

**HARNESSING PEAT-BASED GNOTOBIOTIC PLANT GROWTH TO
CHARACTERIZE MICROBIOTA-MEDIATED IMMUNOCOMPETENCE IN
*ARABIDOPSIS***

By

Bradley Carlton Paasch

A DISSERTATION

**Submitted to
Michigan State University
in partial fulfillment of the requirements
for the degree of**

Biochemistry and Molecular Biology – Doctor of Philosophy

2021

ABSTRACT

HARNESSING PEAT-BASED GNOTOBIOTIC PLANT GROWTH TO CHARACTERIZE MICROBIOTA-MEDIATED IMMUNOCOMPETENCE IN *ARABIDOPSIS*

By

Bradley Carlton Paasch

The increasingly evident involvement of microbes in basic host function has led to a more holistic perspective of plants to be considered. Here, plants and their associated microbiotas interact with each other as holobionts in performing various biological functions in natural ecosystems and crop fields as a single ecological unit. The extent to which microbial components of the holobiont contribute to host health, however, is not fully understood, especially in natural environments. Here, I applied the use of peat-based gnotobiotic growth systems to generate plants grown with and without exposure to microbiota to characterize the role of microbiota on the development of plant immunocompetence.

In my *first chapter*, I review the current understanding on the interplay between microbiota and plant health and immunity. I begin with background on microbial detection and response in plants. I then discuss plant-associated microbiota and provide examples of how perturbation to microbiota homeostasis, such as during dysbiosis for example, can be associated with positive and negative impacts on host health. Host factors regulating microbiota homeostasis in plants are discussed. Lastly, I describe tools and approaches that can be used to the study of plant-microbiota interactions and highlight recent findings involving the modulation of plant immune responses by plant microbiotas.

In my ***second chapter***, I highlight the contributions I made to the improvement of two peat-based gnotobiotic plant growth systems for plant microbiome research recently developed in Dr. Sheng Yang He's laboratory: the FlowPot and GnotoPot systems. I adapted the FlowPot system to use a field soil, highlighting its versatility, and optimized several abiotic conditions associated with plant growth in GnotoPots. Additionally, I used 16S rRNA gene amplicon sequencing to characterize the colonization of a natural, soil-derived microbial community and several preparations of a synthetic bacterial community, demonstrating the use of GnotoPots for colonization studies. We expect both systems to be useful tools for the research community to address a wide variety of questions related to plant-microbiota interactions.

In my ***third chapter***, I implement the optimizations made to peat-based gnotobiotic growth systems described in the previous chapter to characterize the role of basal microbiota colonization on plant immunocompetence. I found that compared to plants colonized by a soil-derived microbiota, axenic plants grown without exposure to a microbiota lacked robust age-dependent immunity. Axenic plants were defective in several aspects of pattern-triggered immunity including flg22-induced production of reactive oxygen species, signaling through MAPK pathways, and induction of defense-related genes and hypersusceptible to disease a bacterial foliar pathogen. Additionally, I found that a synthetic microbiota composed of culturable leaf endosphere bacteria was able to restore immunocompetence similar to plants inoculated with a soil-derived community in a growth substrate-dependent manner. These results demonstrate a role of microbiota in immunocompetence and age-dependent immunity, which was previously thought to be an intrinsic trait of plants.

ACKNOWLEDGEMENTS

First, I would like to give my heartfelt thanks to my graduate advisor Sheng Yang He for your guidance, support, and patience. You have been a truly fantastic mentor and have been instrumental to my success and growth as a scientist. I will forever be grateful the opportunities you have given me. I would also like to thank the many members of the He Lab, past and present, for all the wonderful help and feedback you have offered over the years. In particular, I would like to thank the many team microbiome undergraduate students I've had the pleasure of working with, especially Caleigh Griffin, Franchesca Dion, Trevor Ulrich, Jennifer Martz, and Timothy Johnson. Many of these experiments would not have been possible without your hard work and dedication. I would also like to give a special thanks to friend and colleague James Kramer for laying the framework for this entire project and actively providing valuable advice and insight both in and out of the lab. Lastly, I would like to thank my lovely wife Qiwen for always being by my side and believing in me.

TABLE OF CONTENTS

LIST OF TABLES	vii
LIST OF FIGURES	viii
KEY TO ABBREVIATIONS	x
CHAPTER 1: INTRODUCTION	1
1.1. <i>Arabidopsis</i> innate immunity	2
1.2. Plant defense hormones	3
1.3. Age-dependent immunity	5
1.4. Defining the “core” microbiota in plants.....	6
1.5. Eubiotic microbiota homeostasis	7
1.6. Microbiota homeostasis and plant health.....	8
1.7. Plant factors regulating microbiota homeostasis.....	10
1.8. Gnotobiotic plant growth systems for plant microbiome research.....	14
1.9. Microbiota and plant innate immunity	15
1.10. Aim of the work	17
REFERENCES	19
CHAPTER 2: OPTIMIZATION OF PEAT-BASED GNOTOBIOTIC SYSTEMS FOR PLANT-MICROBIOME RESEARCH	26
2.1. Abstract.....	27
2.2. Introduction	28
2.3. Results.....	34
2.3.1. Features of the FlowPot system.....	34
2.3.2. Adaptation of FlowPots to use field soil.....	36
2.3.3. Features of the GnotoPot system.....	38
2.3.4. Optimization of the GnotoPot system.....	39
2.3.5. Bacterial community colonization in GnotoPots	45
2.3.6. Optimization of SynCom inoculum preparation and storage	46
2.4. Discussion	50
2.5. Methods	55
2.5.1. <i>Arabidopsis</i> growth conditions	55
2.5.2. Adaptation of FlowPots to use field soil.....	55
2.5.3. Preparation of SynCom ^{Col-0} inoculum.....	56
2.5.4. Sample collection and DNA extraction for 16S rRNA gene profiling	57
2.5.5. 16S rRNA gene fragment amplification and MiSeq library preparation	58
2.5.6. Processing of 16S rRNA gene fragment amplicons	59
APPENDICES	61

APPENDIX A: Protocol for the FlowPot and GnotoPot gnotobiotic plant growth systems.....	62
APPENDIX B: Supplementary information	92
REFERENCES.....	98
CHAPTER 3: A MICROBIOTA IS REQUIRED FOR PROPER IMMUNOCOMPETENCE IN <i>ARABIDOPSIS</i>	103
3.1. Abstract.....	104
3.2. Introduction	105
3.3. Results.....	108
3.3.1. Age-related flg22-mediated resistance in potting soil-grown <i>Arabidopsis</i>	108
3.3.2. Optimization of FlowPots and GnotoPots for studying immunocompetence.....	110
3.3.3. Immune maturation is dependent of colonization of plant tissues by microbiota	115
3.3.4. Axenic <i>Arabidopsis</i> exhibit defects in pattern-triggered immunity	117
3.3.5. A bacterial synthetic community (SynCom) confers immunocompetence.....	123
3.3.6. Microbiota-conferred immunocompetence is dependent on growth substrate	125
3.4. Discussion	127
3.5. Methods.....	133
3.5.1. <i>Arabidopsis</i> growth conditions	133
3.5.2. Bacterial infection assays.....	134
3.5.3. ROS burst assay	135
3.5.4. RT-qPCR analysis of flg22-induced gene expression	135
3.5.5. Quantification of SA and SAG.....	137
3.5.6. Protein extraction and immunoblot.....	138
REFERENCES.....	140

LIST OF TABLES

Table 2.1: Advantages and disadvantages of substrates used in gnotobiotic systems	30
Table A2.1: FlowPot and GnotoPot troubleshooting guide.....	90
Table B2.1: Compressed substrate pellets sourced for GnotoPot optimization experiments	96

LIST OF FIGURES

Figure 1.1:	Schematic overview of select flg22-activated PTI responses	4
Figure 1.2:	Host control of microbiota homeostasis in plants	12
Figure 2.1:	<i>Arabidopsis thaliana</i> growth in peat-based FlowPots	35
Figure 2.2:	<i>Arabidopsis</i> growth in soil-based FlowPots.....	37
Figure 2.3:	Effect of LS nutrient solution concentration on <i>Arabidopsis thaliana</i> growth in GnotoPots	40
Figure 2.4:	Effect of humidity on hyperhydricity	41
Figure 2.5:	Typical <i>Arabidopsis</i> vegetative growth in GnotoPots	42
Figure 2.6:	Pellet type impacts <i>Arabidopsis</i> growth in GnotoPots.....	44
Figure 2.7:	Endophytic leaf bacterial colonization in GnotoPots	47
Figure 2.8:	Endophytic leaf bacterial colonization by cryopreserved SynCom ^{Col-0}	49
Figure B2.1:	Basic setup of the FlowPot system	93
Figure B2.2:	Basic setup of the GnotoPot system.....	94
Figure B2.3:	<i>Arabidopsis</i> growth in GnotoPots using peat pellets amended with vermiculite.....	95
Figure B2.4:	<i>Arabidopsis</i> growth phenotype of plants used in 16S rRNA gene profiling experiments.....	97
Figure 3.1:	Immunity undergoes a maturation process in <i>Arabidopsis</i> plants conventionally grown in potting soil.....	109
Figure 3.2:	Excess nutrients and humidity suppresses flg22-induced immune responses in GnotoPots.....	111
Figure 3.3:	Optimized nutrient and humidity conditions promote more robust immune responses in colonized plants grown in GnotoPots.....	114
Figure 3.4:	Role of microbiota in immune maturation.....	116

Figure 3.5: Role of microbiota in maturation of PTI.....	118
Figure 3.6: Axenic Arabidopsis plants exhibit defects in PTI compared to colonized plants	120
Figure 3.7: PTI-associated protein abundance in AX versus HO plants	122
Figure 3.8: SynCom ^{Col-0} restores immunocompetence similar to a natural soil-derived microbial community	124
Figure 3.9: Microbiota-mediated immune phenotype is dependent on growth substrate	126

KEY TO ABBREVIATIONS

ARR	Age-related resistance
ASV	Amplicon sequence variant
AX	Axenic
BAK1	BRASSINOSTEROID INSENSITIVE 1-ASSOCIATED KINASE 1
BGLU42	BETA-GLUCOSIDASE 42
BIK1	BOTRYTIS-INDUCED KINASE
BTH	Benzothiadiazole
CAD1	CONSTITUTIVELY ACTIVATED CELL DEATH 1
cfu	Colony-forming unit
csp22	22 amino acid peptide from bacterial cold shock protein
elf18	18 amino acid peptide from elongation factor Tu
ET	Ethylene
ETI	Effector triggered immunity
flg22	22 amino acid peptide from bacterial flagellin
FLS2	FLAGELLIN SENSITIVE 2
FRK1	FLG22-INDUCED RECEPTOR-LIKE KINASE 1
HO	Holoxenic
JA	Jasmonic acid
LS	Linsmaier and Skoog plant nutrient media
MAPK	Mitogen-activated protein kinase
MIN7	HOPM INTERACTOR 7

MYB72	MYB DOMAIN PROTIEN 72
NPR1	NONEXPRESSOR OF PATHOGENESIS-RELATED GENES 1
OD	Optical density
PAMP	Pathogen-associated molecular pattern
PE	Polyethylene
Pi	Orthophosphate
PLA	Polylactic acid
PP2A	PRPTEIN PHOSPHATASE 2 A
PR	PATHOGENESIS RELATED
PRR	Pattern recognition receptor
PSR	Phosphate starvation response
<i>Pst</i> DC3000	<i>Pseudomonas syringae</i> pv. <i>tomato</i> DC3000
R protein	Resistance protein
RBOHD	RESPIRATORY BURST OXIDASE HOMOLOG D
RH	Relative humidity
ROS	Reactive oxygen species
RT-qPCRq	Reverse transcription-quantitative polymerase chain reaction
SA	Salicylic acid
SDS-PAGE	Sodium dodecyl sulfate-polyacrylamide gel electrophoresis
SynCom	Synthetic community

CHAPTER 1: INTRODUCTION

Parts of this chapter are adapted from portions of a previously published review article entitled “Toward understanding microbiota homeostasis in the plant kingdom” in *PLoS Pathogens*, volume 17(4): e1009472.

Authors: Bradley C. Paasch^{1, 2, 3} and Sheng Yang He^{1, 3, 4}

Affiliations: ¹Department of Energy Plant Research Laboratory, Michigan State University, East Lansing, MI, USA; ²Department of Biochemistry and Molecular Biology, Michigan State University, East Lansing, MI, USA; ³Department of Biology, Durham, NC, USA; ⁴Howard Hughes Medical Institute, Duke University, Durham, NC, USA.

1.1. *Arabidopsis* innate immunity

Plants are exposed to a wide diversity of microorganisms, many of which come from the soil and, to a lesser extent, the air [1-3]. To fight off infection by pathogenic or opportunistic microorganisms found among plant microbiota, plants possess two apparent layers of innate immunity: pattern-triggered immunity (PTI) and effector-triggered immunity (ETI). PTI represents the first layer of plants defense after physical barriers have been breached. It is initiated upon recognition of pathogen-associated molecular pattern (PAMPs) by a pattern recognition receptor (PRR) [4]. PAMP recognition initiates downstream signaling events leading to transcriptional reprogramming of defense-related genes [5, 6]. PAMPs are conserved motifs that occur widely among pathogenic and non-pathogenic microbes. Examples of characterized PAMPs include microbial peptides corresponding to segments of flagellin (flg22), elongation factor Tu (elf18), or cold shock protein (csp22); and oligosaccharides such as lipopolysaccharide, peptidoglycan, or chitin, among others [7]. ETI, on the other hand, serves as a second layer of defense and involves a gene-for-gene interaction where virulence proteins, such as the type III effectors from *Pseudomonas syringae*, introduced into plant cells by potentially pathogenic microorganisms are recognized by plant resistance (R) proteins [4].

The flg22 peptide is a commonly used and well characterized elicitor of PTI in *Arabidopsis*. Here, perception of flg22 by the PRR FLAGELLIN SENSITIVE 2 (FLS2) induces rapid assembly of an immune receptor complex at the plasma membrane composed of FLS2, BRASSINOSTEROID INSENSITIVE 1-ASSOCIATED KINASE 1 (BAK1), and BOTRYTIS-INDUCED KINASE 1 (BIK1). Auto- and transphosphorylation

events facilitate signal transduction through the immune receptor complex, which eventually results in the activation of mitogen-activated protein kinase (MAPK) cascades resulting in transcriptional reprogramming and expression of PTI-responsive genes [8], including *FLG22-INDUCED RECEPTOR-LIKE KINASE 1 (FRK1)*. In addition to proteins facilitating activation of MAPK cascades, BIK1 activates a calcium-dependent NADPH oxidase which is involved in the generation of bursts of reactive oxygen species (ROS) upon the activation of PTI [6] (Figure 1.1). FLS2 is eventually endocytosed and shuttled to the proteasome for degradation [9]. Exogenous application of purified PAMPs, such as flg22 peptide, induces activation of PTI and “primes” plant defenses for enhanced protection during subsequent infections [10]. Activation of PTI also induces closure of gas exchange pores in the leaf called stomata and accumulation of callose on the cell wall, among other physical defense mechanisms [4]. As a result, PAMP-induced protection against bacterial growth, ROS bursts, MAPK activation, defense-related marker gene expression (including FRK1), and callose deposition, are all associated with activation of PTI, and thus, are commonly used to approximate its activation.

1.2. Plant defense hormones

Phytohormones are another important class of signaling molecules plants employ in the coordination of immune responses against non-self entities. Jasmonic acid (JA), ethylene (ET), and salicylic acid (SA) are three major hormones that play a key role in various aspects of plant defense. JA and ET are important for defense against herbivory and necrotrophic pathogens while SA is primarily involved in defense against biotrophic

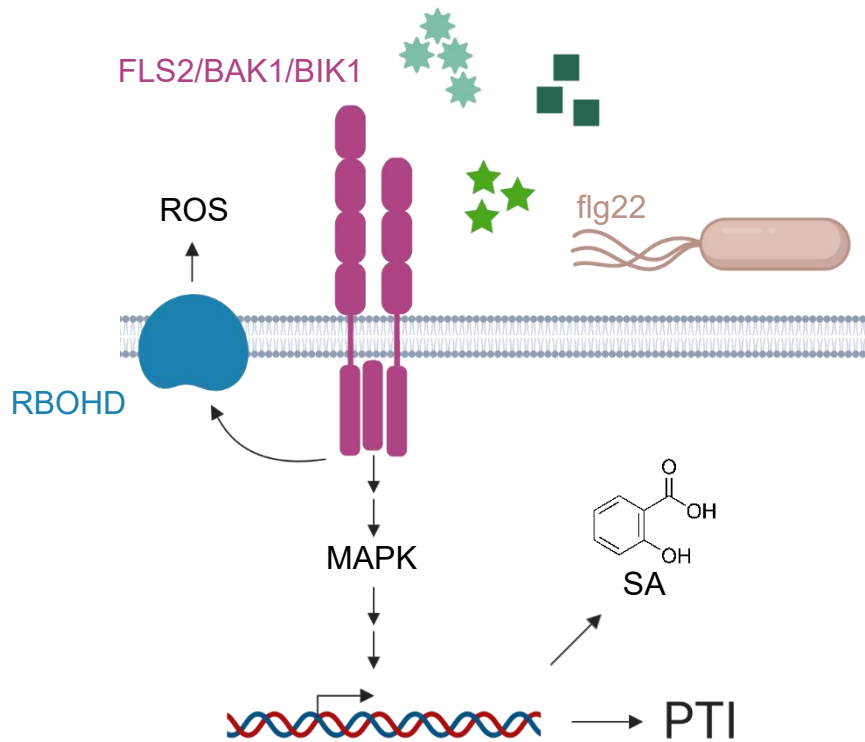


Figure 1.1: Schematic overview of select flg22-activated PTI responses.

PTI signaling is initiated by perception of flg22 by pattern recognition receptor FLAGELLIN SENSITIVE 2 (FLS2) which forms an immune receptor complex with BRASSINOSTEROID INSENSITIVE 1-associated receptor kinase 1 (BAK1), and BOTRYTIS-INDUCED KINASE 1 (BIK1). BIK1 directly phosphorylates NADPH/RESPIRATORY BURST OXIDASE HOMOLOG D (RBOHD) which generates superoxide that is converted to hydrogen peroxide by a superoxide dismutase. Activation of the FLS2/BAK1/BIK1 immune receptor complex also initiates PTI signaling through mitogen-activated protein kinase (MAPK) cascade via an unknown mechanism and ultimately results in the expression of defense-related genes and activation of PTI responses, including accumulation of defense hormone salicylic acid (SA). Created with BioRender.

pathogens [11]. Regulatory protein NONEXPRESSOR OF PATHOGENESIS-RELATED GENES 1 (NPR1) is a major regulator of SA signaling. When challenged with a biotrophic or hemibiotrophic pathogen, SA accumulates within the cytoplasm of plant cells. This stimulates a conformational change in NPR1, which results in its monomerization and translocation into the nucleus [12]. In the nucleus, NPR1 initiates defense gene expression through its interaction with TGA transcription factors [13-17]. Genes activated by SA include various PATHOGENESIS RELATED (PR) genes, including PR1, which is often used as a marker gene for SA-mediated defense. Exogenous application of SA or benzothiadiazole (BTH), a functional analog of SA, induces activation of SA-mediated defense and primes plant defenses for faster and stronger response in an NPR1-dependent manner [18, 19].

1.3. Age-dependent immunity

In nature, many flowering plant species exhibit increased resistance to pathogenic infection as an individual ages [20] and is often referred to as age-related resistance (ARR) in this context. Examples of ARR are widespread and have been described in *Arabidopsis*, tomato, potato, tobacco, barley, rice, wheat, and cotton, among many other plant species [21]. One form of age-related resistance occurs during the first several weeks of plant growth, prior to floral transition. During this time, *Arabidopsis*, for example, becomes more resistant to multiple pathogens including the necrotrophic fungal pathogen *Sclerotinia sclerotiorum* and the hemibiotrophic bacterial pathogens *Xanthomonas oryzae* pv. *oryzae*, *Pseudomonas syringae* pv. *tabaci*, and *P. syringae* pv. *tomato* DC3000 [22]. ARR has historically been associated with transitions

between developmental stages, where intrinsically programmed developmental processes are hypothesized to modulate immune responses [23], though in many cases the underlying cause is still unclear. The potential role of exogenous factors in ARR, such as the contribution of microbiota, is still an area that warrants further investigation.

1.4. Defining the “core” microbiota in plants

A plant microbiome consists of the assemblage of microorganisms residing within or on various plant tissues and their activities. In the past decade, many studies have surveyed microbiota composition in plants. Despite diverse microbes found in plants, overall bacterial composition seems to be conserved at the phylum level. In flowering plants that have been surveyed, the above-ground tissues (phyllosphere) are associated with bacterial assemblages dominated by Proteobacteria, Actinobacteria, Bacteroidetes and Firmicutes. These bacterial phyla are also enriched in below-ground tissues (rhizosphere) compared to bulk soil [24, 25]. Nonvascular plants such as liverwort and moss are also dominated by these phyla [26-28], suggesting possible conservation of core microbiota across plant lineages. It should be pointed out that, so far, most microbiota surveys have been focused on bacterial components of plant-associated microbial communities. As fungi [29], viruses [30], and protozoa [31] are also common residents on or inside the plant, more efforts are needed in the future to systematically define fungal, viral and protozoa microbiota members across plant taxa. Additionally, biogeography plays an important role in determining the reservoir of microbes from which a plant selects members of its microbiota [32]. Because different microbial taxa may provide functionally redundant traits to a plant host [33], detection of

dissimilar taxa in different plants, especially at lower taxonomical levels, may not necessarily indicate functionally distinct microbiotas, an important topic that requires rigorous future investigations.

1.5. Eubiotic microbiota homeostasis

Regardless of whether there is a functionally conserved core microbiome in plants, increasing evidence suggests that microbiota homeostasis may be intimately linked to host processes and, in turn, plant health and immunity. Microbiota homeostasis in eukaryotic organisms is likely dynamic in both space and time. Here, we use *eubiosis* to describe the state of microbiota homeostasis that is necessary for maintaining typical host health and physiology under optimal, non-stressful conditions. The eubiotic state for an individual plant is not static, but instead dynamic over a plant's lifetime. For example, microbiota of healthy plants can vary temporally based on the time of year [1] or developmental stage [34]. Stress or other perturbations may induce changes to the microbiota which could disrupt eubiosis. Disruption to microbiota eubiosis can be associated with negative impacts on host health and is often called dysbiosis in this context [35]. Deviation from eubiosis, however, is not always detrimental and may help plants cope with various forms of stress. The observed correlation between microbiota homeostasis and plant health and immunity highlights a potential role of microbiota in maintaining normal host health and function.

1.6. Microbiota homeostasis and plant health

Deviations of microbial compositions from what is typically observed in health individuals, such as during dysbiosis, can sometimes be linked to changes in host health. In humans, dysbiosis is associated with ailments such as inflammatory bowel disease, diabetes, allergies, and other health issues [36] and is often accompanied by a lower diversity microbial community with altered metabolic function [37]. However, broad use of the term “dysbiosis” in mammalian literature has come under scrutiny, particularly for its inconsistent definition and ambiguity as often no distinction can be made between it being a cause or effect of a specific disease [38]. A recent study showed an example of dysbiosis as the causal agent for tissue damages in plants. Several *Arabidopsis* immune-compromised mutants were found to harbor an increased amount and altered composition of phyllosphere microbiota and display leaf-tissue damage under high humidity [39]. The Shannon diversity index and the relative abundance of Firmicutes were markedly reduced, whereas Proteobacteria were enriched inside the leaves of these mutant plants, bearing cross-kingdom resemblance to some aspects of the dysbiosis that occurs in human inflammatory bowel disease. Importantly, bacterial community transplantation experiments showed that the application of the dysbiotic leaf bacterial community to otherwise healthy plants resulted in tissue damages, demonstrating that, in this case, dysbiosis is causative to negative impact on host health [39].

Tissue damage-associated deviations from eubiosis have also been observed during insect and pathogen attacks, which often compromise host immune responses. For example, herbivory of bittercress plants by the leaf-mining fly causes a significant

shift in phyllosphere microbiota, resulting in an increased abundance of bacteria on damaged leaves. Growth of *Pseudomonas* spp. (belonging to Proteobacteria) was found to largely account for the increased abundance of microbiota [40]. Another study found that fungal pathogen *Zymoseptoria tritici* suppresses immune responses in susceptible wheat cultivars, resulting in an increase in bacteria members of the leaf microbiome near fungal infection sites [41]. Together, these examples imply that immune suppression during pathogen infections is associated with shifting the composition of microbiota, similar to what is observed in immune-compromised plant mutants [39]. This may be a broadly applicable principle. Indeed microbiota changes have been described across many plant species upon biotic challenge, including citrus greening in citrus [42], parasitic nematode *Meloidogyne graminicola* infection in rice [43], Yellow Canopy Syndrome in sugarcane [44], and protist *Plasmodiophora brassicae* in Chinese cabbage [45]. However, in these cases, it is not yet known whether the observed changes in microbiota contribute causally to (or a consequence of) tissue damages in disease.

It should be noted that deviation from eubiosis is not always associated with reduced plant performance. Microbiota changes (referred to hereafter as *meliorbiosis*; from the Latin root *melior*- meaning “to make better, improve”) that enable positive effects on plant performance under stressful conditions have been described. In the case of biotic stress, the fungal pathogen *Fusarium graminearum* was shown to induce shifts to rhizosphere microbiota of barley plants, including apparent recruitment of bacterial taxa that are enriched with antifungal traits [46]. In Arabidopsis, infection of leaves with oomycete *Hyaloperonospora arabidopsidis*, a causative agent of downy

mildew, resulted in enrichment of specific rhizosphere bacteria that were able to induce systemic resistance against downy mildew [47]. Insect herbivory can also induce changes to the plant microbiota. For example, aphid [48] and whitefly [48, 49] feeding of above-ground pepper plant tissues results in restructuring of rhizosphere microbiota and enhanced resilience to belowground bacterial pathogens.

Abiotic stress can also induce shifts in microbiota composition. Drought stress, for instance, induces a large restructuring of below-ground communities across diverse plant hosts [50-52]. This shift is generally associated with enrichment of Actinobacteria in the root endosphere relative to the rhizosphere or bulk soil [51]. The enrichment of specific strains under drought conditions, but not water replete conditions, is correlated with increased plant root biomass [52] which could contribute to improved drought resilience [53].

As is in the case of dysbiosis, the cause-and-effect relationship during meliorbiosis is still not so clear in many cases. While changes in microbiota composition are sometimes associated with positive effects on plant fitness, causality still needs to be demonstrated in most instances. Further, a fundamental understanding of the contribution that the basal abundance and composition of a microbiota during eubiosis has on specific plant phenotypes, such as ARR and immune maturation, is still lacking in many instances.

1.7. Plant factors regulating microbiota homeostasis

If proper microbiota homeostasis is critical for plant health, one would expect that plants would have evolved mechanisms to prevent health-damaging dysbiosis and allow

health-promoting meliorbiosis under stressful conditions. Indeed, recent studies have begun to identify host factors that are involved in mediating microbiome homeostasis in plants (Figure 1.2). While it is well established that plant defense hormones SA and JA play an important role in limiting the growth of virulent pathogens in plants, it is becoming increasingly evident that they also play a critical role in mediating the homeostasis of commensal microbiota members. *Arabidopsis* mutants with constitutively elevated levels of SA-mediated immune response harbor reduced bacterial diversity in the endophytic leaf microbiota, while mutants deficient in JA-mediated immune response harbor an increased bacterial diversity in epiphytic leaf microbiota [54]. Activation of JA pathways by application of methyl-JA also alters the composition of the rhizosphere microbiota [55], further implicating the role of JA pathways in the regulation of microbiome homeostasis in plants. A study involving multiple hormone mutants identified defense hormone SA is required to establish a normal rhizosphere microbiota and that SA-mediated modulation of the rhizosphere microbiota is likely to occur at the family level, instead of impacting only a select few largely abundant strains [56]. In addition to SA and JA, *Arabidopsis ein2* mutants defective in ethylene signaling harbor distinct phyllosphere microbial communities compared to wildtype plants [57]. However, it remains to be determined whether the observed microbiota alterations in these defense hormone mutants causally impact plant fitness, either positively or negative, an area of great interest for future research.

In addition to defense hormones, recent studies have begun to show a critical role of PTI in regulating modulating microbiota homeostasis in plants [39, 58, 59]. An *Arabidopsis* quadruple mutant lacking three PRRs/co-receptors (recognizing bacterial

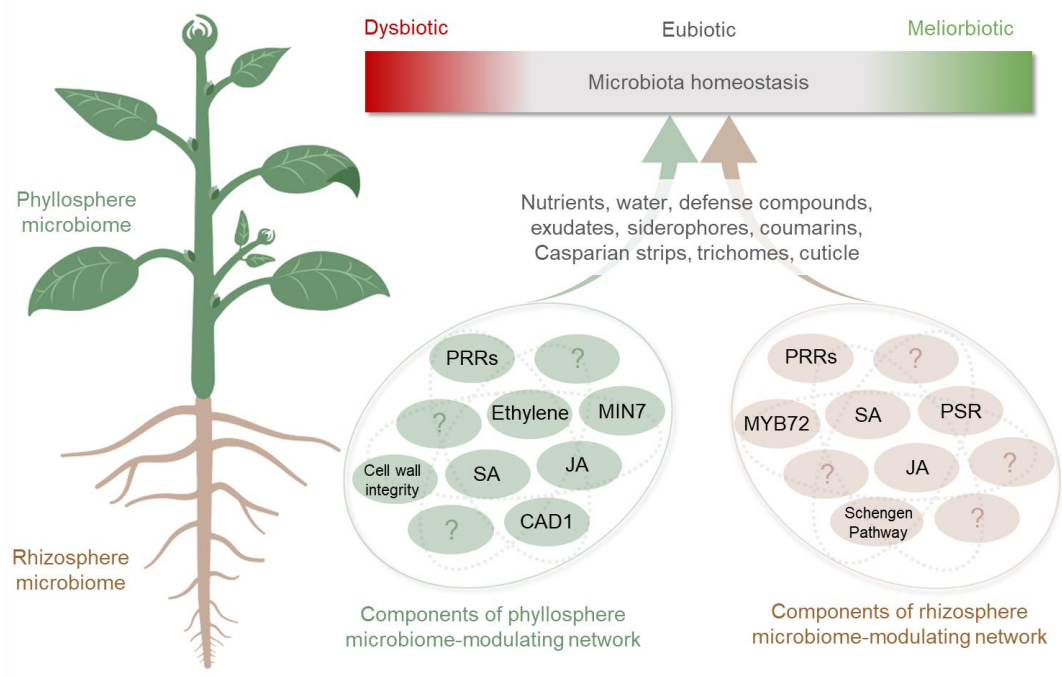


Figure 1.2: Host control of microbiota homeostasis in plants. Microbiota eubiosis represents a normal range of microbiota abundance and composition in healthy plants grown under optimal conditions. If eubiosis is disrupted, either by host mutations, abiotic stress or infections or a combination thereof, homeostasis can shift towards a dysbiotic state associated with negative impacts on plant health or towards a meliorbiotic state associated with positive impacts on plant health. Examples of host factors that contribute to microbiota homeostasis in the phyllosphere (green) and rhizosphere (brown) are depicted in circles below. Not all known factors are depicted. Abbreviations: CAD1, CONSTITUTIVELY ACTIVATED CELL DEATH 1; JA, jasmonic acid; MIN7, HOPM INTERACTOR 7; MYB72, MYB DOMAIN PROTIEN 72; PRRs, pattern recognition receptors; PSR, phosphate starvation response; SA, salicylic acid. Created with BioRender.

flagellin, elongation factor Tu and peptidoglycan, respectively) and a vesicle traffic regulator, the MIN7 protein, displayed a dysbiotic shift in the quantity and composition of the endophytic leaf microbiota [60]. Similar alterations in endophytic leaf microbiota were found in an *Arabidopsis* mutant that carries a S205F mutation in a membrane-attack-complex/perforin-domain protein, CAD1 [39]. The involvement of plant immunity in regulating some aspects of microbiota homeostasis illustrates a conceptual parallel to mammalian-microbiome interactions, as PRR gene mutations (e.g., NOD2) have been shown to be linked to dysbiosis in humans [61] and members of the MACPF protein family, such as human C9 and perforin in particular, have been shown to be involved in innate and adaptive immunity in mammals [62].

In addition to defense-related plant processes, physical barriers and leaf-surface structures such as the plant cell wall and trichomes, may play a role in influencing microbiota homeostasis based on a genome-wide association study examining 196 accessions of *Arabidopsis* grown in the field and their associated bacterial and fungal communities [63]. Furthermore, *Arabidopsis* mutants with altered cuticle formation possess altered epiphytic phyllosphere bacterial communities [57, 64]. A recent study further confirmed the role of physical structures in contributing to microbiota homeostasis [65]. Here, *Arabidopsis* mutants defective in genes controlling the function of endodermal root diffusion barriers, including those in the Schengen pathway required for Casparian strip formation and those involved with suberin deposition, possessed rhizosphere bacterial communities with altered composition [65].

Finally, pathways involved in plant nutrient response also play a role in microbiota homeostasis. For instance, under iron- and phosphate-limiting conditions,

plants can induce the secretion of coumarins which, in addition to aiding in plant nutrient uptake, possess selective antimicrobial activity and can shape the root microbiota [66]. *Arabidopsis*, for instance, secretes iron-mobilizing coumarin scopoletin under iron-limiting conditions in response to beneficial bacteria in a manner dependent on the MYB72 transcription factor and a β -glucosidase, BGLU42. Scopoletin was found to have high antimicrobial activity against fungal pathogens *Fusarium oxysporum* and *Verticillium dahlia*, whereas many beneficial rhizobacteria are tolerant [67]. Additionally, several *Arabidopsis* mutants defective in components regulating phosphate starvation response (PSR) and inorganic phosphate availability in plant tissues were found to harbor endophytic root microbial communities that are significantly different compared to wildtype plants [68].

1.8. Gnotobiotic plant growth systems for plant microbiome research

In *Arabidopsis*, one approach to study the function of a gene of interest is to generate a knockout mutant and characterize how removal of the unknown gene influences plant processes. Similar to how a host phenotype is influenced by the collection of genes that make up the host genotype (genome), the manifest phenotype of a particular microbiota is the consequence of their collective genetic make-up (metagenome) [69]. Therefore, removal of microbiota could provide a basis of comparison to study functions of a microbial community in colonized plants. Indeed, gnotobiotic plant growth systems have been used to generate and characterize microbiota metagenomic 'knock outs'.

Gnotobiotic plant growth systems facilitate the growth of axenic plants (plants devoid of microbiota) and plants colonized with user-defined input microbiota. Gnotobiotic plant growth in these systems is generally accomplished by isolating plants from the surrounding environment, while at the same time making available the resources needed for growth, such as nutrients, light, and gas exchange. A prominent difference between various gnotobiotic growth systems is the composition of the growth substrate. Field soil is notoriously difficult to sterilize so early systems designed for gnotobiotic plant growth utilized liquid media or nutrient agar [70], however these systems lack the physical structure and organic matter relevant to soil. More recently, mineral-based substrates such as sand, quartz, vermiculite, and calcined clay have been utilized. Gnotobiotic systems utilizing substrates based on these materials provide a soil-like scaffold but lack organic matter. Edaphic factors greatly influence associated microbial communities. For example, soil pore size along the root-soil interface has been found to have an impact on rhizosphere microbiome structure and function [71]. Therefore, for studying eubiosis and the resulting contribution that the basal abundance and composition a microbiota has on plant phenotypes, mimicking natural conditions similar to field soil is ideal.

1.9. Microbiota and plant immunity

Initial characterization of axenic seedlings grown in FlowPots indicated that 21-day-old axenic plants lacked normal basal expression of immune-associated genes compared to holoxenic plants inoculated with a complex microbial community extracted from field soil [72]. Further characterization revealed that axenic plants were

hypersusceptible to infection by foliar pathogen *Pst* DC3000 and compromised in various aspects of flg22-induced PTI. These findings indicated that exposure to microbiota contribute to immunocompetence and robust PTI in *Arabidopsis* [72] and served as the basis for this dissertation. Similar findings were subsequently made in a separate report using FlowPots which found that a 183-member multikingdom synthetic community composed of bacteria, fungi, and oomycetes could modulate *Arabidopsis* immune responses in a light-dependent manner and, compared to axenic plants, colonized plants were more resistant to the fungal pathogen *Botrytis cinerea* B05.10 and bacterial pathogen *Pst* DC3000 [73].

On the other hand, a recent study performed using 7-day-old *Arabidopsis* seedlings grown on nutrient agar found that a 35-member synthetic community composed of bacterial *Arabidopsis* root commensals largely suppressed flg22-induced expression of defense-related transcripts in colonized plants compared to axenic controls [74]. When strains within the synthetic community were characterized individually, the immunomodulatory effect was found to be strain-specific and some strains induced immune responses while others suppressed immune responses and that suppressors could not be predicted taxonomically [74]. Indeed, a separate report also found specific non-pathogenic microbes can suppress various plant immune responses individually [59, 75] and that an imbalance of immune suppressive bacteria can suppress immune function of plate-grown plants in a community context [59]. Since the plant growth conditions of these study are different compared to those conducted with FlowPots (i.e. agar vs peat), the question remains whether the observed immunomodulatory effects of microbiota are dependent on some unidentified

environmental condition, such as abiotic factors like nutrient availability that could be influenced by growth substrate. Indeed, plant microbiota colonization can be modulated by environmental factors like salinity, pH, phosphate availability, and temperature [32, 76]. Additionally, given the age differences between the plants used in the studies, a question is raised about whether there is a temporal immunomodulatory effect in *Arabidopsis* facilitated by exposure to microbiota during vegetative growth. Lastly, given the difference in input microbiota, it is not clear whether fungi and oomycetes are required for robust PTI in colonized plants, or whether colonization by bacteria is sufficient.

1.10. Aim of the work

While the apparent cases of dysbiosis and meliorbiosis discussed in previous sections highlight the impact aberrant microbiota compositions may have on plant health, the contributions eubiotic microbiota homeostasis has to *typical* host health and physiology is still not well understood in many cases. One particular area that lacks this clarity is the contribution of microbiota to plant innate immunity. I chose to approach this gap in understanding with a “whole community” knock-out approach by comparing uncolonized axenic plants to colonized plants that were otherwise grown with the same conditions through the implementation of peat-based gnotobiotic plant growth systems recently developed in Dr. Sheng Yang He’s lab. However, since this project began a few notable findings were made were identified. Namely, I found that long-term vegetative growth in FlowPots can be highly variable and that in some gnotobiotic system setups, PTI can be dramatically suppressed by abiotic conditions irrespective of microbial

colonization. Thus, the goal of this work was twofold. First, I sought to improve on an emerging gnotobiotic plant growth system and optimize them to allow for extended plant growth and robust PTI. Second, I sought use this newly redesigned system to assess the role of microbiota on the maturation of plant innate immunity during vegetative growth, using the characterization of flg22-induced immune responses as a starting point.

REFERENCES

REFERENCES

1. Grady, K.L., et al., *Assembly and seasonality of core phyllosphere microbiota on perennial biofuel crops*. Nature communications, 2019. **10**(1): p. 1-10.
2. Compant, S., et al., *A review on the plant microbiome: ecology, functions, and emerging trends in microbial application*. Journal of advanced research, 2019. **19**: p. 29-37.
3. Abdelfattah, A., et al., *Revealing cues for fungal interplay in the plant–air interface in vineyards*. Frontiers in plant science, 2019. **10**: p. 922.
4. Jones, J.D. and J.L. Dangl, *The plant immune system*. nature, 2006. **444**(7117): p. 323-329.
5. Navarro, L., et al., *The transcriptional innate immune response to flg22. Interplay and overlap with Avr gene-dependent defense responses and bacterial pathogenesis*. Plant physiology, 2004. **135**(2): p. 1113-1128.
6. Bigeard, J., J. Colcombet, and H. Hirt, *Signaling mechanisms in pattern-triggered immunity (PTI)*. Molecular plant, 2015. **8**(4): p. 521-539.
7. Zipfel, C., *Pattern-recognition receptors in plant innate immunity*. Current opinion in immunology, 2008. **20**(1): p. 10-16.
8. Zipfel, C., *Early molecular events in PAMP-triggered immunity*. Current opinion in plant biology, 2009. **12**(4): p. 414-420.
9. Robatzek, S., D. Chinchilla, and T. Boller, *Ligand-induced endocytosis of the pattern recognition receptor FLS2 in Arabidopsis*. Genes & development, 2006. **20**(5): p. 537-542.
10. Macho, A.P. and C. Zipfel, *Plant PRRs and the activation of innate immune signaling*. Molecular cell, 2014. **54**(2): p. 263-272.
11. Pieterse, C.M., et al., *Hormonal modulation of plant immunity*. Annual review of cell and developmental biology, 2012. **28**: p. 489-521.
12. Dong, X., *NPR1, all things considered*. Current opinion in plant biology, 2004. **7**(5): p. 547-552.
13. Chern, M.S., et al., *Evidence for a disease-resistance pathway in rice similar to the NPR1-mediated signaling pathway in Arabidopsis*. The Plant Journal, 2001. **27**(2): p. 101-113.

14. Després, C., et al., *The Arabidopsis NPR1/NIM1 protein enhances the DNA binding activity of a subgroup of the TGA family of bZIP transcription factors*. *The Plant Cell*, 2000. **12**(2): p. 279-290.
15. Niggeweg, R., et al., *Tobacco TGA factors differ with respect to interaction with NPR1, activation potential and DNA-binding properties*. *Plant molecular biology*, 2000. **42**(5): p. 775-788.
16. Zhang, Y., et al., *Interaction of NPR1 with basic leucine zipper protein transcription factors that bind sequences required for salicylic acid induction of the PR-1 gene*. *Proceedings of the National Academy of Sciences*, 1999. **96**(11): p. 6523-6528.
17. Zhou, J.-M., et al., *NPR1 differentially interacts with members of the TGA/OBF family of transcription factors that bind an element of the PR-1 gene required for induction by salicylic acid*. *Molecular Plant-Microbe Interactions*, 2000. **13**(2): p. 191-202.
18. Cao, H., et al., *The Arabidopsis NPR1 gene that controls systemic acquired resistance encodes a novel protein containing ankyrin repeats*. *Cell*, 1997. **88**(1): p. 57-63.
19. Huot, B., et al., *Dual impact of elevated temperature on plant defence and bacterial virulence in Arabidopsis*. *Nature communications*, 2017. **8**(1): p. 1-12.
20. Develey-Rivière, M.P. and E. Galiana, *Resistance to pathogens and host developmental stage: a multifaceted relationship within the plant kingdom*. *New Phytologist*, 2007. **175**(3): p. 405-416.
21. Panter, S. and D.A. Jones, *Age-related resistance to plant pathogens*. 2002.
22. Xu, Y.P., et al., *Leaf stage-associated resistance is correlated with phytohormones in a pathosystem-dependent manner*. *Journal of integrative plant biology*, 2018. **60**(8): p. 703-722.
23. Carella, P., D.C. Wilson, and R.K. Cameron, *Some things get better with age: differences in salicylic acid accumulation and defense signaling in young and mature Arabidopsis*. *Frontiers in plant science*, 2015. **5**: p. 775.
24. Müller, D.B., et al., *The plant microbiota: systems-level insights and perspectives*. *Annual review of genetics*, 2016. **50**: p. 211-234.
25. Bulgarelli, D., et al., *Structure and functions of the bacterial microbiota of plants*. *Annual review of plant biology*, 2013. **64**: p. 807-838.

26. Alcaraz, L.D., et al., *Marchantia liverworts as a proxy to plants' basal microbiomes*. Scientific reports, 2018. **8**(1): p. 1-12.
27. Bragina, A., et al., *The S phagnum microbiome supports bog ecosystem functioning under extreme conditions*. Molecular ecology, 2014. **23**(18): p. 4498-4510.
28. Ma, J., et al., *Illumina sequencing of bacterial 16S rDNA and 16S rRNA reveals seasonal and species-specific variation in bacterial communities in four moss species*. Applied microbiology and biotechnology, 2017. **101**(17): p. 6739-6753.
29. Bergelson, J., J. Mittelstrass, and M.W. Horton, *Characterizing both bacteria and fungi improves understanding of the Arabidopsis root microbiome*. Scientific reports, 2019. **9**(1): p. 1-11.
30. Roossinck, M.J., *A new look at plant viruses and their potential beneficial roles in crops*. Molecular plant pathology, 2015. **16**(4): p. 331.
31. Gao, Z., et al., *Protists: puppet masters of the rhizosphere microbiome*. Trends in Plant Science, 2019. **24**(2): p. 165-176.
32. Fitzpatrick, C.R., et al., *The plant microbiome: from ecology to reductionism and beyond*. Annual review of microbiology, 2020. **74**: p. 81-100.
33. Louca, S., et al., *Function and functional redundancy in microbial systems*. Nature ecology & evolution, 2018. **2**(6): p. 936-943.
34. Chaparro, J.M., D.V. Badri, and J.M. Vivanco, *Rhizosphere microbiome assemblage is affected by plant development*. The ISME journal, 2014. **8**(4): p. 790-803.
35. Petersen, C. and J.L. Round, *Defining dysbiosis and its influence on host immunity and disease*. Cellular microbiology, 2014. **16**(7): p. 1024-1033.
36. Blum, H.E., *The human microbiome*. Advances in medical sciences, 2017. **62**(2): p. 414-420.
37. DeGruttola, A.K., et al., *Current understanding of dysbiosis in disease in human and animal models*. Inflammatory bowel diseases, 2016. **22**(5): p. 1137-1150.
38. Hooks, K.B. and M.A. O'Malley, *Dysbiosis and its discontents*. MBio, 2017. **8**(5): p. e01492-17.
39. Chen, T., et al., *A plant genetic network for preventing dysbiosis in the phyllosphere*. Nature, 2020. **580**(7805): p. 653-657.

40. Humphrey, P.T. and N.K. Whiteman, *Insect herbivory reshapes a native leaf microbiome*. *Nature ecology & evolution*, 2020. **4**(2): p. 221-229.
41. Seybold, H., et al., *A fungal pathogen induces systemic susceptibility and systemic shifts in wheat metabolome and microbiome composition*. *Nature communications*, 2020. **11**(1): p. 1-12.
42. Trivedi, P., et al., *Huanglongbing alters the structure and functional diversity of microbial communities associated with citrus rhizosphere*. *The ISME journal*, 2012. **6**(2): p. 363-383.
43. Masson, A.-S., et al., *Deep modifications of the microbiome of rice roots infected by the parasitic nematode *Meloidogyne graminicola* in highly infested fields in Vietnam*. *FEMS Microbiology Ecology*, 2020. **96**(7): p. f1aa099.
44. Hamonts, K., et al., *Field study reveals core plant microbiota and relative importance of their drivers*. *Environmental microbiology*, 2018. **20**(1): p. 124-140.
45. Lebreton, L., et al., *Temporal dynamics of bacterial and fungal communities during the infection of *Brassica rapa* roots by the protist *Plasmodiophora brassicae**. *PLoS One*, 2019. **14**(2): p. e0204195.
46. Dudenhöffer, J.H., S. Scheu, and A. Jousset, *Systemic enrichment of antifungal traits in the rhizosphere microbiome after pathogen attack*. *Journal of Ecology*, 2016. **104**(6): p. 1566-1575.
47. Berendsen, R.L., et al., *Disease-induced assemblage of a plant-beneficial bacterial consortium*. *The ISME journal*, 2018. **12**(6): p. 1496-1507.
48. Lee, B., S. Lee, and C.-M. Ryu, *Foliar aphid feeding recruits rhizosphere bacteria and primes plant immunity against pathogenic and non-pathogenic bacteria in pepper*. *Annals of botany*, 2012. **110**(2): p. 281-290.
49. Yang, J.W., et al., *Whitefly infestation of pepper plants elicits defence responses against bacterial pathogens in leaves and roots and changes the below-ground microflora*. *Journal of Ecology*, 2011. **99**(1): p. 46-56.
50. Santos-Medellín, C., et al., *Drought stress results in a compartment-specific restructuring of the rice root-associated microbiomes*. *MBio*, 2017. **8**(4): p. e00764-17.
51. Fitzpatrick, C.R., et al., *Assembly and ecological function of the root microbiome across angiosperm plant species*. *Proceedings of the National Academy of Sciences*, 2018. **115**(6): p. E1157-E1165.

52. Xu, L., et al., *Drought delays development of the sorghum root microbiome and enriches for monoderm bacteria*. Proceedings of the National Academy of Sciences, 2018. **115**(18): p. E4284-E4293.
53. Fang, Y. and L. Xiong, *General mechanisms of drought response and their application in drought resistance improvement in plants*. Cellular and molecular life sciences, 2015. **72**(4): p. 673-689.
54. Kniskern, J.M., M.B. Traw, and J. Bergelson, *Salicylic acid and jasmonic acid signaling defense pathways reduce natural bacterial diversity on Arabidopsis thaliana*. Molecular plant-microbe interactions, 2007. **20**(12): p. 1512-1522.
55. Carvalhais, L.C., et al., *Activation of the jasmonic acid plant defence pathway alters the composition of rhizosphere bacterial communities*. PLoS One, 2013. **8**(2): p. e56457.
56. Lebeis, S.L., et al., *Salicylic acid modulates colonization of the root microbiome by specific bacterial taxa*. Science, 2015. **349**(6250): p. 860-864.
57. Bodenhausen, N., et al., *A synthetic community approach reveals plant genotypes affecting the phyllosphere microbiota*. PLoS genetics, 2014. **10**(4): p. e1004283.
58. Song, Y., et al., *Loss of a plant receptor kinase recruits beneficial rhizosphere-associated Pseudomonas*. BioRxiv, 2020.
59. Ma, K.-W., et al., *Coordination of microbe–host homeostasis by crosstalk with plant innate immunity*. Nature Plants, 2021. **7**(6): p. 814-825.
60. Xin, X.-F., et al., *Bacteria establish an aqueous living space in plants crucial for virulence*. Nature, 2016. **539**(7630): p. 524-529.
61. Lauro, M.L., J.M. Burch, and C.L. Grimes, *The effect of NOD2 on the microbiota in Crohn's disease*. Current opinion in biotechnology, 2016. **40**: p. 97-102.
62. Liu, X. and J. Lieberman, *Knocking'em dead: pore-forming proteins in immune defense*. Annual review of immunology, 2020. **38**: p. 455-485.
63. Horton, M.W., et al., *Genome-wide association study of Arabidopsis thaliana leaf microbial community*. Nature communications, 2014. **5**(1): p. 1-7.
64. Reisberg, E.E., et al., *Distinct phyllosphere bacterial communities on Arabidopsis wax mutant leaves*. PloS one, 2013. **8**(11): p. e78613.
65. Salas-González, I., et al., *Coordination between microbiota and root endodermis supports plant mineral nutrient homeostasis*. Science, 2021. **371**(6525).

66. Voges, M.J., et al., *Plant-derived coumarins shape the composition of an Arabidopsis synthetic root microbiome*. Proceedings of the National Academy of Sciences, 2019. **116**(25): p. 12558-12565.
67. Stringlis, I.A., et al., *MYB72-dependent coumarin exudation shapes root microbiome assembly to promote plant health*. Proceedings of the National Academy of Sciences, 2018. **115**(22): p. E5213-E5222.
68. Castrillo, G., et al., *Root microbiota drive direct integration of phosphate stress and immunity*. Nature, 2017. **543**(7646): p. 513-518.
69. Vandenkoornhuysen, P., et al., *The importance of the microbiome of the plant holobiont*. New Phytologist, 2015. **206**(4): p. 1196-1206.
70. Hale, M., D. Lindsey, and K. Hameed, *Gnotobiotic culture of plants and related research*. The Botanical Review, 1973. **39**(3): p. 261-273.
71. Song, C., K. Jin, and J.M. Raaijmakers, *Designing a home for beneficial plant microbiomes*. Current Opinion in Plant Biology, 2021. **62**: p. 102025.
72. Kremer, J.M., *Characterization of axenic immune deficiency in Arabidopsis thaliana*. 2017: Michigan State University.
73. Hou, S., et al., *A microbiota–root–shoot circuit favours Arabidopsis growth over defence under suboptimal light*. Nature Plants, 2021. **7**(8): p. 1078-1092.
74. Teixeira, P.J., et al., *Specific modulation of the root immune system by a community of commensal bacteria*. Proceedings of the National Academy of Sciences, 2021. **118**(16).
75. Teixeira, P.J.P., et al., *Beyond pathogens: microbiota interactions with the plant immune system*. Current opinion in microbiology, 2019. **49**: p. 7-17.
76. Finkel, O.M., et al., *A single bacterial genus maintains root growth in a complex microbiome*. Nature, 2020. **587**(7832): p. 103-108.

CHAPTER 2: OPTIMIZATION OF PEAT-BASED GNOTOBIOTIC SYSTEMS FOR PLANT-MICROBIOME RESEARCH

Parts of this chapter are adapted from a previously published research article entitled “Peat-based gnotobiotic plant growth systems for *Arabidopsis* microbiome research” in *Nature Protocols*, volume 16(5): pages 2450-2470.

Authors: James M. Kremer^{#,1, 2, 3, 4}, Reza Sohrabi^{#, 1, 5, 6}, Bradley C. Paasch^{#, 1, 7, 6}, David Rhodes¹, Caitlin Thireault¹, Paul Schulze-Lefert⁸, James M Tiedje^{2, 3}, Sheng Yang He^{1, 2, 5, 6, 9}

Affiliations: ¹MSU-DOE Plant Research Laboratory, Michigan State University, East Lansing, MI, USA; ²Department of Microbiology and Molecular Genetics, Michigan State University, East Lansing, MI, USA; ³Center for Microbial Ecology, Michigan State University, East Lansing, MI, USA; ⁴Joyn Bio, Boston, MA, USA; ⁵Plant Resilience Institute, Michigan State University, East Lansing, MI, USA; ⁶Department of Biology, Duke University, Durham, NC, USA; ⁷Department of Biochemistry and Molecular Biology, Michigan State University, East Lansing, MI, USA; ⁸Department of Plant Microbe Interactions, Max Planck Institute for Plant Breeding Research, Cologne, Germany; ⁹Howard Hughes Medical Institute, Duke University, Durham, NC, USA; [#]Equal contribution.

2.1. Abstract

The structure and function of a given plant microbiota is driven by many variables, including the environment, microbe-microbe interactions, and host factors. Likewise, resident microbiota may influence many host phenotypes. Gnotobiotic growth systems and controlled environments empower researchers to isolate these variables, and standardized methods could equip a global research community to harmonize protocols, replicate experiments, and collaborate broadly. Currently, plant microbiome research is in need of gnotobiotic systems that could simulate organic-matter-containing substrates where plants often grow in nature. Two peat-based gnotobiotic growth platforms were recently introduced from Dr. Sheng Yang He's laboratory – the FlowPot system and the GnotoPot system. Sterile peat is amenable to colonization by microbiota and supports growth of the model plant *Arabidopsis thaliana* in the presence or absence of microorganisms. A defining feature of the FlowPot system is the ability to flush the substrate with water, nutrients, and/or suspensions of microbiota via an irrigation port located on the bottom of each pot. A mesh retainer prevents the loss of substrate during flushing steps and permits a range of downstream manipulations such as inversion of plants for dip or vacuum infiltrations. The irrigation port also facilitates passive drainage during plant growth. In contrast, the GnotoPot system implements the use of a compressed peat pellet as the primary growth substrate, which is widely used in the horticultural industry. GnotoPot construction has fewer steps and requires less user handling, thereby reducing the risk of contamination. In this chapter I provide a characterization of each system and describe optimization for select system components, including as nutrients, humidity, and substrate composition.

2.2. Introduction

Multicellular organisms are in constant contact with diverse microbial communities, which reside in and on their body parts. These microbes, collectively called microbiota, play important roles in modulating their host health and disease [1-3]. Much progress has been made to elucidate plant-microbiome interactions in open field or greenhouse conditions, but there are limitations to resolve the cause and effect of many plant-microbiome interactions under such conditions [4, 5]. In particular, soils vary tremendously in their biochemical composition, microbial composition, and geochemical and physical attributes. Likewise, the air to which plants are exposed in open systems in different locations fluctuates in microbial composition and load. These variations are not amenable for a global research community to replicate experiments easily. A deep mechanistic understanding of plant-microbiome interactions, especially the cause-and-effect relationship, could benefit from the development of a common set of standardized experimental platforms. Indeed, a current research priority for the plant microbiome community is to develop standardized methods to elucidate the rules of microbiome assembly and functional plant-microbiome interactions, including plant genotype-by-environment-by-microbiome-by-management interactions [4, 5]. Development of a set of gnotobiotic plant growth systems that can be widely adopted by the research community could facilitate the advancement of global plant microbiome studies.

Several aspects should be considered to minimize system artifacts which may impact plant growth or microbiota colonization when designing a gnotobiotic plant growth system. Environmental factors such as temperature and humidity, for instance, can affect both plant-associated phenotypes as well as microbial community

composition. Elevated temperatures, for example, are associated with altered plant development [6] and reduced defense [7]. Similarly, high humidity can promote defects in plant growth and development and encourage disease [8]. Environmental variables such as temperature and humidity have also been demonstrated to have an impact on plant-associated bacterial community colonization [9, 10]. In addition, edaphic factors such as pH, organic matter content, carbon content, moisture, porosity, gaseous composition, cation exchange, and other physical or chemical properties of the soil are key determinants of plant and soil microbiota composition [11-13]. Therefore, when conducting microbiota colonization experiments to compare plants colonized by a microbial community with uncolonized, axenic plants, consideration of both environmental and edaphic factors is important.

Several gnotobiotic plant growth systems capable of producing axenic and microbiota-colonized plants have been described in the literature (Table 2.1). A common way to grow axenic plants in the laboratory employs the use of tissue culture methodology using nutrient agar contained in a gas-permeable container. Agar-based substrates, however, lack the physical structure, organic matter, and carbon typical of soil. Furthermore, size and diffusion limitations can result in non-uniform nutrient and O₂ delivery after extended plant growth [14]. Enclosed hydroponic systems that circulate a sterile, aerated nutrient solution have also been used to generate axenic plants [15] and provide more uniform nutrient and O₂ delivery compared to nutrient agar, however hydroponic systems still lack the physical structure, organic matter, and carbon relevant to soil. The additional complexity associated with hydroponic systems can also make them more susceptible to contamination compared to agar-based systems. Mineral-

Table 2.1: Advantages and disadvantages of substrates used in gnotobiotic systems.

Growth system	Advantage	Disadvantage
Nutrient agar	<ul style="list-style-type: none"> • Chemically-defined substrate. • Routine tissue culture methodology. 	<ul style="list-style-type: none"> • Lacks the physical structure of soil for plants and microbes. • Lack of organic matter relevant to soil. • Non-uniform nutrient and O₂ delivery over time. • Highly dissimilar to field condition.
Hydroponic	<ul style="list-style-type: none"> • Chemically-defined substrate. • Easily accessible roots for exudate collection. • No substrate to interfere with imaging technology. 	<ul style="list-style-type: none"> • Lacks soil-like physical structure for plants and microbes. • Lack of organic matter relevant to soil. • Highly dissimilar to field conditions. • Susceptible to contamination.
Mineral substrates (calcined clay, zeolite, sand, quartz, vermiculite)	<ul style="list-style-type: none"> • Provides soil-like scaffold. • Substrate highly accessible. • Easy to sterilize. • Roots are easily extracted from substrate. 	<ul style="list-style-type: none"> • Lack of organic matter. • Lacks significant organic carbon, unless supplemented. • Variable labile ions. • Maybe difficult to maintain water flow.
Sterilized Soil	<ul style="list-style-type: none"> • Natural substrate for plant growth. • Easily accessible. 	<ul style="list-style-type: none"> • Soil is a generic term that includes many diverse substrates with different edaphic features. • Different soils are differentially impacted by autoclaving, and other sterilization methods. • Not easy to standardize for a global research community. • Roots not easily removed from substrate.
Peat (FlowPot and GnotoPot)	<ul style="list-style-type: none"> • Peat is standard potting mix, and easily accessible around the world. • Organic matter supports microbial growth and plant growth. • Commonly used in commercial greenhouse operations. 	<ul style="list-style-type: none"> • For the FlowPot system, assembly requires significant hands-on time. • Roots not easily removed from substrate.

based substrates such as calcined clay, zeolite, sand, quartz, and vermiculite have also been used as a substrate for gnotobiotic plant growth [16-20]. While these substrates are porous and provide a soil-like scaffold, they generally lack organic matter and carbon, unless supplemented with an exogenous carbon source such as sucrose. Furthermore, mineral-based substrates can have highly variable sorptive properties among production lots which can dramatically alter the labile concentrations of micronutrients available to plants and, in some cases, cause nutrient limitations or phytotoxic excesses [21]. Nevertheless, compared to peat-based gnotobiotic systems described here, non-soil substrates, such as phytonutrient agar, hydroponics, and calcined clay, may be suitable to mimic defined mineral nutrient deficiencies and other specific applications, thus highlighting the importance of multiple standardized gnotobiotic system methodologies.

Field soils have also been used as substrate for gnotobiotic plant growth in laboratory settings, however the use of soil often presents challenges. Soil can be difficult to effectively sterilize. Several methods have been described for the sterilization of soil including autoclaving, dry heat, gamma-irradiation, microwave, and chemical sterilants by either fumigation or saturation. [22]. Soil sterilization methods need to be carefully optimized for plant growth due to potential phytotoxic effects of chemical residue and unintended artifacts of the sterilization process. For example, autoclaving can acidify soil and increase levels of water-soluble carbon and other ions such as manganese [23]. Together these can lead to nutritional imbalances and/or phytotoxic effects [24]. However, subjecting a thin layer of soil to multiple consecutive autoclave cycles spaced 24 h apart, some soils can be sterilized with little chemical modification

[25-27]. In our hands, gnotobiotic systems based on heat-sterilized soils often do not provide a conducive environment for growing healthy *Arabidopsis* plants, unless amended with certain inert materials and aseptically flushed with a nutrient solution, as will be described in this chapter.

Recently, two peat-based gnotobiotic plant growth systems were developed in Dr. Sheng Yang He's laboratory: the FlowPot system and the GnotoPot system. These systems implement a peat-based growth substrates, like those that are commonly used in greenhouse settings, which is relatively easy to sterilize and provides both the physical structure as well as organic carbon typical to soil. FlowPots and GnotoPots allow for the growth of *Arabidopsis* in axenic (no viable microorganisms detected), gnotobiotic (inoculated with a defined community of bacteria), and holoxenic (inoculated with undefined microbiota extracted directly from a natural environment) conditions. Both systems also implement a gas-permeable Microbox tissue culture container (SacO2, Belgium) which provides a microbial barrier and sequesters plant growth from surrounding environments while permitting necessary gas exchange. While the peat-based nature of the growth substrate used in either system is similar, nuances between the growth apparatus construction makes the FlowPot and GnotoPot systems unique in terms of their potential applications and versatility.

A major effort of my dissertation research was devoted to the characterization and subsequent optimization of FlowPots and GnotoPots for gnotobiotic growth of *Arabidopsis*. Here, I will highlight these findings. These efforts ultimately aided in the improvement of both systems and contributed to the creation of the published protocols [28], which are presented in Appendix A. In subsequent sections, I will describe the

basic set up of FlowPots and GnotoPots, as well as results that highlight my contributions to each system.

2.3. Results

2.3.1. Features of the FlowPot system

The FlowPot system was developed by Dr. James Kremer prior to the start of this dissertation research. It utilizes a sterile substrate composed of equal parts peat and vermiculite as the growth medium (Supplementary Figure B2.1). Individual FlowPots containing the substrate are constructed using truncated syringe barrels with a mesh retainer. The mesh retainer allows inversion and subsequent down-stream manipulation of individual FlowPots while the Luer lock fitting facilitates bottom-irrigation. Bottom irrigation is a critical step that enables robust plant growth, presumably by flushing out phytotoxic byproducts released from the substrate during autoclaving steps. During preparation FlowPots are aseptically supplemented with nutrients and optionally inoculated with a microbiota via the irrigation port. In the case of axenic plant growth, FlowPots are mock-inoculated with a heat-killed version of the inoculum. Prepared FlowPots are then placed into sterile Microboxes prior to sowing.

To limit the risk of contamination by environmental microbes, the essential factors required for plant growth (i.e., nutrients and water) are incorporated into the FlowPot system prior to sealing microboxes lids. Although the FlowPot system had been used to sustain *Arabidopsis* plant growth and to conduct microbiota study prior to this dissertation work, the duration the FlowPot system can reliably sustain healthy plant growth had not been extensively characterized. Over the course of at least 18 months of my Ph.D. program, I observed that plants grown in FlowPots could vary in size and appearance (Figures 2.1 A-C), especially after prolonged growth. Deviation from typical, healthy plant growth was sporadic but frequent enough to complicate inter-experiment

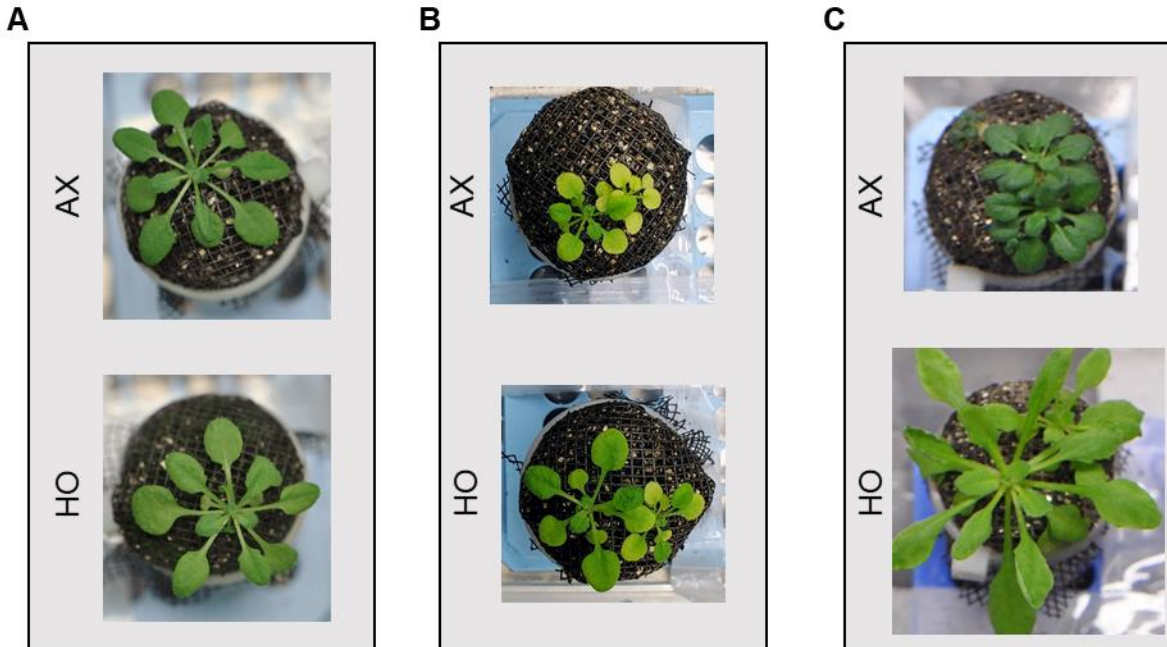


Figure 2.1: *Arabidopsis thaliana* growth in peat-based FlowPots.

(A-C) Axenic (AX) and holoxenic (HO) *Arabidopsis* plants grown in sterile peat substrate photographed approximately 4.5 weeks post germination. AX plants were mock-inoculated with an autoclaved slurry extracted from soil (MSU18). Holoxenic HO plants were inoculated with a viable MSU18 soil slurry. Each axenic/holoxenic pair is from a separate experiment: (A) Represents expected plant growth typical to FlowPots. (B) An example experiment where both axenic plants are stunted in growth and both axenic and holoxenic plants displayed chlorosis. (C) An example experiment where axenic plants displayed darker green pigmentation and holoxenic plants were larger than expected and with an altered leaf shape.

reproducibility of sequential experiments. Variation typically manifested as differences in leaf color (e.g. chlorosis or altered pigmentation), leaf shape, plant size, or a combination thereof. Experiment-to-experiment variation was typically most profound, though variation within an experiment was also observed on occasion. When experimental variation did occur, indications typically did not appear until after week 3 and became most pronounced around week 5-6. Taken together, these results suggest that the basic FlowPot system is best used to characterize plant-microbe interactions during the first 3 weeks post-germination. For experiments that require longer plant growth periods, a greater number of FlowPots need to be prepared so that enough healthy plants are available for experimental treatments.

2.3.2. Adaptation of FlowPots to use field soil

Along with undergraduate researcher Trevor Ulrich, I next tested the possibility to adapt the FlowPot system to include the use of natural soil. We substituted the peat substrate with field soil harvested from a *Miscanthus* plot located at a research farm on campus at Michigan State University (and introduced several modifications to the FlowPot setup. First, sterile FlowPots were made by replacing the peat/vermiculite mix with a soil/vermiculite mix. Addition of vermiculate was important as unamended soils were unable to sustain robust *Arabidopsis* growth, even without autoclaving, presumably because unamended soil was too dense for *Arabidopsis* root development. In addition, we found that standard “bottom-up” FlowPot irrigation steps (Supplementary Figure B2.1) would wash out much of the soil, likely owing to its finer particle size compared to peat. We therefore modified irrigation steps to slowly flush liquids through



Figure 2.2: *Arabidopsis* growth in soil-based FlowPots.

Axenic (AX) and holoxenic (HO) plant pairs grown in FlowPots utilizing either sterile soil or peat as a growth substrate. Photographed at 5 weeks post germination. Soil (MSU19) was harvested from an agricultural plot at MSU. Prior to FlowPot construction substrates were amended with vermiculite and autoclaved. Holoxenic plants were inoculated with a slurry derived from unautoclaved soil.

FlowPots from the top of FlowPots and out the irrigation port on the bottom to prevent soil loss. Vacuum applied to the irrigation port of FlowPots aided this process. Mesh retainers on top of FlowPots were removed to accommodate this modified flushing step. We sowed *Arabidopsis* and examined plant growth five weeks after germination. After 5 weeks of growth, plants appeared healthy without visible signs of stress in FlowPots constructed with soil (Figure 2.2). Axenic plants were subsequently harvested and plated on R2A agar plates. No microbial growth was detected. Thus, we successfully adapted FlowPots to use natural soil as a substrate for growing *Arabidopsis* under gnotobiotic conditions.

2.3.3. Features of the GnotoPot system

The concept for the GnotoPot system was conceived by Dr. Reza Sohrabi several years after the FlowPot system was established. A distinguishing feature of this gnotobiotic plant growth system is its use of commercially available peat pellets (Supplementary Figure B2.2). Overall, the use of pre-manufactured peat pellets results in reduced handling and a simplified setup procedure compared to the FlowPot system. During setup of the GnotoPot system, compressed peat pellets are expanded in a nutrient solution and placed into small nursery pots to form a GnotoPot. Individual GnotoPots are then placed inside a Microbox and sterilized in an autoclave. After sterilization, additional nutrient solution is aseptically added the system, creating a reservoir of excess nutrient solution. Seeds are then sown onto individual GnotoPots and subsequently inoculated with a microbiota from above. For axenic plant growth individual GnotoPots can be mock inoculated with an autoclaved inoculum.

2.3.4. Optimization of the GnotoPot system

Nutrient supplementation: Early versions of GnotoPots utilized full-strength (1x) Linsmaier and Skoog (LS) basal medium as nutrient solution. In initial experiments I found that plants often grew larger when lower concentrations of nutrient solution were used (Figure 2.3 A). Elevated nutrient concentrations also masked plant immunity phenotypes (discussed in detail in Chapter 3). When nutrients were reduced, however, colonized plants grown with LS nutrient solution concentrations of 0.25x or less often developed hyperhydricity in leaf tissues (Figure 2.3 B), characterized by a translucent and water-soaked appearance due to excessive hydration (Figure 2.3 C, D). Symptoms of hyperhydricity were not observed in plant grown without exposure to microbiota. Incidences of hyperhydricity observed in colonized plants could be mitigated by reducing the relative humidity on the exterior of GnotoPot boxes (Figure 2.4 A), which increased the rate of evaporation from GnotoPot Microboxes (Figure 2.4 B). Plants also appeared to grow larger when external RH was decreased. Given other gnotobiotic plant growth systems utilized LS (or similar nutrient solutions) in the range of 0.25x-0.5x [20, 29], in my thesis research standard nutrient levels used in subsequent GnotoPot experiments were reduced from 1x to 0.25x-0.5x LS and plants were grown in tissue culture chambers with RH maintained below 50%.

Compared to the FlowPot system, the GnotoPot system implements a larger pot size (Figure 2.5 A) and a nutrient reservoir which was thought to passively replenish depleted nutrients and moisture to individual pots (Figure 2.5 B). I qualitatively characterized long-term growth of *Arabidopsis* in GnotoPots over the course of several months. Robust plant growth throughout vegetative stages of development was

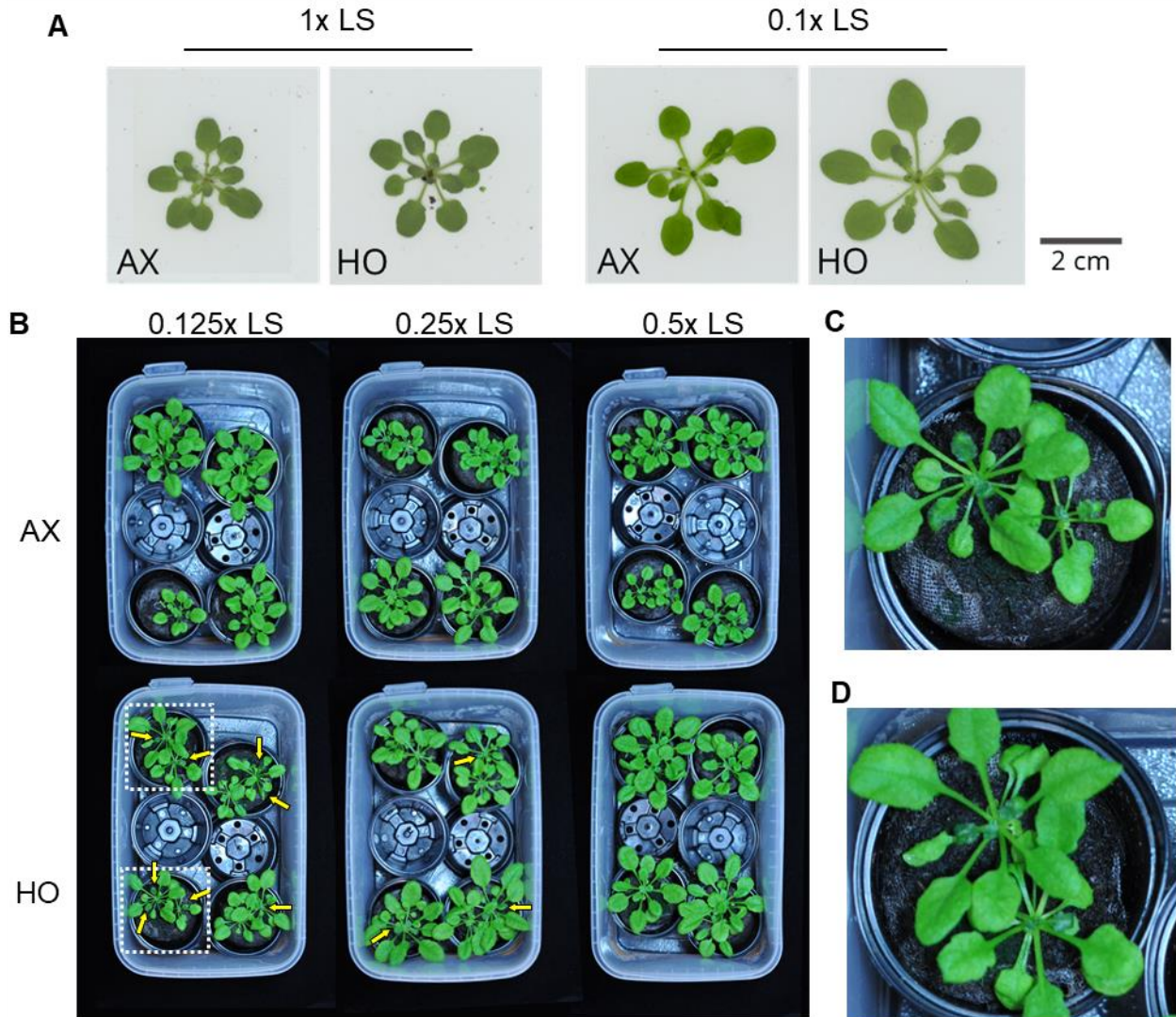


Figure 2.3: Effect of LS nutrient solution concentration on *Arabidopsis thaliana* growth in GnotoPots.

(A) Axenic (AX) and holoxenic (HO) *Arabidopsis* grown in GnotoPots using 1x LS or 0.1x LS nutrient solution concentration. Whole rosettes were removed prior to imaging. Scale bar represents 2 cm. (B) AX and HO *Arabidopsis* grown in GnotoPots using 0.125x LS, 0.25x LS, or 0.5x LS nutrient solution concentration. Microboxes were housed in a tissue culture chamber without humidity control ($RH \geq 80\%$) during plant growth. Leaf tissues indicating symptoms of hyperhydricity are noted with yellow arrows. Photographs taken after 4.5 weeks of plant growth. Areas indicated by white boxes enlarged in panel (C) and (D). For all experiments, MSU19 soil served as source for input microbiota.

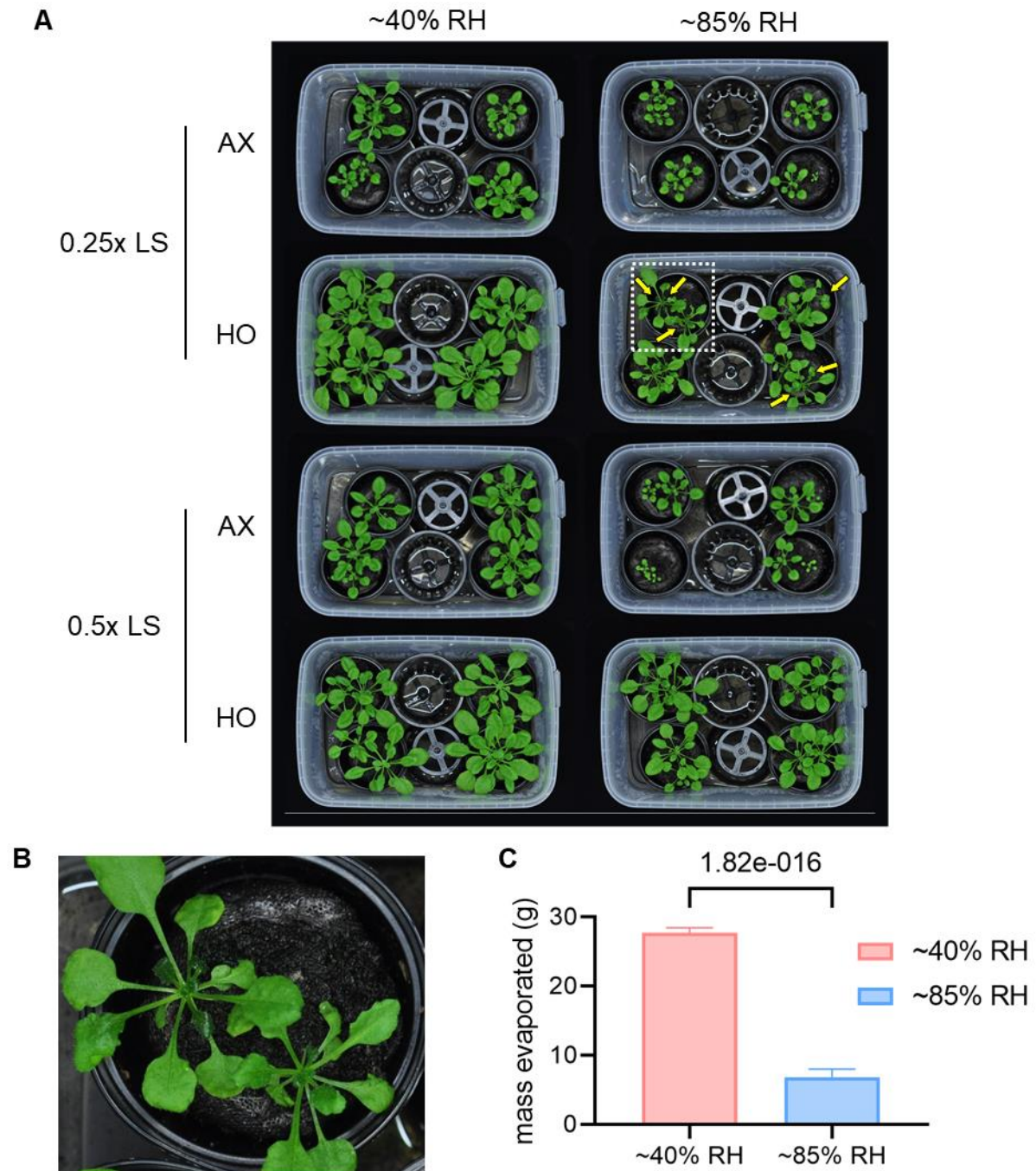


Figure 2.4: Effect of humidity on hyperhydricity.

(A) Axenic (AX) and holoxenic (HO) *Arabidopsis* grown in GnotoPots using 0.25x LS or 0.5x LS nutrient solution concentration with ~40% RH or ~85% RH. Leaf tissues indicating symptoms of hyperhydricity are noted with yellow arrows. Photographs taken after 4.5 weeks of plant growth. MSU19 soil served as source for input microbiota. Area indicated by white box enlarged in panel (B). (C) Average mass evaporated per Microbox after 4.5 weeks when plants are grown at ~40% RH or ~85% RH ($p = 1.82 \times 10^{-16}$, Student's *t*-test).

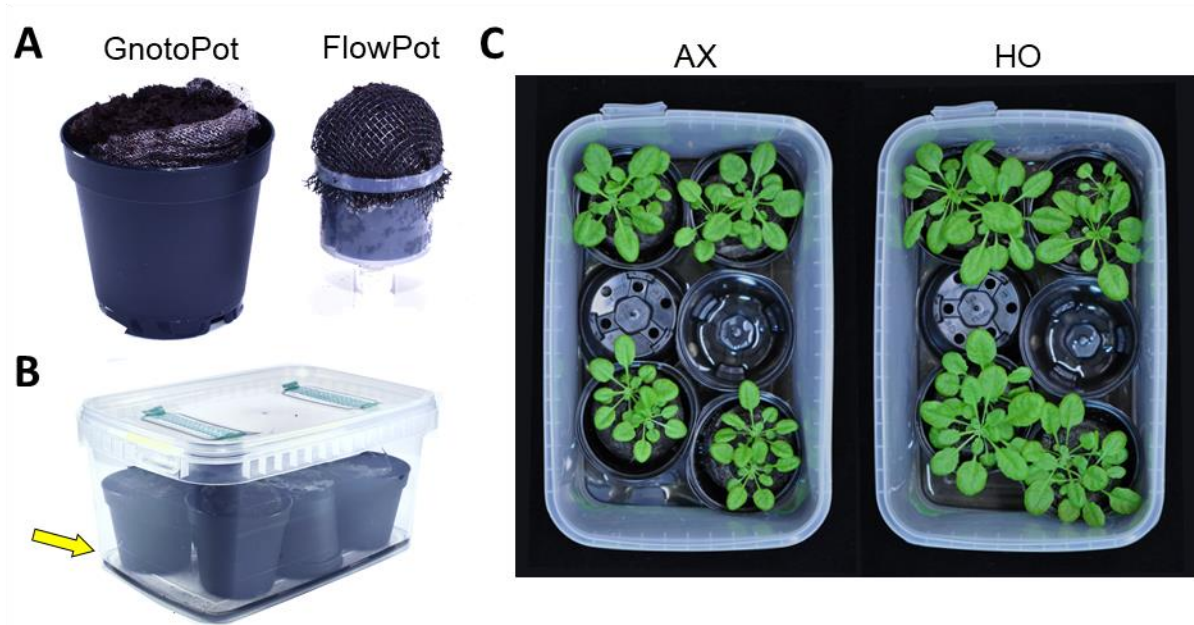


Figure 2.5: Typical *Arabidopsis* vegetative growth in GnotoPots.

(A) Relative size difference between FlowPots and GnotoPots. (B) A reservoir at the bottom of a GnotoPot Microbox contains approximately 60 mL of nutrient solution indicated by the yellow arrow. (C) Photographs of *Arabidopsis thaliana* plants grown in GnotoPots taken 5 weeks post-germination. Axenic (AX) plants were mock-inoculated with an autoclaved slurry extracted from soil (MSU19). Holoxenic (HO) plants were inoculated with a viable MSU19 soil slurry.

observed (Figure 2.5 C) and, in general, was less variable compared to plants grown for the same duration in the FlowPot system. Plants grown in GnotoPots were able to consistently reach reproductive stages of growth without visible signs of stress.

Substrate composition: The GnotoPot system protocol described in this chapter is based on commercially available Jiffy-7 peat pellets. However, there are several types of Jiffy-7 peat pellet from Jiffy Group, as well as various types of pellets from other manufacturers. During characterization of plant growth in the GnotoPot system I tested several pellet types. The pellets I tested varied in composition (peat, coir, or a peat/coir mixture), netting type (inert polyethylene or biodegradable polylactic acid), and proprietary manufacturer-added amendments such as wetting agent and nutrient starting charge. Supplementary Table B2.1 contains a description of the pellet types tested. Most pellets could not sustain robust plant growth after autoclaving, which is an essential step in GnotoPot construction. Plants would germinate but were significantly stunted in growth and often appeared chlorotic (Figure 2.6 A, B, D). I conducted experiments to determine the cause(s). First, each Jiffy-7 pellet is wrapped by a netting to keep peat substrate in shape. I tested the hypothesis that different nettings may contain unknown chemicals that could impact plant growth. However, removal of netting did not improve plant growth (Figure 2.6 A, B). Next, I tested the possibility that plant performance was linked to pellet substrate composition. Indeed, only plants grown in pellets composed a mixture of peat and coir substrates exhibited robust, uniform growth (Figure 2.6 C). Coir is a growth media produced from the mesocarp of coconut (*Cocos nucifera* L.). While particle size is a factor in its physical properties, coir typically possesses a reduced bulk density, increased total pore space, and increased water-

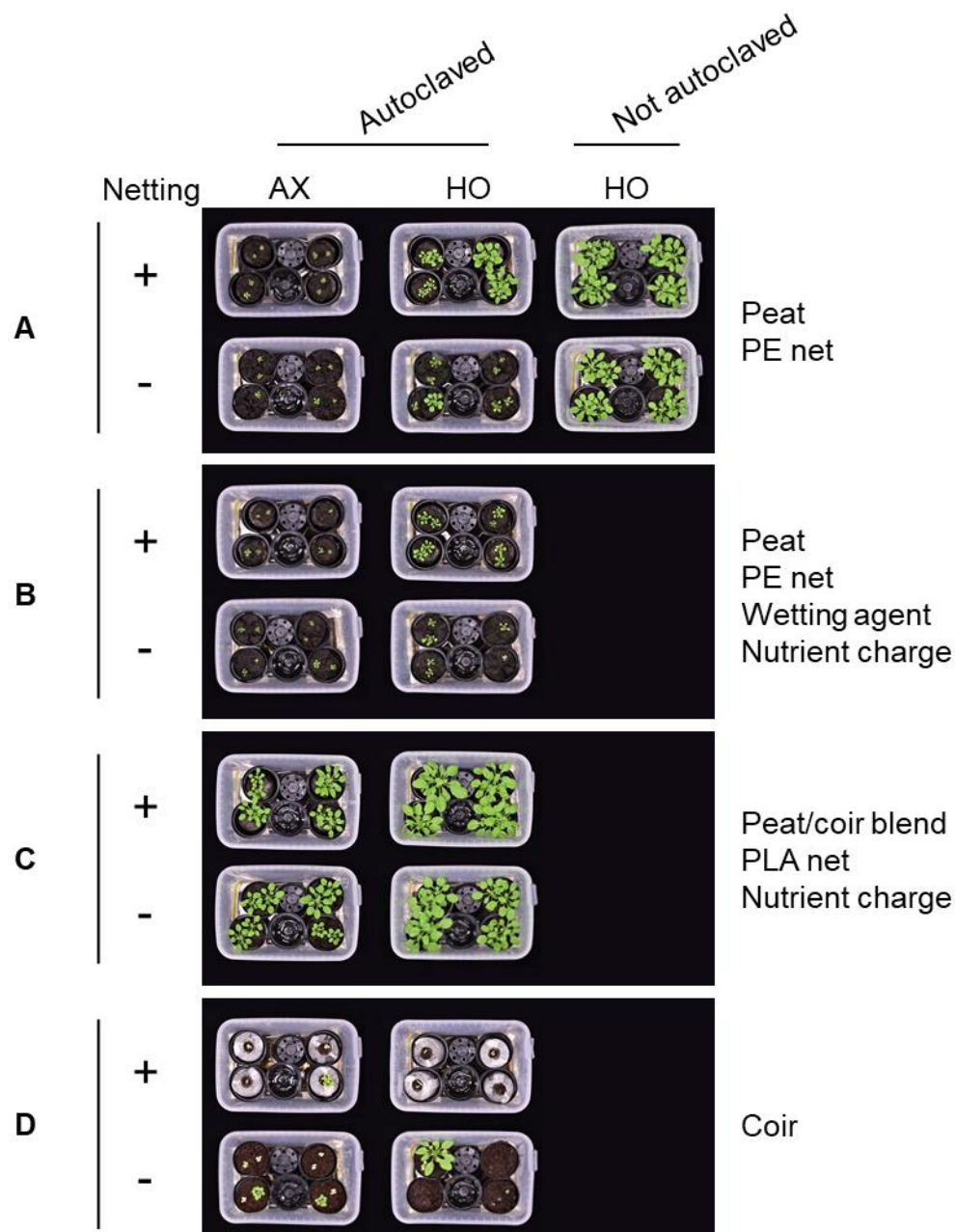


Figure 2.6: Pellet type impacts *Arabidopsis* growth in GnotoPots.

(A-D) Plant growth in GnotoPots constructed with pellets made of various materials. Netting retained (+) or removed (-) prior to autoclaving. Autoclaved pellets mock-inoculated with an autoclaved (AX) microbial community or inoculated with a viable microbial community derived a soil slurry (MSU19). Unautoclaved pellets prepared in parallel, omitting autoclave steps. 0.5x LS and chamber humidity ~40% RH. Additional pellet details available in Supplementary Table B2.1. Photographs taken after five weeks of plant growth.

holding capacity compared to peat [30]. Additionally, coir is less acidic (pH ~5-6 compared to pH ~4-5 for peat) and has altered sorptive properties [31]. To further verify that physical composition of substrate was contributing to poor plant growth, the contents of peat pellets (which grew plants poorly) were removed and amended with equal parts vermiculite. This resulted in a peat/vermiculite mixture similar in composition to FlowPots. Robust plant growth was observed in deconstructed peat pellets amended with vermiculite, but not in unamended peat (Supplementary Figure B2.3), further implicating the physical composition of the peat substrate as a contributor to robust plant growth in the GnotoPot system.

2.3.5. Bacterial community colonization in GnotoPots

Having optimized FlowPot and GnotoPot systems for plant growth, I next conducted microbiota colonization experiments. The FlowPot system has been used in a number of microbiome colonization studies [2, 28, 32]. In contrast, the GnotoPot system has not been tested in such study. Therefore, I focused on the GnotoPot system for microbiota colonization by working with and mentoring an undergraduate researcher, Timothy Johnson. We performed 16S rRNA gene amplicon sequencing to identify bacteria associated with the leaf endosphere of 4.5-week-old *Arabidopsis* plants grown in GnotoPots. Two distinct input microbiotas were used: a natural community composed of a complex consortium of microorganisms (“MSU19” community) extracted from Michigan agricultural field soil and a 48-member bacterial synthetic community (SynCom^{Col-0}) composed of culturable leaf endophytes isolated from *Arabidopsis* [1]. Alpha and beta diversity were calculated on an OTU table rarefied to 1705 reads. Alpha

diversity was estimated using the Shannon Diversity Index, richness, and phylogenetic diversity. We observed that the input microbiota extracted from field soil was more diverse than the SynCom^{Col-0} input, but the diversity associated with the leaf endosphere of 4.5-week-old plants was similar, regardless of which input microbiota was used (Figure 2.5 A-C). This result suggests that plant leaves pose a strong selection on the types of bacteria that can colonize the endosphere regardless of the microbiota input. Principle coordinate analysis of 16S profiles based on weighted UniFrac distances revealed that both leaf endosphere sample groups clustered together and away from their respective inputs (Figure 2.5 D), indicating the leaf endosphere community between “MSU19” community-inoculated and SynCom^{Col-0}-inoculated plants are phylogenetically similar in composition, despite distinct inputs. The most abundantly observed phyla in endosphere samples were Alphaproteobacteria and Bacteroidetes, which were enriched compared to inputs. Firmicutes were also abundant in plants inoculated with a soil-derived community. Taxa classified as Betaproteobacteria, on the other hand, were markedly reduced in both groups (Figure 2.5 E).

2.3.6. Optimization of SynCom inoculum preparation and storage

Finally, I devoted effort to optimize the preparation of storage of SynComs for gnotobiotic research. In most current protocols that describe inoculation of a synthetic community, individual isolates are grown separately and subsequently combined to produce a final mixed community for inoculation in each experiment [1, 2, 16, 33, 34]. This involves a substantial amount of work and often poses a time constraint to completing subsequent experimental steps. I evaluated whether a pre-prepared and

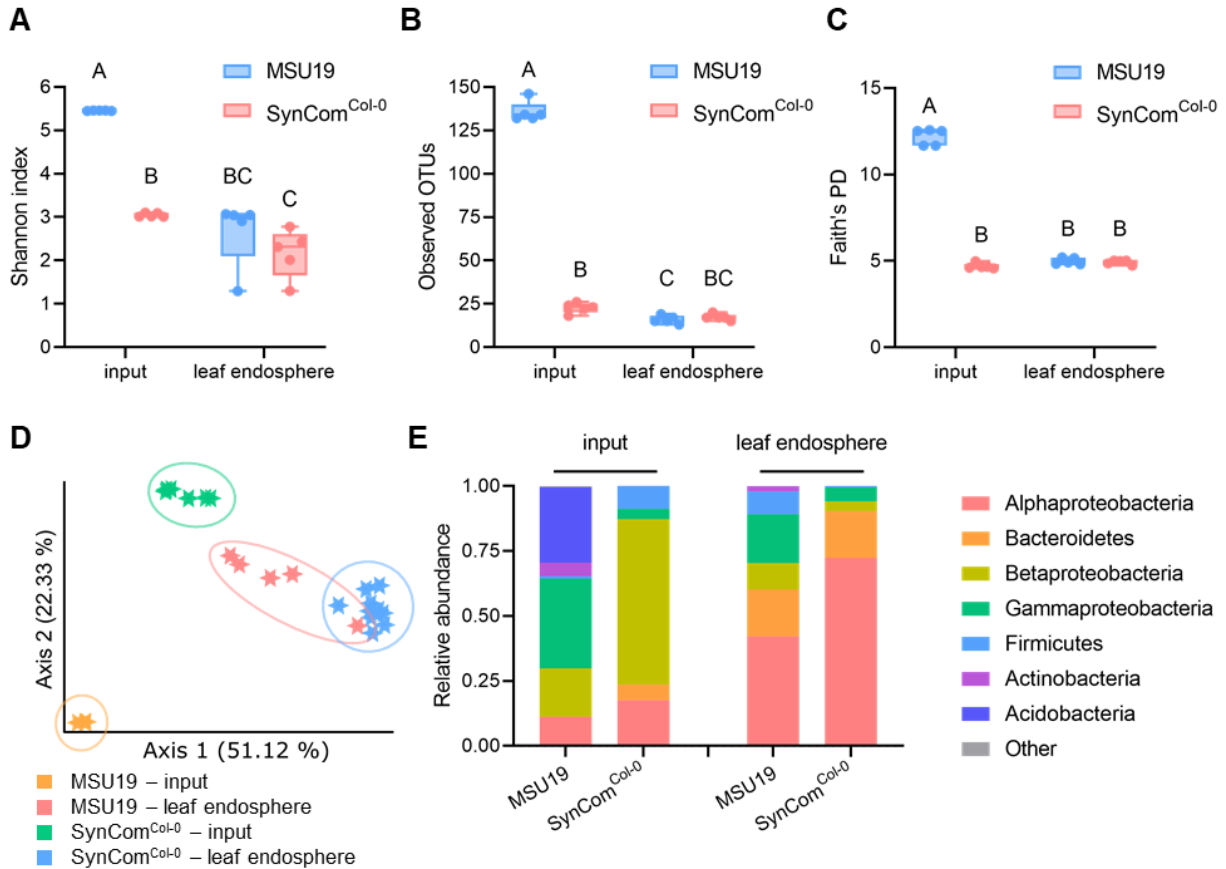


Figure 2.7: Endophytic leaf bacterial colonization in GnotoPots.

(A-C) Alpha diversity of the initial microbiota input and the resulting leaf endosphere of plants inoculated with a soil-derived microbiota (MSU19) or SynCom^{Col-0}. (A) Shannon Diversity Index, (B) richness, and (C) Faith's Phylogenetic Diversity. Different letters represent a significant difference ($p < 0.05$, two-way ANOVA with Tukey's HSD post-hoc test). (D) PCA based on weighted UniFrac distances for leaf endosphere communities from plants inoculated with MSU19 or SynCom^{Col-0} or their respective inputs. Groups circled for emphasis. (E) Relative abundance profiles of the top 7 phyla of the initial microbiota input and the resulting leaf endosphere of plants inoculated with a soil-derived microbiota or SynCom^{Col-0}. Proteobacteria phylum subdivided into classes.

cryogenically preserved SynCom^{Col-0} could colonize plants in the GnotoPot system similar to a freshly-prepared SynCom^{Col-0}. Cryoprotective agents and thaw temperatures can have a differential impact the functionality and colonization patterns of some mixed microbial communities after post-freezing resuscitation [35], therefore cryopreserved aliquots of pre-mixed SynCom^{Col-0} were prepared using two distinct cryoprotectants: 10% glycerol or 5% DMSO. Additionally, frozen aliquots of SynCom were thawed at two distinct temperatures: slowly (1 hr) at 4°C or rapidly (30 s) at 37°C. This resulted in four distinct SynCom preparations. Sterile *Arabidopsis* seeds were subsequently inoculated with a freshly prepared SynCom^{Col-0} (from combining 48 freshly grown bacteria) or one of the four cryopreserved SynComs and grown in GnotoPots. Four and a half weeks after sowing, no qualitative differences in plant growth could be discerned between plants inoculated with cryopreserved SynComs or fresh SynCom^{Col-0} (Supplementary Figure B2.6). 16S rRNA gene sequencing indicated microbial alpha diversity was not significantly different among any of the treatment groups, as judged by Shannon Diversity index (Figure 2.6 A). Further, principal coordinate analysis of weighted UniFrac distances did not reveal a significant effect of cryoprotection on community composition, regardless of the cryoprotectant type or thaw method used (Figure 2.6 B), indicating a cryogenically preserved bacterial SynCom can reproduce leaf endosphere-associated taxonomic distribution associated with freshly SynCom upon host colonization.

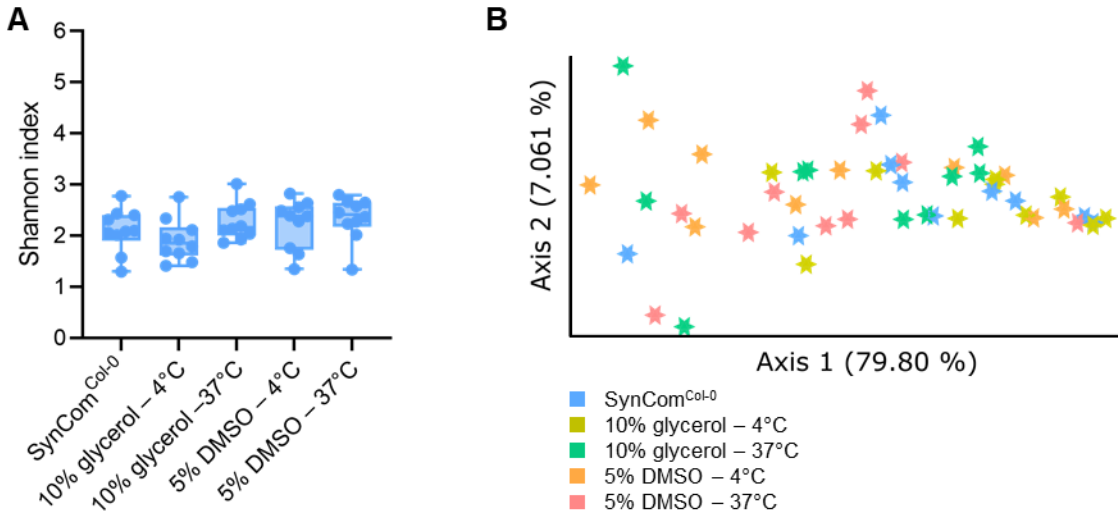


Figure 2.8: Endophytic leaf colonization by cryopreserved SynCom^{Col-0}. (A) Alpha diversity associated with the leaf endosphere of plants inoculated with various preparations of SynCom^{Col-0}. No significant difference ($p > 0.98$, two-way ANOVA). (B) PCA based on weighted UniFrac distances for the initial microbiota input and resulting leaf endosphere communities associated with plants inoculated with a soil-derived microbiota (MSU19) or SynCom^{Col-0} or their respective inputs.

2.4. Discussion

Gnotobiotic plant growth systems present a way for researchers to control variables associated with plant growth and plant-microbiome interactions in a reproducible manner. The FlowPot and GnotoPot plant growth systems are two such systems to maintain axenic plant growth in a peat-based substrate. Both systems implement a commercially available Microbox tissue culture container to sequester plant growth from surrounding environments and utilize similar peat-based potting soil substrates which provide a soil-like matrix and organic carbon that more closely approximates natural soil compared to systems which use agar or mineral-based substrates.

After extensive use of the FlowPot system I found that *Arabidopsis* growth beyond 4-5 weeks was occasionally associated with indications of stress. This stress presented in multiple ways including chlorosis or darker green leaf pigments which indicates the accumulation of anthocyanins. Both chlorosis and anthocyanin accumulation are associated with various forms of abiotic stress, including certain nutritional deficiencies and drought-induced osmotic stress. However, the transient and sporadic nature of the growth variation made empirical determination of the underlying causes elusive. At the time of these observations, FlowPots were typically prepared in bulk on a per week basis by a number of individuals. I speculate week-to-week inconsistency in physical FlowPot construction may have at least partially contributed to nonuniformity in FlowPots. Given their small volume and relatively involved procedure, slight variations in fill density or compaction could affect the amount of moisture or nutrients able to be contained within individual pots which, in turn, could have resulted

in the variation of plant growth consistent with what was observed. This likely could be partially mitigated through the use of larger syringes when making FlowPots. Larger 140 mL syringes are available however they are not as universally available as the 60 mL syringes used in the FlowPot protocol (Appendix A).

While the physical construction of individual pots is potential contributor to unevenness of individual FlowPots, it also makes the FlowPot system highly versatile by allowing a multitude of different user-defined substrates to be implemented. Plants grown under standard laboratory conditions differ considerably compared to those grown in the field and there is often a disconnect between results obtained in the lab versus results obtained in the field [36-38]. Minimizing differences between the laboratory and the field has been proposed as one way to make translation more amenable [38]. The FlowPot system attempts to mimic the physical attributes of soil by implementing a peat-based substrate. A peat substrate harbors a more diverse microbial community compared to commonly used laboratory substrates, like calcined clay [29]. This results in more diverse colonization of plant hosts [29] and highlights the impact growth substrates can have on host colonization within a gnotobiotic system. Whether or how substrate-induced differences in microbiota contribute to host phenotype in gnotobiotic systems remains an outstanding question and will be discussed in more detail in Chapter 3. Nonetheless, edaphic factors are an important driver in the structure and function of plant-associated microbial communities [39-41] and implementing a true field soil could prove useful in certain contexts. To highlight its versatility, we used the FlowPot system to grow axenic and holoxenic *Arabidopsis* in field soil (Figure 2.2). My experiments also showed that each soil would need to be

individually optimized for use in FlowPots as most soils perform poorly as substrates in containers and the impact of soil amendments would need to be resolved.

As noted in the Results section, the FlowPot system may not be optimal for gnotobiotic experiments that require plant growth for a long period of time. GnotoPots, on the other hand, were found to consistently grow *Arabidopsis* into reproductive stages of development. Compared to FlowPots, the extended duration of uniform growth was likely aided by the increased pot size and inclusion of a nutrient reservoir into the GnotoPot design which could passively replenish depleted nutrients. Additionally, the peat pellets which comprise the GnotoPot growth substrate are commercially manufactured which standardizes variation and minimizes inconsistencies that result during pot construction. Together, these features make GnotoPots more amenable for long-term studies during vegetative growth and even the reproductive stage of plant-microbiota interactions. This advantage does come at the expense of customizability (an advantage of the FlowPot system) as the substrate cannot be defined by the user.

Of the factors tested, the most important for robust growth in the GnotoPot system appeared to be pellet type/composition, humidity, and nutrients. I optimized nutrient content to 0.25x-0.5x LS and external humidity to ~40% RH (Figure 2.4). The pellet type warrants further discussion. In particular, pellets made with peat or coir as their sole component performed very poorly after autoclaving. This likely was the result of physical growth substrate properties as amending poor performing peat pellets with vermiculite yielded more robust plant growth. Vermiculite can increase water and nutrient retention and improve aeration and drainage of peat. Relative to peat, coir can increase aeration and drainage, however primarily coir substrates can suffer from water

and nutritional limitations. For example, substrates composed of greater than 50% coir suffer from high nitrogen immobilization [31]. During development of the GnotoPot system the manufacturer was in the process of transitioning Jiffy-7 pellets from a biologically inert polyethylene (PE) netting to a biodegradable polylactic acid (PLA) netting [42, 43]. However, netting type did not appear to adversely affect plant growth as both PE- and PLA-netted pellets could sustain robust plant growth.

The use of synthetic microbial communities to apply reductionist approaches can be used to disentangle plant-microbiota interactions and help gain mechanistic understanding on microbiome function [5]. In this context, the use gnotobiotic systems can limit the colonization of unwanted microorganisms by isolating samples within a common growth chamber and prevent cross-contamination between samples and contamination by environmental microorganisms. In GnotoPots, we found that plants inoculated with SynCom^{Col-0} had similar levels of Shannon diversity, richness, and phylogenetic diversity compared to plants inoculated with a soil-derived microbiota. Principle coordinate analysis of 16S profiles based on weighted UniFrac distances further revealed that soil-inoculated plants and SynCom^{Col-0}-inoculated plants were more similar to one another compared to their respective inputs, suggesting that the reduced complexity bacterial synthetic community SynCom^{Col-0} colonizes *Arabidopsis* grown in GnotoPots reminiscent of a holistic, soil-derived microbiota. Furthermore, I demonstrated that frozen mixtures of SynComs colonize similarly compared to a freshly prepared SynComs, which greatly facilitate gnotobiotic experiments.

In summary, FlowPot and GnotoPot systems described here provide new tools for the at-large research community to understand plant-microbiota interactions. My

findings presented in this chapter helped the development of both gnotobiotic plant growth systems and contributed to the creation of the published protocol presented below (Appendix A).

2.5. Methods

2.5.1. *Arabidopsis* growth conditions

FlowPots, GnotoPots, soil extracts, and sterile seeds were prepared as described in Appendix A. 0.5x LS nutrient solution concentration was used unless noted otherwise. For GnotoPots, 0.5x LS or the indicated LS nutrient solution concentrations indicated was used for both the initial rehydration and subsequent supplementation steps. The soil used for the preparation of soil extracts was collected from a research farm at Michigan State University (N42°43'1.5492", W84°27'45.7855") in October 2018 and again in November 2019 (MSU19). After harvesting, soil was sifted through a 3 mm test sieve to remove large debris, aliquoted into 50 g aliquots, and stored in Whirl-Pak bags (Nasco) at 4°C in the dark until use. Microboxes containing assembled FlowPots or GnotoPots were sown with sterile *Arabidopsis* and plants were grown in a Percival tissue chamber using the following conditions: 19-21°C (inside the box) with 12 h day/12 h night photoperiod cycle and provided with a daytime photon flux of ~90-100 $\mu\text{mol m}^{-2} \text{s}^{-1}$ (inside the box). Ambient chamber humidity was below 50% RH, unless otherwise noted.

2.5.2. Adaptation of FlowPots to use field soil

Soil-based FlowPots were prepared with procedure indicated in Appendix A with modifications described here. First, peat was replaced with MSU19 soil during substrate preparation. Here, equal volumes of MSU19 soil and medium horticultural grade vermiculite were hydrated to approximately 60% moisture, mixed, and subsequently autoclaved twice with 24-48 hours between cycles. Soil-based FlowPots were then

assembled using the sterile soil/vermiculite mix. To accommodate modified flushing steps Glass wool (Sigma) was used for FlowPot construction instead of glass beads. Consistent with the procedure for peat-based FlowPots, soil-based FlowPots were autoclaved after construction, resulting in a total of three autoclave cycles. Flushing steps were also modified to accommodate the smaller particle size of soil in the soil-based FlowPots. Here, liquids were aseptically flushed through FlowPots in reverse by applying fluids to the top of the FlowPot and a vacuum fitted with a collection vessel to the irrigation port. All irrigation and inoculation solutions (water, nutrients, and soil extracts) were flushed through individual FlowPots with house-supplied vacuum pressure. The mesh retainer was removed prior to flushing to aid this process. Assembled, flushed FlowPots were transferred to sterile Microboxes (SacO₂) and sown with sterile *Arabidopsis* seed for plant growth.

2.5.3. Preparation of SynCom^{Col-0} inoculum

SynCom^{Col-0} was prepared as previously described [1]. Briefly, lawns of 48 individual strains were streaked from glycerol stocks onto R2A agar and grown at 21 °C for three days. After three days growth, bacterial lawns were scraped from agar plates with a sterile L-shaped cell spreader (Fisher) and taken up into 2 mL 10 mM MgCl₂. The resulting bacterial suspensions were normalized by optical density to OD₆₀₀ = 1.0 and equal volumes of each suspension were combined to make a concentrated mixed bacterial community. After mixing, the suspension was adjusted down to OD₆₀₀ = 0.04 (~2×10⁷ cfu/mL) and 2 mL was used to inoculate each GnotoPot. For cryoprotection experiments, the concentrated SynCom^{Col-0} was diluted to OD₆₀₀ = 0.4 and

cryoprotectant agents (CPAs) were added to a final concentration of 10% glycerol or 5% DMSO. Aliquots were then snap frozen in liquid N₂ and stored at -80°C. Immediately prior to inoculation into GnotoPots, frozen aliquots of concentrated SynCom^{Col-0} with CPAs were thawed either slowly on ice at approximately 4°C, or quickly in a 37°C water bath until thaw (approximately 1 min). Upon thawing, concentrated SynCom^{Col-0} with CPAs were diluted 10-fold with 10 mM MgCl₂ to a final OD₆₀₀ = 0.04 (~2×10⁷ cfu/mL). Individual GnotoPots were then inoculated with 2 mL of the resulting bacterial suspension.

2.5.4. Sample collection and DNA extraction for 16S rRNA gene profiling

The 16S rRNA gene profiling experiments presented here were performed concurrently. GnotoPots were inoculated with a soil slurry (50 g MSU19 soil/ 1 L water), a freshly prepared SynCom^{Col-0}, or one of the four preparations of cryopreserved SynCom^{Col-0} as described above. For each input microbiota, two Microboxes containing four GnotoPots with two seeds each were inoculated. At the time of inoculation three ~0.5 g aliquots of the MSU19 soil used to prepare the soil slurry and six 250 µL aliquots of the fresh SynCom^{Col-0} suspension were collected, snap frozen in liquid N₂, and stored at -80°C until further processing. After four and a half weeks of growth, five representative plants were harvested from each Microbox, surface sterilized in 5% bleach for 1 min, and rinsed twice in sterile-filtered water. This yielded a total of 10 individual plants for SynCom^{Col-0}-inoculated samples and 5 individual plants for MSU19-inoculated samples. Individual plants were then placed in 2 mL impact-resistant tubes, snap frozen in liquid N₂ and stored at -80°C until further processing.

DNeasy PowerSoil kits (Qiagen) were used for total DNA extraction. First, frozen samples were ground to fine powders with a TissueLyser (Qiagen) using two 45 s cycles at 28 Hz. PowerBead Pro tube solution from the extraction kit was then used to take up frozen sample powders and transfer them to PowerBead Pro tubes. Remaining kit steps were performed according to the manufacturer's instructions. DNA was eluted in water and stored at -20°C until further processing.

2.5.5. 16S rRNA gene fragment amplification and MiSeq library preparation

16S rRNA gene amplification and MiSeq library preparation was performed as previously described [1]. In brief, the V5-V7 hypervariable region of bacterial 16S rRNA gene was amplified using AccuPrime high-fidelity Taq DNA polymerase and the following barcoded 799F/1193R [17] primers (underlined sequences indicate Fluidigm CS1/CS2 adapters):

799F: 5'-ACACTGACGACATGGTTCTACAAACMGGATTAGATACCCCKG-3'

1193R: 5'-TACGGTAGCAGAGACTTGGTCTACGTCATCCCCACCTTCC-3'

PCR was performed in duplicate in 40 µL reaction volumes containing 0.24 µL AccuPrime high-fidelity Taq DNA polymerase, 1.6 µL DMSO, 4 µL Buffer II, 0.8 µL of each primer (10 µM), and 3.2 µL template DNA with the following parameters: 94°C for 60 s, followed by 35 cycles of denaturation at 94°C for 20 s, annealing at 53°C for 30s, and extension at 68°C for 30 s, with a final extension at 68°C for 2 min. PCR products were separated on 1% agarose and the band corresponding to amplified bacterial 16s rRNA gene was excised. Upon excision Zymoclean Gel DNA Recovery Kit (Zymo Research) was used to purify and concentrate DNA according to the manufacturer's

instructions. DNA was normalized to 1 ng/uL using the Quant-iT PicoGreen dsDNA Assay Kit (Life Technologies) for quantification before submission to the Research Technology Service Facility (RTSF) at Michigan State University (MSU) for library preparation and sequencing.

RTSF Genomics Core at MSU performed secondary PCR using dual-indexed Illumina-compatible primers which targeted the Fluidigm CS1/CS2 oligomer sequences of primary PCR products. Final PCR products were normalized in bulk using SequalPrep DNA Normalization plates (Invitrogen) and pooled. Pools were cleaned up and quantified using Qubit dsDNA HS kit (Life Technologies), TapeStation HS DNA1000 (Agilent), and Colibri Library Quantification qPCR (Invitrogen) assays. The pool was then loaded onto a single MiSeq v2 flow cell and sequencing was performed in a 2x250 format using a MiSeq v2 500 cycle reagent kit. Sequencing and indexing primers corresponding to the Fluidigm CS1/CS2 oligomer were added to the applicable wells of the reagent cartridge. Illumina Real Time Analysis (RTA) v1.18.54 was used for base calling and output RTA was demultiplexed and converted to FastQ format with Illumina Bcl2fastq v2.20.0.

2.5.6. Processing of 16S rRNA gene fragment amplicons

Raw Illumina fastq reads were quality filtered and processed using QIIME 2 Core 2018.11 distribution [44]. DADA2 [45] was used to trim, quality filter and denoise samples, remove chimeras, and resolve amplicon sequence variants (ASVs). ASVs were assigned taxonomy with a naïve Bayes classifier [46] pre-trained on version 13_8 of the Greengenes 16S rRNA gene reference database [47]. Unassigned sequences

and sequences classified as plant chloroplast or mitochondria were subsequently removed. Diversity calculations were performed using QIIME 2 using data rarefied to the highest number of reads which retained all samples. Alpha diversity calculations exported to GraphPad Prism v9.2.0 for visualization and statistical testing. For comparisons between MSU19 and SynCom^{Col-0}, data was rarefied to 1705 reads and for comparisons between SynCom^{Col-0} and cryopreserved variants of SynCom^{Col-0}, data was rarefied to 3170 reads. The sequence analysis workflow and QIIME 2 output files are available on GitHub (<https://github.com/BradCP/GnotoPot-community-analysis>). Raw source Illumina fastq files from this project are available upon request.

APPENDICES

APPENDIX A:

Protocol for the FlowPot and GnotoPot gnotobiotic plant growth systems

A2.1 Overview

For the FlowPot system (Procedure 1), each FlowPot (the gnotobiotic pot holding the substrate) is assembled using inexpensive and routinely available labware. In short, each FlowPot is prepared by truncating a 50 mL syringe (Steps 1-4), followed by the preparation of autoclaved soil or peat substrates (Steps 5-7), which is then added to the FlowPot, covered with a mesh retainer, and secured with a cable tie (Steps 8-10) (Supplemental Figure 2.1 A). The FlowPot system features an inoculation port on each vessel (Fig. 1a) that enables substrate rinsing to remove soluble byproducts of soil sterilization, provides drainage, and accommodates homogenous inoculation with microbiota and/or nutrients. Assembled FlowPots are then autoclaved once more and aseptically irrigated from the inoculation port with nutrients and any desired input microbial suspensions (Steps 11-14) (Supplemental Figure B2.1 B). Subsequently each FlowPot is placed into a sterile Microbox supported by a stand, and microbiota-free *Arabidopsis* seeds are sown on each FlowPot (Steps 15-16). The tissue culture boxes containing FlowPots are placed in a plant growth chamber with desired lighting and temperature conditions to support plant growth (Steps 17-18).

For the GnotoPot system (Procedure 2), the assembly of each unit begins with an initial hydration step of a compressed Jiffy-7® pellet. Here, a dry pellet is placed inside a small polypropylene pot and hydrated with a nutrient solution (Steps 1-2) (Supplemental Figure B2.2 A). Next, GnotoPots are transferred to the Microboxes and secured in place with empty plastic pots (Steps 3-7) (Supplemental Figure B2.2 B). Then, Microboxes containing GnotoPots are placed inside an autoclavable plastic bag, loosely sealed, and autoclaved (Steps 8-12). At the final preparation steps

(Supplemental Figure B2.2 C,D), *Arabidopsis* seeds are sown aseptically on GnotoPots, desired input microbiota communities are inoculated and the Microboxes are placed inside a tissue culture growth chamber with desired lighting and temperature conditions to support plant growth (Steps 22-26).

A2.2. Preparation of the soil extract source microbiota

This section provides information on how to collect and store soil for extraction of complex microbial communities. Soil is collected when there have not recently been extreme conditions, such as rain 3–5 days prior to sampling. Procurement of source microbiota can be performed in advance of the experiment and modified depending on the input community characteristics and experimental parameters of your choosing.

Equipment

- Whirl-Pak sterile sampling bags (Nasco, cat. no. B01065WA)
- Soil/sediment sifter (VWR, cat. no. 470014-728)
- Soil/sediment sifter (VWR, cat. no. 470014-728)

Collection method

Collect and store soil using the following steps:

1. Remove topsoil (typically 10–15 cm), including any vegetation. At the sites of our soil collection, this helps to avoid variability of surface debris and organic matter. However, less topsoil can be removed if soil surfaces are less variable in debris and organic matter. Then collect >5 cm deep soil and transfer to the lab.
2. Let the soil sit for 1 week at RT with ~50% relative humidity.
3. Next, sift soil through a soil sifter to remove large debris.

4. Prepare 100 g aliquots of soil and store at 4 °C in Whirl-Pak bags up to 1 year.

A2.3. Seed preparation, sterilization and stratification • TIMING 3 days

Arabidopsis seed sterilization can be performed via a variety of methods [48]. Here we describe vapor phase sterilization as it allows high-throughput processing of multiple aliquots of different genotypes at once and can be performed in advance. To promote uniform germination and plant growth, seeds are first selected based on size using a sieve. Additionally, proper seed storage and cold stratification help ensure higher germination rates. As FlowPot and GnotoPot systems can be used to study plant interactions with vertically transmitted endophytes, specialized steps, such as antibiotic or fungicide treatment before seed harvest in the prior generation insect-free growth chambers, will need to be developed.

Reagents

- *Arabidopsis* seeds (from ABRC, <https://abrc.osu.edu/>)
- Bleach (common household bleach, 5.25% sodium hypochlorite (wt/vol); e.g., Clorox)

! CAUTION: Bleach is corrosive. Use protective equipment.

! CRITICAL: Use freshly opened bleach.

- Hydrochloric acid (HCl, 37% (vol/vol); Sigma-Adrich, cat. no. 320331)

! CAUTION: HCl is corrosive. Use protective equipment.

Equipment

- Metal Sieve, US Standard 60 mesh (250 µm) (Fisher Scientific, cat. no. AA41200ON)

- Metal Sieve, US Standard 50 mesh (300 μm) (Fisher Scientific, cat. no. AA39985ON)
- Microcentrifuge tubes (USA Scientific, cat. no. 1415-2500)
- Polypropylene storage box (USA Scientific, cat. no. 2310-5848)
- Erlenmeyer flask (Corning, cat. no. 4980-500)
- Glass pipette and bulb (Fisher Scientific, cat. nos. 13-678-20 and 03-448-25, respectively)
- Glass desiccator (Corning, cat. no. 3081-250)
- Vacuum grease (Dow Corning, cat. no. 1597418)
- Chemical fume hood
- Biosafety cabinet or laminar flow hood (e.g., Logic+ Class II A2 Biological Safety Cabinet, Labconco, cat. no. 302611100; or Console Horizontal Airflow Workstation, Nuaire, cat. no. NU-301-530)
- Auto-desiccator cabinet (Bel-Art, cat. no. F42074-0116)

Seed preparation • **TIMING** 5 min

1. Pass dried *Arabidopsis* seeds harvested from healthy plants through two metal sieves with sieve mesh size 50 placed on top of sieve mesh size 60. Only collect the seeds in between two sieves. This will result in selection of seeds with sizes between 250 μm and 300 μm and reduce variation in germination rates.

PAUSE POINT: Seeds can be stored under dry, cool conditions for at least one year prior to further processing.

Seed sterilization • TIMING 6-8 hr

2. Aliquot approximately 50-250 seeds into a labeled 1.5 mL microcentrifuge tube.

Do not close the lid. Repeat for the desired number of aliquots.

CRITICAL STEP Chlorine gas generated in subsequent steps will react with some commonly used inks and may interfere with sample labeling. Use chemical-resistant inks.

3. Place open microcentrifuge tubes in a plastic microcentrifuge storage box, but do not close the box lid. Place the open microcentrifuge storage box with open microcentrifuge tubes containing seeds and an Erlenmeyer flask containing 100 mL undiluted bleach in a glass desiccator located in a chemical fume hood.
4. Carefully add 1-2 mL of concentrated HCl using a glass pipette to the Erlenmeyer flask containing bleach and immediately place the lid on the glass desiccator, ensuring a proper seal. Sterilize seeds for 6-8 hrs [48].

! CAUTION: Chlorine gas is toxic to humans! Use proper safety precautions.

! CRITICAL STEP: Vacuum grease can help ensure a sufficient seal is made.

5. After sterilization, allow seed aliquots to off-gas residual chlorine gas before closing the lids on individual seed aliquots. Close the storage box lid and store the entire box containing seed aliquots at 4°C. For long-term cold storage, store seeds in the dark under low humidity. We found seeds stored in an auto-desiccator cabinet were sterile and viable after more than one year in storage.

! CAUTION: Chlorine gas is caustic! Use proper safety precautions.

! CRITICAL STEP: Residual chlorine gas can be removed by cracking the lid to the desiccator for several minutes and moving the seeds to a laminar flow hood. It is important to maintain sterile technique upon sterilization.

! CRITICAL STEP: Checking for effective decontamination of an aliquot of seeds is crucial for maintaining axenic growth conditions (see Section A2.5).

! CRITICAL STEP: Storing seeds in the dark at low humidity is important to maintain high germination rates.

PAUSE POINT: Aliquots of seed can be sterilized in bulk and stored under appropriate conditions for future use.

Seed stratification • TIMING 2 days

6. Prior to an experiment, allow seeds to imbibe during a 48-hour stratification period in sterile Milli-Q water at 4°C in the dark prior to sowing. This helps promote uniform germination.

? TROUBLESHOOTING

A2.4. Plant growth conditions

A plant tissue culture growth chamber (Percival) was used for growing plants in gnotobiotic setups. We routinely use the following conditions for *Arabidopsis* plant growth: 22 °C with 12 h day/12 h night photoperiod cycle at ~90-100 $\mu\text{E m}^{-2} \text{s}^{-1}$. The light intensity and temperatures on the tissue culture chamber were adjusted based on measurement done using probes placed inside the Microboxes to attain the expected growth parameters. We recommend rotating gnotobiotic boxes in a growth chamber

every 2-3 days to ensure uniform plant growth. Since Microboxes are engineered to have a high water retention capacity inside the containers make sure to adapt Microbox-grown plants to desired relative humidity at the time of performing experiments, if relevant.

A2.5. Assessment of the sterility of gnotobiotic systems

This section presents culture-based methods for testing the sterility of the gnotobiotic systems. To ensure axenic conditions are maintained throughout plant growth, it is important to check the sterility both before the experiment and after plant growth. For plants grown in the FlowPot system we test 7-10 days old seedlings at the time of thinning (Procedure1, Step 20) and again at the time of using plants for planned experiments. For plants grown in the GnotoPot system we check sterility of axenic plants and peat substrate at the time of using plants for planned experiments.

Reagents

- R2A agar medium (DIFCO, cat. no. 218263)
- Potato dextrose agar (PDA) (BD Difco, BD 213400)
- Standard sterile Petri plates, 100 x 15 mm (VWR, cat. no. 25384-302)
- Sterile tweezers or disposable inoculation loops (Fisher Scientific, cat no. 16-100-110 or 08-757-133, respectively)

Reagent setup

R2A

- Dissolve 18.2 g of powder in 1 L of water. Mix thoroughly. Autoclave at 121°C for 20 minutes on liquid cycle. Cool the medium to ~65°C and pour it into petri

dishes in a sterile hood. Once solidified, the plates can be stored at 4°C for at least three months. R2A media from Difco contains: yeast extract (0.5 g/L), proteose peptone No.3 (0.5 g/L), casamino acids (0.5 g/L), dextrose (0.5 g/L), soluble starch (0.5 g/L), sodium pyruvate (0.3 g/L), dipotassium phosphate (0.3 g/L), magnesium sulfate (0.05 g/L), agar (15 g/L).

PDA

- Dissolve 39 g of powder in 1 L of water. Mix thoroughly. Autoclave at 121°C for 30 min on liquid cycle. Cool the medium to ~65°C and pour it into petri dishes in a sterile hood. Once solidified, the plates can be stored at 4°C for at least three months. PDA from Difco contains: potato starch (4 g/L), dextrose (20 g/L), agar (15 g/L).

Testing for culturable microbial contamination of seeds • TIMING 2-7 days

1. Check for seed-borne contaminants and germination efficiency by incubating an aliquot of sterilized seeds on R2A agar at 22°C for at least one week.

? TROUBLESHOOTING

Testing for culturable microbial contamination of plants and substrate • TIMING 2-7 days

2. To test for bacterial contamination after plant growth, transfer plant material or small amounts of peat substrate to R2A agar plates. Spread peat material evenly. Incubate for at least one week at 22°C looking for any possible bacterial contamination.

3. Use the same approach and plate on PDA to test for fungal contamination.
Incubate for at least one week at 22°C looking for any possible fungal contamination.

? TROUBLESHOOTING

A2.6. Procedure 1: The FlowPot system

In this procedure, a FlowPot is described as an individual growth vessel that contains peat substrate, and the final assembled setup consists of four assembled FlowPots within a Microbox. FlowPots are reusable. Steps 1-4 of the procedure only need to be performed for initial construction.

Reagents

- *Arabidopsis* seeds (from ABRC, <https://abrc.osu.edu/>). See Section A2.3 for seed preparation, sterilization, and stratification and Section A2.4 for plant growth conditions.
- Sample containing input microbiota (e.g., from soil, see Section A2.2)
- Sterile Milli-Q water (reverse osmosis filtered, or an equivalent quality water)
- Multi-Terge™ detergent (EMD Millipore, cat. no. 65068); diluted to 2% (v/v)

! CAUTION: Multi-Terge detergent may be corrosive to metals and cause skin irritation. Use personal protective equipment as described by the manufacturer.

- Spor-Klenz™ disinfectant (Steris, USA, cat. no. 652026); diluted to 3% (v/v)

! CAUTION: Spor-Klenz is a strong oxidizer and corrosive. Use personal protective equipment as described by the manufacturer.

- Linsmaier & Skoog (LS) medium buffered with 2-(N-morpholino) ethanesulfonic acid (MES) to pH 5.7 (Caisson Labs, cat. no. LSP03)
- Ethanol, 100% or 95% (v/v) (Fisher Scientific, cat. no. 04-355-451)

! CAUTION: Avoid ignition sources and ensure proper ventilation when working with fire and flammable solvents such as ethanol.

Equipment

- Luer lock PP syringes, 50 mL (Jensen Global, cat. no. JG50CC-LL)
- Female Luer x female Luer adapter, nylon (autoclaved prior to use; Cole-Parmer, cat. no. EW-45502-22)
- Mesh fiberglass “Phiferglass”, 18 x 14 standard charcoal mesh (Phifer Incorporated, cat. no. 3003906)
- Soda-glass beads, 3 mm (Sigma-Aldrich, cat. no. Z265926)
- Microbox container (SacO2, cat. no., TP1600+TPD1200; #40 green filter, autoclavable)
- Filament tape model 893, 18 mm (Scotch Company)
- Redi-Earth plug and seedling mix (Sun Gro Horticulture, Canada). Contains fine Canadian sphagnum peat moss, vermiculite, dolomitic limestone, and a wetting agent

! CRITICAL: This can be substituted with alternative substrates, but plant performance may vary.

- Medium vermiculite, horticultural grade
- Polypropylene trays (United Scientific Supplies, cat. no. 81701)
- Sterilization wrap (Medline, cat. no. GEM1124S)

- Cable ties, 22 mm (TENAX Corporation, Baltimore, USA, cat. no. 120094)
- Sun bags (Sigma-Aldrich, cat. no. B7026)
- Cell strainer, 70 µm (Celltreat Scientific, cat. no. 229483)
- Drill bit, 8.8 mm (e.g., Chicago-Latrobe, cat no. 47329)
- Blocks of polypropylene, 12 cm x 8 cm x 1 cm (United States Plastic Corp, cat. no. 42605); alternatively, use Rainin RT-L1000 or similar tip box inserts

General equipment

- Biosafety cabinet or laminar flow hood (e.g., Logic+ Class II A2 Biological Safety Cabinet, Labconco, cat. no. 302611100; or Console Horizontal Airflow Workstation, Nuair, cat. no. NU-301-530)
- Test tube clamp or clamp modified hemostat (e.g., Stoddard Clamp, United Scientific Supplies, cat. no. TTCL03)
- Pipet and 1 mL filter tips (e.g., classic PR-1000 pipette and 1 mL RT-LTS filter tips, Rainin, cat. nos. 17008653 and 30389214)
- Funnel, 150 mm (Fisher Scientific, cat. no. 10-500-3)
- Glass Erlenmeyer flasks, 2 L (Corning, cat. no. 4980-2L)
- Sterile glass media bottles with screw cap, 2 L (Corning, cat. no. 1395-2L)
- Sterile graduated cylinders, 500 mL (Thermo Scientific, cat. no. 36620500)
- Bunsen burner (e.g., Humboldt Manufacturing Company, cat. no. H5870)
- Test tube racks (Thermo Scientific, cat. no. 59700020)
- Miter saw (e.g., Ryobi, cat. no. DC970K-2)
- Drill (e.g., 18-Volt Compact Drill/Driver, Dewalt, cat. no. DC970K-2)
- Growth chamber with desired lighting (e.g., Percival cat. no. CU36L5)

Reagent Setup

Multi-Terge detergent

- Dilute Multi-Terge concentrate to 2% (v/v) in water. Diluted detergent can be stored at room temperature (22-25°C) for several weeks.

Spor-Klenz disinfectant

- Dilute Spor-Klenz concentrate to 3% (v/v) in water. Prepare fresh solution daily.

LS nutrient solution

- Prepare LS solutions by dissolving the LS powder in water at 4.73 g/L for a 1x solution. Autoclave the solution for 45 min. After autoclaving, cool down the media bottles to room temperature (22-25°C) then tighten the lid. Prepared LS nutrient solution can be stored at room temperature for at least three months. A 1x concentrate of buffered LS from Caisson Labs contains: NH_4NO_3 (1650 mg/L), H_3BO_3 (6.2 mg/L), CaCl_2 (332.2 mg/L), $\text{CoCl}_2 \cdot 6\text{H}_2\text{O}$ (0.025 mg/L), $\text{CuSO}_4 \cdot 5\text{H}_2\text{O}$ (0.025 mg/L), EDTA disodium dihydrate (37.26 mg/L), MES (200 mg/L), MgSO_4 (180.7 mg/L), $\text{MnSO}_4 \cdot \text{H}_2\text{O}$ (16.9 mg/L), $\text{Na}_2\text{MoO}_4 \cdot 2\text{H}_2\text{O}$ (0.25 mg/L), Myo-Inositol (100 mg/L), KHCO_3 (98 mg/L), KI (0.83 mg/L), KNO_3 (1900 mg/L), KH_2PO_4 (170 mg/L), Thiamine hydrochloride (0.4 mg/L), $\text{ZnSO}_4 \cdot 7\text{H}_2\text{O}$ (8.6 mg/L).

Construction of FlowPots • TIMING ~1.5 hr

1. For each individual FlowPot, remove the piston from a 50 mL polypropylene (PP) Luer taper syringe. Using a miter saw with a fine-tooth blade, cut the syringe at the “20 mL” mark, retaining only the portion with the Luer connector. Mount the blade on the miter saw backwards for a smoother cut, and sand if needed.

Remove any residual shards with a vacuum and a moist cloth. Soak the syringe tops for 20 minutes in 2% (v/v) Multi-Terge ionic detergent, and subsequently rinse the syringe top in Milli-Q water to remove all traces of the detergent.

Autoclave prior to FlowPot construction.

! CRITICAL STEP: Avoid syringes that have silicon oil or other lubricants within the barrel or wash thoroughly prior to initial use.

! CAUTION: Use proper eye protection and keep hands out of the path of the blade when cutting plastic.

2. Cut 5 x 5 cm squares of mesh fiberglass. Autoclave prior to FlowPot construction.
3. Rinse 3 mm soda-glass beads 6 times with Milli-Q water. Dry and autoclave prior to FlowPot construction.
4. To construct a FlowPot stand, drill four holes in a 12 x 8 x 1 cm block of autoclave-compatible plastic (polypropylene or polycarbonate; e.g. disposable inserts from Rainin RT-L1000 or other pipette tip boxes) using an 8.8 mm drill bit. Orient the holes so they are evenly distributed with adequate spacing from stand edge so that the FlowPots do not exceed the stand boundaries.

! CAUTION: Use proper eye protection and keep hands out of the path of blades and drill bits when cutting plastic and drilling inserts.

Sterilization of the substrate • **TIMING** ~3 days

5. Blend a 1:1 (vol:vol) ratio of peat potting mix and medium vermiculite (substrate). Moisten with Milli-Q water to achieve moisture content of approximately 60% moisture content. Evenly distribute the substrate on clean polypropylene

laboratory trays at a depth of approximately 2 cm. Cover the surface of each tray with sterilization wrap in such a way that liquid will not collect on top during autoclaving and flow onto the substrate. Autoclave for 30 minutes on liquid cycle (121°C, 18 PSI, slow exhaust with forced liquid cooling) and bring to room temperature (22-25°C) immediately after autoclaving.

! CRITICAL STEP: Do not let materials sit in the autoclave after cycling because this may cause the substrate to dry out, resulting in increased hydrophobicity and suboptimal plant growth.

6. Homogenize substrate in a sterile container and subsequently distribute on polypropylene laboratory trays. Let sit covered with sterilization wrap at room temperature for 24-48 hours.

! CRITICAL STEP: The rest between autoclave cycles provides an opportunity for dormant microbial spores to germinate, which can then be killed during the second autoclave cycle.

7. Autoclave the substrate a second time (to kill any spores) for 30 minutes on liquid cycle (121°C, 18 PSI, slow exhaust with forced liquid cooling). Pre-clean the surface of a laminar flow hood using Spor-Klenz. Immediately after autoclaving, place the autoclaved trays of substrate in the pre-cleaned laminar flow hood and bring to room temperature. Once at room temperature, aseptically homogenize the substrate in the sterile laminar flow hood. Cover the trays of substrate with sterilization wrap. Leave covered at room temperature for 24-48 hours.

! CRITICAL STEP: Depending on the moisture content of your substrate, relative humidity, and the calibration of your autoclave, autoclave

parameters may need to be optimized to ensure sterility whilst preserving the integrity of the substrate.

! CAUTION: Spor-Klenz is caustic and an eye/skin irritant. Use personal protective equipment as described by the manufacturer.

Assembly of FlowPots • TIMING ~2 hr

8. Aseptically place 10 sterile glass beads (from Step 3) into each of autoclaved syringe tops (from Step 1). To stabilize FlowPots during assembly, use a sterile test tube rack (from Step 4). Gently fill each syringe top with the twice-autoclaved substrate mixture (from Step 7) until slightly heaping (~0.5 cm). Cover barrel end of the syringe top with the square mesh (from Step 2) and secure with a cable tie. Trim the excess edges of the square mesh.

! CRITICAL STEP: Do not overpack the substrate. Compaction can lead to suboptimal plant growth. Within an experiment, it is critical to maintain the same relative compaction for all FlowPots.

! CRITICAL STEP: We recommend using a cable tie gun: Thomas & Betts Ty-Rap Tool (<http://www.cableorganizer.com/thomas-betts/ty-rap-tool.html>).

9. Once the test tube rack is full, place the test tube rack full of assembled FlowPots in a Sun bag and loosely close the end with autoclave tape such that the risk of contamination is minimized when the bag is removed from the autoclave, yet steam may still permeate the bag during sterilization. Autoclave for 30 minutes on liquid cycle (121°C, 18 PSI, slow exhaust with forced liquid cooling).

Immediately after autoclaving, seal the opening of the Sun bag and move to a sterile hood.

! CRITICAL STEP: Alternative autoclave-safe bags can be used instead of Sun bags. FlowPots can also be autoclaved directly in Microboxes as well, as long as care is taken to ensure steam can penetrate assembled FlowPots during autoclaving.

PAUSE POINT: Sterile FlowPots inside sealed Sun bags can be stored for several days.

10. Center and fasten the drilled FlowPot stand to the inside bottom of a Microbox tissue culture vessel using filament tape. Autoclave constructed boxes and lids according to the manufacturer's instructions prior to use. Immediately after autoclaving, aseptically move to a sterile hood and place four assembled, autoclaved FlowPots into each Microbox.

! CRITICAL STEP: We routinely use 18 mm filament tape model 893 (Scotch, USA), but alternative tapes are suitable.

PAUSE POINT: Upon cooling, autoclaved Microboxes containing sterile, assembled FlowPots can be snapped closed and stored for several weeks.

? TROUBLESHOOTING

FlowPot irrigation and inoculation • TIMING ~2 hr

11. Add 950 mL of sterile distilled H₂O and 50 g of sieved soil (see Section A2.2) to a sterile 2-L Erlenmeyer flask. Agitate soil slurry on a rotary shaker for 20 minutes at room temperature at 100-200 rpm, and subsequently let settle for 5

minutes. Filter the supernatant through a 40 µm cell strainer into a sterile 2-L Nalgene media bottle.

! CRITICAL STEP: Allowing the slurry to settle increases reproducibility of colonization³¹ and reduces filter clogging.

12. Divide the soil slurry into two. Prepare the holoxenic inoculum by directly mixing the strained soil slurry with equal parts 1x LS media. To prepare a sterile mock inoculum, autoclave the remaining portion of the strained soil slurry for 45 minutes (121°C, 18 PSI, slow exhaust with forced liquid cooling), then mix with equal parts 1x LS media in a sterile laminar flow hood, bringing the final concentration of LS to 0.5x.

! CRITICAL STEP: The amount of inoculum needed for each condition will be determined by the number of FlowPots being prepared.

13. In a sterile hood, attach a sterile female Luer x female Luer adapter to a sterile 50 mL syringe. Using a flame-sterilized test tube clamp, grasp each FlowPot (from Step 10) and invert over a sterile funnel placed atop a waste flask. While inverted, use the sterile 50 mL syringe with attached adapter to aseptically infiltrate each FlowPot with 50 mL of sterile H₂O. Apply even pressure during the infiltration. After water infiltration, place the FlowPot back into its Microbox or on a sterile test tube rack. To reduce the risk of contamination, we recommend ethanol-flaming the test tube clamps between each FlowPot infiltration. The preparation of axenic FlowPots should be performed separately from those that are holoxenic and in a Biosafety cabinet or laminar flow hood.

! CAUTION: Avoid ignition sources and ensure proper ventilation when working with fire and flammable solvents such as ethanol.

! CRITICAL STEP: Occasionally, the glass beads become oriented in a way that the infiltration port is obscured. In this case, a sterile syringe needle may be inserted into the infiltration port to clear the blockage.

! CRITICAL STEP: An alternative to the test tube clamp holder is a modified hemostat with semicircular stainless steel bands to grip the FlowPots.

? TROUBLESHOOTING

14. Let water-infiltrated FlowPots sit for 30 minutes, then infiltrate the FlowPots with 50 mL of a desired input community mixture (from Step 12). Evenly mix the input community prior to infiltration. Because of the small size of seeds to be placed on the surface of a prepared pot (see step 15), colonization of germinating plants is not expected to need inoculation of the entire system. For some other applications where a total saturation of the systems becomes necessary (e.g., study of microbial activities in different locations within a pot), an investigation of the evenness of inoculation within a pot will need to be conducted.

15. Place irrigation port of inoculated FlowPots in the drilled holes of the FlowPots stand within the sterile Microboxes. We recommend 4 FlowPots per Microbox for plants to receive even light coverage.

Sowing seeds • TIMING ~30 min

16. Aseptically sow approximately 8 seeds per FlowPot using a pipette with filter tips.

! CRITICAL STEP: Prepare surface-sterilized seeds using information from Section A2.3.

Plant growth • TIMING Up to 4.5 weeks

17. Place Microboxes with planted FlowPots in the plant tissue culture growth chamber (see Section A2.4).

! CRITICAL STEP: After sowing, make sure the Microbox lids are completely sealed to maintain consistent humidity and sterility.

18. Aseptically thin boxes to 3 plants per pot using flamed forceps 7-10 days after germination.

! CRITICAL STEP: Check sterility of plants and substrate during plant growth by using information from Section A2.5.

! CRITICAL STEP: The syringe barrels can be reused after the experiment is completed to construct new FlowPots. In order to do so, discard contents, rinse thoroughly, and autoclave before storage or new FlowPot construction.

? TROUBLESHOOTING

A2.7. Procedure 2: The GnotoPot system

In this procedure, a hydrated Jiffy-7® peat pellet inside a plastic pot is referred to as a GnotoPot, and the final assembled setup consists of four GnotoPots within a Microbox. This procedure is for preparing 48 GnotoPots for within 12 Microboxes.

Reagents

- *Arabidopsis* seeds (from ABRC - Arabidopsis Biological Research Center; <https://abrc.osu.edu/>). See Section A2.3 for seed preparation, sterilization, and stratification and Section A2.4 for plant growth conditions.
- Sample containing input microbiota (e.g., from soil, see Section A2.2).
- Linsmaier & Skoog (LS) medium buffered with 2-(N-morpholino) ethanesulfonic acid (MES) to pH 5.7 (Caisson Labs, cat. no. LSP03).
- Sterile Milli-Q water (reverse osmosis filtered, or an equivalent quality water)
- Spor-Klenz™ disinfectant (Steris, USA, cat. no. 652026); dilute to 3% (v/v)

! CAUTION: Spor-Klenz is a strong oxidizer and corrosive. Use personal protective equipment as described by the manufacturer.

Equipment

- Biosafety cabinet or laminar flow hood (e.g., Logic+ Class II A2 Biological Safety Cabinet, Labconco, cat. no. 302611100; or Console Horizontal Airflow Workstation, Nuair, cat. no. NU-301-530)
- Standard Sterile Petri plates, 100 x 15 mm (VWR, cat. no. 25384-302)
- Jiffy-7® peat pellet, 36mm (Jiffy Group, cat. no. 32170236)
- Small (2 inch) polypropylene nursery pots (Amazon, cat no. B00LH1NMV0)
- Microbox container (SacO2, cat. no., TP1600+TPD1200; #40 green filter, autoclavable)
- Sun bags (Sigma-Aldrich, cat. no. B7026)
- 25 mL disposable serological pipets (Genesee Scientific, cat. no.12-106)
- Electronic pipette controller (Scilogex, cat. no. 740200029999)

- Cell strainer, 70 μm (Celltreat Scientific, cat. no. 229483)
- Sterilization wrap (Medline, cat. no. GEM1124S)
- Pipet with 1 mL and 20 μL filter tips (e.g., classic PR-1000 pipette with 1 mL and 20 μL RT-LTS filter tips, Rainin, cat. nos. 17008653, 30389214, and 30389296, respectively)
- Growth chamber with desired lighting (e.g., Percival cat. no. CU36L5)

Reagent Setup

LS nutrient solution

- Prepare LS solutions by dissolving the LS powder in water at 4.73 g/L or 2.37 g/L for 1x or 0.5x solution, respectively. Autoclave the solution for 45 min. After autoclaving, cool down the media bottles to room temperature (22-25°C) then tighten the lid. Prepared LS nutrient solution can be stored at room temperature for at least three months. A 1x concentrate of buffered LS from Caisson Labs contains: NH_4NO_3 (1650 mg/L), H_3BO_3 (6.2 mg/L), CaCl_2 (332.2 mg/L), $\text{CoCl}_2 \cdot 6\text{H}_2\text{O}$ (0.025 mg/L), $\text{CuSO}_4 \cdot 5\text{H}_2\text{O}$ (0.025 mg/L), EDTA disodium dihydrate (37.26 mg/L), MES (200 mg/L), MgSO_4 (180.7 mg/L), $\text{MnSO}_4 \cdot \text{H}_2\text{O}$ (16.9 mg/L), $\text{Na}_2\text{MoO}_4 \cdot 2\text{H}_2\text{O}$ (0.25 mg/L), Myo-Inositol (100 mg/L), KHCO_3 (98 mg/L), KI (0.83 mg/L), KNO_3 (1900 mg/L), KH_2PO_4 (170 mg/L), Thiamine hydrochloride (0.4 mg/L), $\text{ZnSO}_4 \cdot 7\text{H}_2\text{O}$ (8.6 mg/L).

Spor-Klenz solution

- Dilute Spor-Klenz concentrate to 3% (v/v) in water. Prepare fresh solution daily.

Preparation of the GnotoPot system (day 1) • TIMING ~45 min

1. Place 48 plastic nursery pots inside a large autoclave bin and add one dry compressed Jiffy-7® disc per pot.
2. Add 3 L of freshly prepared 0.5x LS nutrient solution to completely hydrate the pellets. Wait for 30-40 min. The pellets will expand to seven times the original height of the dry discs.

? TROUBLESHOOTING

3. While pots are being thoroughly soaked in nutrient solution add a small piece of labelling tape to 12 Microbox containers on the side with an opening crack for labelling each box at the time of the experiment.
4. Transfer two empty plastic pots to the center of each Microbox container.
5. Transfer four fully hydrated GnotoPots to each Microbox flanking the central empty pots (Fig. 2b).
6. Add 50 mL of the excess nutrient solution from hydration autoclave bin to each box.
7. Loosely place the Microbox container lid on top of each box. Do not snap close the lids.
8. Transfer two assembled Microboxes with loose lids into an autoclavable bag (Sun bag) and close the bag with a piece of labelling tape after folding the opening of the bag inside and then down.
9. Place assembled bags into an autoclave bin, cover with sterilization wrap and secure the wrap with binder clips.

! CRITICAL STEP: Make sure that the final assembled setup does not go through any strong mechanical disturbances since the pots will tip over and would not be usable after the autoclave cycles.

Sterilization of the GnotoPot system (day 1 and day 3) • TIMING ~3 days

10. Autoclave the assembled setup from Step 9 for 45 min using a liquid cycle at 121°C (18 PSI). After the autoclave cycle is done allow the chamber to cool down to 50°C. Then store the assembled setup at room temperature (22-25°C).
11. After two nights (36 h to 48 h) repeat the autoclave cycle as Step 10 and cool down at room temperature.

! CRITICAL STEP: The rest between autoclave cycles provides an opportunity for dormant microbial spores to germinate, which can then be killed during the second autoclave cycle.

12. After 3-4 h or sufficient cool down remove the sterilization wrap and snap close the lids while inside the Sun Bag. Store the Microboxes containing GnotoPots while inside Sun Bags at room temperature for at least 1 day before sowing seeds (Step 23).

PAUSE POINT: At this stage, Microboxes containing GnotoPots inside the Sun bags could be stored away for future use up to at least two months without any contamination issues.

! CRITICAL STEP: If the external surfaces of the Microbox lids have significant condensation after 1 day, allow more time for drying before use.

Preparation of the complex holoxenic community (day 4) • TIMING ~3 hr

13. Use the soil material prepared based on information in Section A2.2. To extract soil microbial communities, transfer 10 g of the soil aliquot to an autoclaved 1L Erlenmeyer flask and add 200 mL of autoclaved Milli-Q water.
14. Place the flask in a shaker for 20 min at 100-200 rpm at room temperature.
15. Store the flasks on the bench for 5 min allowing for separation of large soil particles from soil slurry.
16. Filter the soil slurry through a cell strainer and split into two 100 mL aliquots inside 1 L round media storage bottles.
17. Add 100 mL of autoclaved 1x LS to 100 mL of soil slurry for viable microbial community inoculation.
18. Autoclave the second half of soil slurry for 45 min for heat-killed community control. After cooling down to room temperature, place the heat-killed community inside a biosafety cabinet and add 100 mL of autoclaved 1x LS solution.

Transferring Microboxes containing GnotoPots to a biosafety cabinet (day 4) • TIMING ~30 min

19. To surface sterilize the interior environment of the biosafety cabinet use the germicidal UV lamp for 10 min. After lifting up the sash spray and wipe out all the working areas with freshly prepared Spor-Klenz solution.

! CAUTION: Spor-Klenz is caustic and an eye/skin irritant. Use personal protective equipment as described by the manufacturer.

! CRITICAL STEP: To ensure that the GnotoPots remain axenic during the handling steps, thorough aseptic practice is recommended.

20. Spray all the items to be used inside the biosafety cabinet with freshly prepared Spor-Klenz solution and store inside the biosafety cabinet.

21. Remove the Microboxes containing GnotoPots from Sun Bags and move the bags out of the biosafety cabinet.

! CRITICAL STEP: In cases that the external surfaces of the Microbox lids are still wet at this point, allow the boxes to dry out further inside the biosafety cabinet before handling.

Seed sowing on GnotoPots (day 4) • TIMING ~45 min

22. Open each Microbox and add 15 mL of 1x LS solution to individual GnotoPots by top irrigation of the pots to restore the Jiffy-7® pellet water content to full saturation. At this step label each Microbox with appropriate information for different plant genotypes and treatments.

23. Using a P20 pipette transfer 1 or 2 seeds (see Section A2.3) per pot to the edge of the central divot of the GnotoPots.

! CRITICAL STEP: To achieve a uniform plant growth in this procedure only one seed per pot is being used, therefore it is important to make sure that the seeds are of high quality with high germination rates following the steps described earlier (Section A2.3).

24. For axenic plants with no further treatments snap close boxes and move them out of the biosafety cabinet.

Inoculation with microbial communities (day 4) • TIMING ~15 min

25. To inoculate with live complex microbial communities or synthetic bacterial communities [1] gradually irrigate the top section of pots with 1 mL of the

microbial community solution (from Step 17) in a dropwise manner covering the entire top surface. For axenic plants treated with heat-killed community as a control uniformly add 1 mL of autoclaved and cooled down solution from Step 22 to the top section of GnotoPots. Then snap close the lids and move boxes out of the biosafety cabinet.

Plant growth • TIMING Up to 6.5 weeks

26. Move the GnotoPots to a plant tissue culture growth chamber (see Section A2.4).

! CRITICAL STEP: Check sterility of plants and substrate during plant growth by using information from Section A2.4.

? TROUBLESHOOTING

Sampling GnotoPots for contamination tests • Timing ~30 min for six Microboxes containing GnotoPots

27. Test for sterility before using germ-free plant material for experiments by sampling the peat pellet from each GnotoPot for microbial contamination. Spray germ-free boxes with Spor-Klenz and store under the biosafety cabinet for 10 min. Then open the boxes and, using a sterile loop, scoop a small amount of peat pellet from any part of the GnotoPots including the central hollow core and process samples using instructions from Section A2.3. Alternatively, test standing liquid inside Microboxes for contamination.

! CAUTION: Spor-Klenz is caustic and an eye/skin irritant. Use personal protective equipment as described by the manufacturer.

! CRITICAL STEP: Make sure that sampling is done without damaging the plant material or contaminating the system. Use this sample in the next step.

A2.8. Troubleshooting

The FlowPot system requires more steps to construct and implement than the GnotoPot system. It is important to minimize the variability associated with construction of FlowPots (Procedure 1 Steps 1-4), and several attempts may be required to optimize Procedure 1. Supplementary Table A2.1 summarizes several troubleshooting suggestions to help facilitate the optimization process. Supplementary Table A2.1 also contains several troubleshooting tips for the GnotoPot system as well.

A2.9. Timing

Any required soil or seed preparation should be performed prior to the start of the experiment.

Procedure 1 for preparation of 12 FlowPots

Pre-experiment preparation:

- Steps 1-4, construction of 12 reusable FlowPots (3 FlowPot boxes): ~1.5 h

Days 1-4:

- Steps 5-7, sterilization of the substrate: ~3 d
- Steps 8-10, assembly of FlowPots: ~2 h
- Steps 11-15, FlowPot irrigation and inoculation: ~2 h
- Steps 16, sowing seeds: ~0.5 h

Table A2.1: FlowPot and GnotoPot troubleshooting guide.

Procedure	Step	Problem	Possible reason	Solution	
Section A2.3	6	Poor root germination	Sterilization is too harsh.	Reduce exposure to chlorine gas or reduce the amount of HCl added to the Erlenmeyer flask. Verify germination rate on 0.5x LS plates without sucrose.	
			Seed storage suboptimal.	Ensure seeds are stored in the dark with low humidity. Verify germination rate on 0.5x LS plates without sucrose.	
Section A2.5	1	Seeds are contaminated	Seeds were not properly decontaminated.	Use fresh bleach during sterilization and ensure adequate sterilization time. Alternatively, increase the exposed surface area of seed aliquots by reducing the number of seeds in each tube. It may be necessary to empirically determine the duration of sterilization based on the volume of seeds in individual aliquots. Alternatively, surface sterilize seeds with Ethanol solution (50% Ethanol (v/v) +0.01% Triton X-100) for 5 min, followed by fresh bleach solution (10% commercial bleach+ 0.01% Triton X-100) for 5 min and wash 4 times with sterile Milli-Q water.	
			3	Plants or substrate are contaminated	Substrate was not properly sterilized. Tissue culture box not sealed. Water or media was contaminated during irrigation or inoculation.
	12	Microbox becomes deformed after autoclaving.	Lid was sealed on the Microbox while autoclaving.	Do not seal lids while autoclaving and follow manufacturer's instructions for Microbox sterilization.	
1 - FlowPot	15	The mesh retainer is dislodged from the FlowPot.	Liquid is unable to be passed through the FlowPot.	Glass beads or debris are obstructing the irrigation port. Insert a sterile needle into the bottom of the FlowPot to clear the irrigation port.	
			The mesh retainer is dislodged from the FlowPot.	Glass beads or debris are partially obstructing the irrigation port, resulting in increased backpressure. Substrate is packed too tightly into the FlowPot, resulting in increased back pressure.	Insert a sterile needle into the bottom of the FlowPot to clear the irrigation port. Assemble FlowPots using less substrate and do not pack.
				The nylon cable tie relaxed during autoclaving.	Do not fully tighten cable ties until after autoclaving or use a cable tie gun. Alternatively, change the material of the cable ties and avoid nylon.
	20	Plants appear chlorotic	Recalcitrant byproducts of sterilization may be deleterious to plant growth.	In our experience, using 50-60 °C water to flush the substrate improves performance if plants appear chlorotic.	
		Excess condensation builds up on the walls of the Microbox during plant growth.	Too much moisture is contained within the system.	The depth filter of the described Microbox is hydrophobic, so water is generally retained within a sealed box for quite some time. Decrease the amount of FlowPots per box to reduce excess moisture. We recommend no more than four FlowPots per Microbox.	
			Temperature fluctuations within the Microbox are increasing the rate of evaporation from FlowPots.	Maintain constant temperatures within the Microbox. Adjusting day/night temperatures can help account for the radiant energy absorbed by the Microboxes from the light source. Alternatively, we found that placing growth chamber temperature probes into sealed Microboxes with humidity levels corresponding to those of boxes growing plants helped mitigate temperature fluctuations. Additionally, insulating Microboxes from metal surfaces by placing them on matte black ceramic tiles may also help reduce thermal fluctuations and the build up of condensation.	
		Plants are water stressed.	Substrate is drying out.	Aseptically apply ~8 mL sterile water with a needle and syringe to the center of each FlowPot, avoiding damage to plant roots. We have found that watering plants after sowing is generally unnecessary and that the substrate sustains plant growth for at least 8 weeks without intervention. In our experience, the drying of substrate is usually due to temperature fluctuations increasing the rate of evaporation. The water is usually retained within the system on the bottom or sides of the Microbox as the filter is hydrophobic.	
	Plants are nutrient stressed.	Nutrients are depleted from the substrate.	Apply ~8 mL 0.5x LS media with a needle and syringe to the center of each FlowPot as needed. We have found that supplementing FlowPots with nutrients after sowing is generally unnecessary and that the substrate sustains plant growth for at least 8 weeks without intervention.		
	Plants fail to germinate.	Seeds sterilized for too long.	Decrease sterilization time. It may be necessary to empirically determine the duration of sterilization based on the volume of seeds in individual aliquots. We found that 6 h sterilization time had no adverse effect on germination rate. Alternatively, liquid bleach can be used to sterilize seeds.		
	2 - GnotoPot	26	Occasionally, the dry pellets do not fully expand.	Variance in manufacturing.	Visually inspect the dry pellets before placing inside the 2 inch pots to make sure that the mesh covering peat is not ruptured. Also after full expansion make sure that the central part of the Jiffy-7® is accessible for placing the seed at the time of seed sowing. If the central hole is not accessible use a pair of tweezers to manually open up the mesh.
Too much algal growth inside the box. The peat pellet looks dry after 6 weeks.			Excess of microbial community inoculum from soil. Excessive water loss	Use a smaller amount of the soil for preparing the soil tea. Also make sure that the soil inoculum is only added to the central area of peat pellet Although the GnotoPots perform very well in retaining the moisture, depending on the changes in the seasonal ambient humidity levels in different geographical locations some pots might have a drier peat pellet later in the growth phase. To hydrate these pots simply raise one side of the Microbox to about 10 degree angle to move the sitting solution to one side of the box and wait for 1-2 minutes. Perform this step for all the relevant controls as well.	

Procedure 2 for preparation of 48 GnotoPots

Days 1-4:

- Steps 1-12, preparation of the 48 GnotoPots (within 12 Microboxes) and two autoclave cycles: 3 d
- Steps 13-18, preparation of the complex holoxenic community: ~3 h

Step 19-25, soil slurry and heat killed community preparation, and seeds sowing in GnotoPot: ~4 hours

APPENDIX B:

Supplementary information

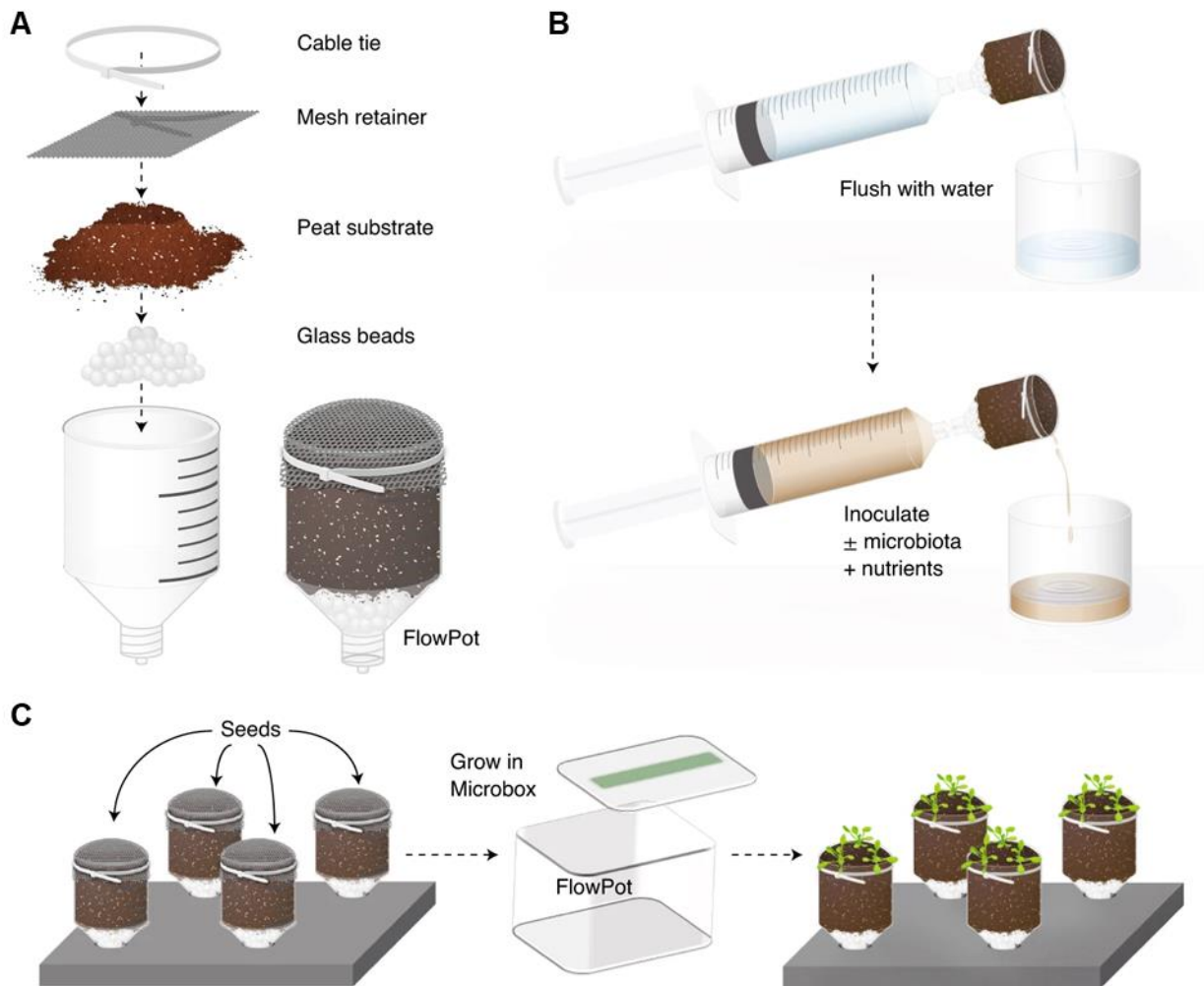


Figure B2.1: Basic setup of the FlowPot system.

(A) Each FlowPot is prepared by adding glass beads to the Luer end of a truncated syringe, followed by the addition of twice-autoclaved peat, covering the peat with a mesh retainer and then securing with a cable tie. (B) Assembled FlowPots are then autoclaved, aseptically irrigated with sterile Milli-Q water and inoculated with nutrients and any desired input microbiota. (C) FlowPots are then aseptically placed into Microboxes on stands and microbe-free *Arabidopsis* seeds are sown onto each FlowPot. The Microboxes containing FlowPots are placed in a growth chamber with the desired lighting and temperature conditions for plant growth. Contributed by James Kremer.

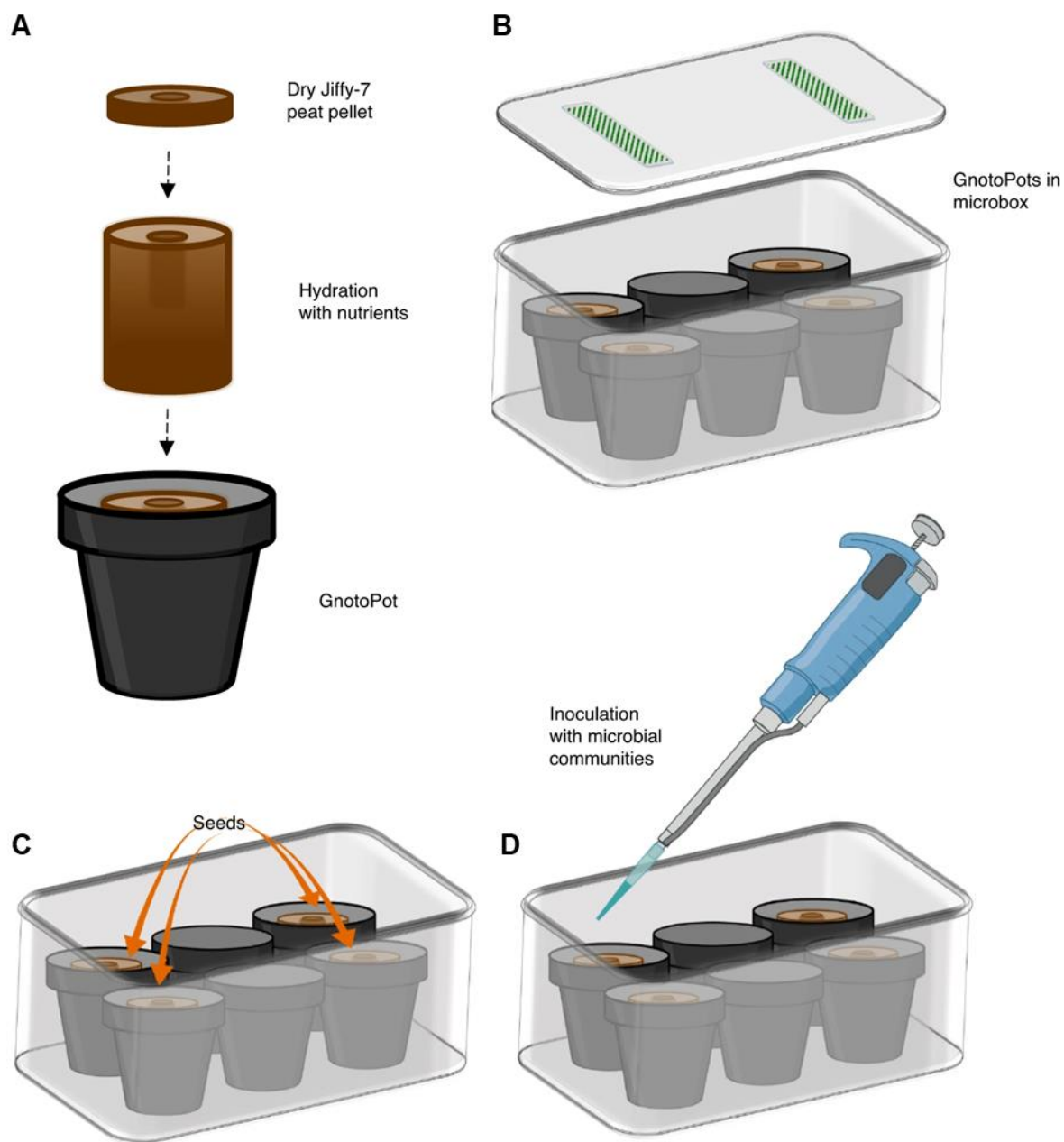


Figure B2.2: Basic setup of the GnotoPot system.

(A) Soaking the Jiffy-7 peat pellet with nutrient solution results in expansion of the dry discs and formation of the GnotoPot. (B) GnotoPots are placed inside the Microboxes flanking two empty pots. (C) After the autoclaving cycles the GnotoPots are rehydrated with nutrient solution and seeds are sown aseptically. (D) Lastly, desired input microbiota is inoculated using a 1 mL pipette, the lids are snapped closed and Microboxes are transferred to growth chambers. Contributed by Reza Sohrabi.

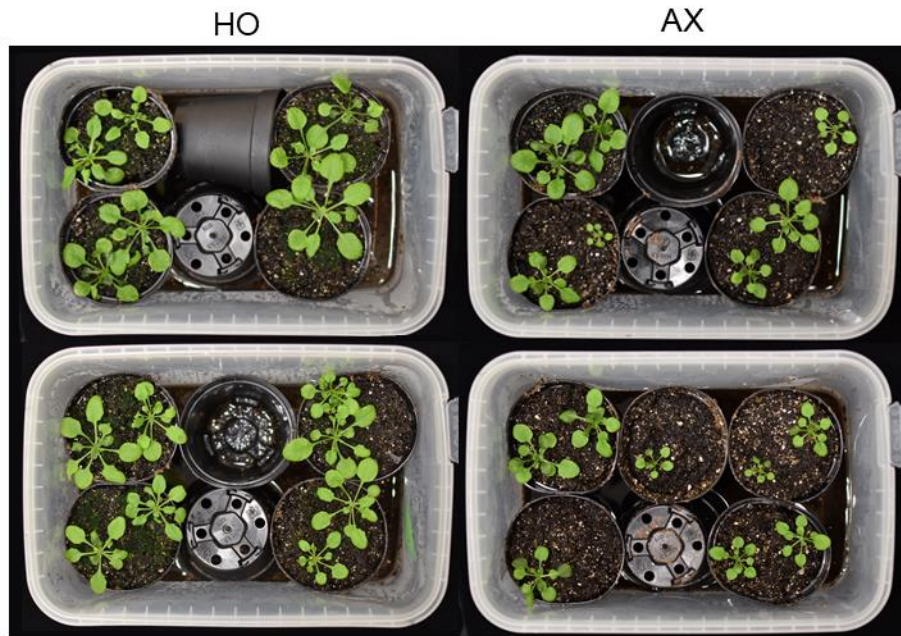


Figure B2.3: *Arabidopsis* growth in GnotoPots using peat pellets amended with vermiculite.

Plant growth 4.5 weeks after germination in GnotoPots containing an amended peat substrate. Substrate from peat pellet (Jiffy Group, #70001091) was removed from netting and mixed with 40% (w/w) medium vermiculite. 0.25x LS was used for rehydration and plant growth. Axenic (AX) plants were mock-inoculated with an autoclaved slurry extracted from soil (MSU19). Holoxenic (HO) plants were inoculated with a viable MSU19 soil slurry. 21.5-23°C inside Microbox. Contributed by Timofey Arapov.

Table B2.1: Compressed substrate pellets sourced for GnotoPot optimization experiments.

Name	Brand	Model	Source	Catalog #	Composition	Netting	Additives
Peat	Jiffy Group	Jiffy-7 Organic	Jiffy Group	70001091	Peat	Polyethylene	Lime
Peat + WA/nutrients	Jiffy Group	Jiffy-7 Horticultural	Jiffy Group	70000809	Peat	Polyethylene	Lime, nutrient charge, wetting agent
Peat/coir	Jiffy Group	Jiffy-7	Jiffy Group	32170236	Peat/coir pith mixture	Polylactic acid	Lime, nutrient charge
Coir	FibreDust	Coco Coir Seed Starter	Amazon	B085WC5HJS	Coir pith/fiber	Unknown, biodegradable	None

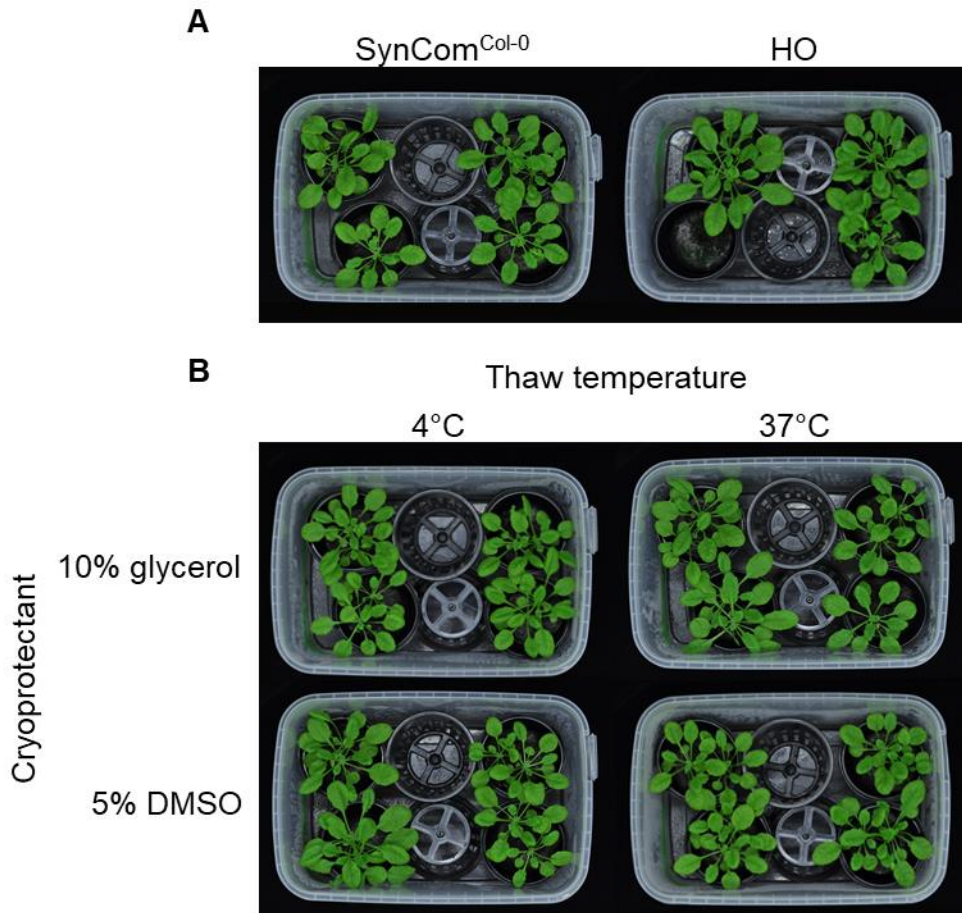


Figure B2.4: *Arabidopsis* growth phenotype of plants used in 16S rRNA gene profiling experiments.

(A) *Arabidopsis* plant inoculated with a MSU19 soil-derived community (HO) or a synthetic community consisting of 48 endophytic leaf bacteria from healthy Col-0 leaves (SynCom^{Col-0}). Photographs taken 4.5 weeks post germination. (B) *Arabidopsis* plants inoculated with SynCom^{Col-0} cryopreserved with 10% glycerol or 5% DMSO cryoprotectants and thawed slowly at 4°C or quickly at 37°C. Photographs taken 4.5 weeks post germination.

REFERENCES

REFERENCES

1. Chen, T., et al., *A plant genetic network for preventing dysbiosis in the phyllosphere*. *Nature*, 2020. **580**(7805): p. 653-657.
2. Durán, P., et al., *Microbial interkingdom interactions in roots promote Arabidopsis survival*. *Cell*, 2018. **175**(4): p. 973-983. e14.
3. Round, J.L. and S.K. Mazmanian, *The gut microbiota shapes intestinal immune responses during health and disease*. *Nature reviews immunology*, 2009. **9**(5): p. 313-323.
4. Busby, P.E., et al., *Research priorities for harnessing plant microbiomes in sustainable agriculture*. *PLoS biology*, 2017. **15**(3): p. e2001793.
5. Liu, Y.-X., Y. Qin, and Y. Bai, *Reductionist synthetic community approaches in root microbiome research*. *Current opinion in microbiology*, 2019. **49**: p. 97-102.
6. Hatfield, J.L. and J.H. Prueger, *Temperature extremes: Effect on plant growth and development*. *Weather and climate extremes*, 2015. **10**: p. 4-10.
7. Huot, B., et al., *Dual impact of elevated temperature on plant defence and bacterial virulence in Arabidopsis*. *Nature communications*, 2017. **8**(1): p. 1-12.
8. Grange, R. and D. Hand, *A review of the effects of atmospheric humidity on the growth of horticultural crops*. *Journal of Horticultural Science*, 1987. **62**(2): p. 125-134.
9. van der Voort, M., et al., *Impact of soil heat on reassembly of bacterial communities in the rhizosphere microbiome and plant disease suppression*. *Ecology letters*, 2016. **19**(4): p. 375-382.
10. Xin, X.-F., et al., *Bacteria establish an aqueous living space in plants crucial for virulence*. *Nature*, 2016. **539**(7630): p. 524-529.
11. Dastogeer, K.M., et al., *Plant microbiome—an account of the factors that shape community composition and diversity*. *Current Plant Biology*, 2020: p. 100161.
12. Andrew, D.R., et al., *Abiotic factors shape microbial diversity in Sonoran Desert soils*. *Applied and environmental microbiology*, 2012. **78**(21): p. 7527-7537.
13. Fierer, N. and R.B. Jackson, *The diversity and biogeography of soil bacterial communities*. *Proceedings of the National Academy of Sciences*, 2006. **103**(3): p. 626-631.

14. Gunning, T. and D.M. Cahill, *A Soil-free Plant Growth System to Facilitate Analysis of Plant Pathogen Interactions in Roots*. Journal of phytopathology, 2009. **157**(7-8): p. 497-501.
15. Kareem, Z.J., et al., *Small-scale bioreactor for sterile hydroponics and hairy roots: Metabolic diversity and salicylic acid exudation by hairy roots of Hyoscyamus niger*. Applied Sciences, 2019. **9**(15): p. 3044.
16. Carlström, C.I., et al., *Synthetic microbiota reveal priority effects and keystone strains in the Arabidopsis phyllosphere*. Nature ecology & evolution, 2019. **3**(10): p. 1445-1454.
17. Bai, Y., et al., *Functional overlap of the Arabidopsis leaf and root microbiota*. Nature, 2015. **528**(7582): p. 364-369.
18. Henry, A., et al., *An axenic plant culture system for optimal growth in long-term studies*. Journal of environmental quality, 2006. **35**(2): p. 590-598.
19. Kloepper, J. and M. Schroth, *Plant growth-promoting rhizobacteria and plant growth under gnotobiotic conditions*. Phytopathology, 1981. **71**(6): p. 642-644.
20. Lebeis, S.L., et al., *Salicylic acid modulates colonization of the root microbiome by specific bacterial taxa*. Science, 2015. **349**(6250): p. 860-864.
21. Adams, C., A. Jacobson, and B. Bugbee, *Ceramic aggregate sorption and desorption chemistry: implications for use as a component of soilless media*. Journal of Plant Nutrition, 2014. **37**(8): p. 1345-1357.
22. Trevors, J., *Sterilization and inhibition of microbial activity in soil*. Journal of Microbiological Methods, 1996. **26**(1-2): p. 53-59.
23. Shaw, L., et al., *Re-inoculation of autoclaved soil as a non-sterile treatment for xenobiotic sorption and biodegradation studies*. Applied Soil Ecology, 1999. **11**(2-3): p. 217-226.
24. Boyd, H., *Manganese toxicity to peanuts in autoclaved soil*. Plant and soil, 1971. **35**(1): p. 133-144.
25. Berns, A., et al., *Effect of gamma-sterilization and autoclaving on soil organic matter structure as studied by solid state NMR, UV and fluorescence spectroscopy*. European journal of soil science, 2008. **59**(3): p. 540-550.
26. Lotrario, J., et al., *Effects of sterilization methods on the physical characteristics of soil: implications for sorption isotherm analyses*. Bulletin of environmental contamination and toxicology, 1995. **54**(5): p. 668-675.

27. Wolf, D., et al., *Influence of sterilization methods on selected soil microbiological, physical, and chemical properties*. 1989, Wiley Online Library.
28. Kremer, J.M., et al., *Peat-based gnotobiotic plant growth systems for Arabidopsis microbiome research*. Nature protocols, 2021. **16**(5): p. 2450-2470.
29. Kremer, J.M., *Characterization of axenic immune deficiency in Arabidopsis thaliana*. 2017: Michigan State University.
30. Abad, M., et al., *Physical properties of various coconut coir dusts compared to peat*. HortScience, 2005. **40**(7): p. 2138-2144.
31. Arenas, M., et al., *Coir as an alternative to peat in media for tomato transplant production*. HortScience, 2002. **37**(2): p. 309-312.
32. Hou, S., et al., *A microbiota–root–shoot circuit favours Arabidopsis growth over defence under suboptimal light*. Nature Plants, 2021. **7**(8): p. 1078-1092.
33. Finkel, O.M., et al., *A single bacterial genus maintains root growth in a complex microbiome*. Nature, 2020. **587**(7832): p. 103-108.
34. Finkel, O.M., et al., *The effects of soil phosphorus content on plant microbiota are driven by the plant phosphate starvation response*. PLoS Biology, 2019. **17**(11): p. e3000534.
35. Kerckhof, F.-M., et al., *Optimized cryopreservation of mixed microbial communities for conserved functionality and diversity*. PloS one, 2014. **9**(6): p. e99517.
36. Patterson, D.T., et al., *Photosynthesis in relation to leaf characteristics of cotton from controlled and field environments*. Plant Physiology, 1977. **59**(3): p. 384-387.
37. Külheim, C., J. Ågren, and S. Jansson, *Rapid regulation of light harvesting and plant fitness in the field*. Science, 2002. **297**(5578): p. 91-93.
38. Poorter, H., et al., *Pampered inside, pestered outside? Differences and similarities between plants growing in controlled conditions and in the field*. New Phytologist, 2016. **212**(4): p. 838-855.
39. Song, C., K. Jin, and J.M. Raaijmakers, *Designing a home for beneficial plant microbiomes*. Current Opinion in Plant Biology, 2021. **62**: p. 102025.
40. Zarraonaindia, I., et al., *The soil microbiome influences grapevine-associated microbiota*. MBio, 2015. **6**(2): p. e02527-14.

41. Sivakumar, N., *Effect of edaphic factors and seasonal variation on spore density and root colonization of arbuscular mycorrhizal fungi in sugarcane fields*. *Annals of microbiology*, 2013. **63**(1): p. 151-160.
42. Jiffy Group. *Jiffy Sustainable Peat Pellets*. 2020 [cited 2021 October 16]; Available from: <https://jiffygroup.com/solutions/jiffy-pellets/>.
43. Williams, P., *Jiffy offers sustainable netting solution for Growblocks and Pellets*, in *Greenhouse Management*. 2020.
44. Bolyen, E., et al., *Reproducible, interactive, scalable and extensible microbiome data science using QIIME 2*. *Nature biotechnology*, 2019. **37**(8): p. 852-857.
45. Callahan, B.J., et al., *DADA2: high-resolution sample inference from Illumina amplicon data*. *Nature methods*, 2016. **13**(7): p. 581-583.
46. Werner, J.J., et al., *Impact of training sets on classification of high-throughput bacterial 16s rRNA gene surveys*. *The ISME journal*, 2012. **6**(1): p. 94-103.
47. DeSantis, T.Z., et al., *Greengenes, a chimera-checked 16S rRNA gene database and workbench compatible with ARB*. *Applied and environmental microbiology*, 2006. **72**(7): p. 5069-5072.
48. Lindsey III, B.E., et al., *Standardized method for high-throughput sterilization of Arabidopsis seeds*. *JoVE (Journal of Visualized Experiments)*, 2017(128): p. e56587.

CHAPTER 3: A MICROBIOTA IS REQUIRED FOR PROPER IMMUNOCOMPETENCE IN *ARABIDOPSIS*

This chapter is adapted from an article that will be submitted for publication (expected 2022).

Authors: Bradley Paasch^{1, 2, 3}, Reza Sohrabi^{1, 3, 4}, James Kremer^{1, 5}, Kinya Nomura^{1, 3}, Brian Kvitko⁶, James Tiedje^{2, 7}, Sheng Yang He^{1, 3, 4, 8}

Affiliations: ¹Department of Energy Plant Research Laboratory, Michigan State University, East Lansing, MI, USA; ²Department of Biochemistry and Molecular Biology, Michigan State University, East Lansing, MI, USA; ³Department of Biology, Duke University, Durham, NC, USA; ⁴Plant Resilience Institute, Michigan State University, East Lansing, MI, USA; ⁵Department of Microbiology and Molecular Biology, Michigan State University, East Lansing, MI, USA; ⁶Department of Plant Pathology, University of Georgia, Athens, GA, USA; ⁷Center for Microbial Ecology, Michigan State University, East Lansing, MI, USA; ⁸Howard Hughes Medical Institute, Duke University, Durham, NC, USA.

3.1. Abstract

A vast array of microorganisms including bacteria, fungi, viruses, and protozoa reside on and within various parts of a plant. Collectively referred to as plant microbiota, a subset of these microorganisms can form a close association with the plant and impact fundamental host processes. Although many studies have shown that microbes can ectopically stimulate plant immune responses, the fundamental question of whether the preexisting microbiota is indeed required for proper development of plant immune response remains unanswered. Here, I optimized a newly developed peat-based gnotobiotic plant growth system to characterize immunocompetence in *Arabidopsis* during vegetative growth. Axenic plants grown in the absence of microbiota were found to possess significantly diminished age-dependent immune responses. Axenic plants were defective in several aspects of pattern triggered immunity, including flg22-induced production of reactive oxygen species, signaling through MAPK pathways, and induction of defense-related genes. Axenic plants were ultimately hypersusceptible to infection by the foliar bacterial pathogen *Pseudomonas syringae* pv. tomato DC3000. A synthetic microbiota composed of culturable bacteria from the leaf endosphere of healthy *Arabidopsis* plants was able to restore immunocompetence similar to plants inoculated with a soil-derived community in a growth substrate-dependent manner. These results demonstrate a role of microbiota in immunocompetence and age-dependent immunity, which was previously thought to be an intrinsic trait of plants.

3.2. Introduction

Plants are colonized by a diverse set of microorganisms resulting in exposure to a variety of mutualistic, commensal, and pathogenic interactions. To protect against pathogenic microorganisms, plants possess an apparent two-tiered defense strategy capable of recognizing evolutionarily conserved pathogen-associated molecular patterns (PAMPs) or specific effector proteins secreted by pathogens into plant cells and mounting a response or via pattern-triggered immunity (PTI) or effector-triggered immunity, respectively. PTI represents an initial line of defense. A 22 amino acid epitope derived from bacterial flagellin (flg22) is a well characterized elicitor of PTI and recognized by the pattern recognition receptor (PRR) FLAGELLIN-SENSITIVE 2 (FLS2). Many other elicitors/receptor pairs have been described, including those for elongation factor TU, cold shock protein, peptidoglycan, lipopolysaccharide, chitin, and β -glucan [1]. In *Arabidopsis*, PTI signaling is initiated upon perception of bacterial flagellin by plasma membrane-localized pattern recognition receptor FLS2 which subsequently forms a complex with co-receptor BRASSINOSTEROID INSENSITIVE 1-ASSOCIATED RECEPTOR KINASE 1 (BAK1). Another kinase, BOTRYTIS-INDUCED KINASE 1 (BIK1) associates with this complex to initiate PTI signaling mediated, in part, through a MAPK cascade. Activation of PTI results in the induction of many physiological responses including the production of reactive oxygen species (ROS) [2] and the expression of defense-related genes [3, 4], among others. Activation of PTI prior to an infection can also result in enhanced pathogen resistance [5].

Age-related resistance (ARR) describes a widely observed phenomenon in which young plants exhibit greater disease susceptibility compared to older plants [6, 7]. This

is observed across many flowering plants and is effective against a variety of host pathogens [8]. In *Arabidopsis*, for instance, the basal susceptibility of young plants to foliar bacterial pathogen *Pseudomonas syringae* pv. *tomato* (*Pst*) DC3000 is greater compared to older plants. One hypothesis involving growth-defense tradeoffs suggests that in order to balance resource restrictions while promoting robust vegetative growth early in life, young plants prioritize growth over defense [9]. Indeed, there is evidence of direct molecular connections between plant growth and immunity [10-12] including common dual-function signaling components as in the case of PTI and brassinosteroid-dependent plant growth [13]. However, it is unclear whether molecular connections such as these are intrinsic to age-dependent immunity in plants. Development of technologies to generate gnotobiotic animals such as germ-free mice have allowed researches to discover an important contribution of endogenous microbiota in postnatal maturation of innate immune responses in newborn vs adult animals [14, 15] This raises the possibility that plant microbiota may also contribute to the maturation of plant immunity. However, it remains an open question whether age-dependent immunity is entirely intrinsic to plant development or whether maturation of PTI is, in part, the result of a naturally colonization of a microbiota. To enable researchers to address questions such as this, two peat-based gnotobiotic plant growth systems, the FlowPot and GnotoPot system (discussed in Chapter 2), were recently developed in Dr. Sheng Yang He's laboratory. These systems, allow the growth of plants with and without exposure to viable microorganisms, under otherwise identical conditions.

In this Chapter, I describe a form of age-dependent flg22-mediated immunity observed in *Arabidopsis* that occurs during vegetative growth from approximately two

weeks to at least six weeks post-germination. I then implement peat-based gnotobiotic plant growth systems to examine the role of microbiota on age-dependent immune maturation. Notably, I found that axenic plants lacked age-dependent flg22-mediated immune responses compared to plants inoculated with a soil-derived microbial community, suggesting a role for plant-associated microbiota in the maturation of host immune responses. I further found that microbially-mediated immune modulation of plant immune responses by a complex soil-derived community could be recapitulated by a 48-member bacterial synthetic community.

3.3. Results

3.3.1. Age-related flg22-mediated resistance in potting soil-grown *Arabidopsis*

To characterize the maturation of flg22-mediated resistance over time in conventionally grown *Arabidopsis* plants, we performed flg22 protection assays using 2.5-week-old and 3.5-week-old *Arabidopsis* plants which were conventionally grown in a potting soil substrate in air-circulating growth chambers. In younger, 2.5-week-old plants we observed modest flg22-mediated resistance in flg22-treated vs mock-treated plants. However, compared to younger plants, older plants exhibited significantly enhanced resistance when treated with the same concentration of flg22 (Figure 3.1 A), suggesting that PTI was not yet fully functional in the younger plants. We hypothesized that the lack of a fully competent immune system may make young plants more susceptible to invaders with low virulence, such as weakly pathogenic or opportunistic microorganisms. To test this hypothesis we used the weakly virulent $\Delta avrPto\Delta avrPtoB$ mutant strain of *Pst* DC3000 in which two of the 36 effector genes are deleted [16]. *AvrPto* and *AvrPtoB* are important virulence factors involved in the suppression of PTI in susceptible plants during DC3000 infection [17, 18]. In older plants, the $\Delta avrPto\Delta avrPtoB$ mutant strain was significantly less virulent compared to wild-type *Pst* DC3000 which was consistent with previous reports [16, 19]. However, no significant difference was observed in younger plants, indicating the $\Delta avrPto\Delta avrPtoB$ strain could more aggressively infect younger plants and further suggested that younger plants have decreased levels of PTI compared to older plants (Figure 3.1 B). We next tested the *Pst* DC3000 *hrcC* mutant strain which is defective in components of the type III protein secretion pathway and thus unable to deliver any of the 36 effector proteins to host cells

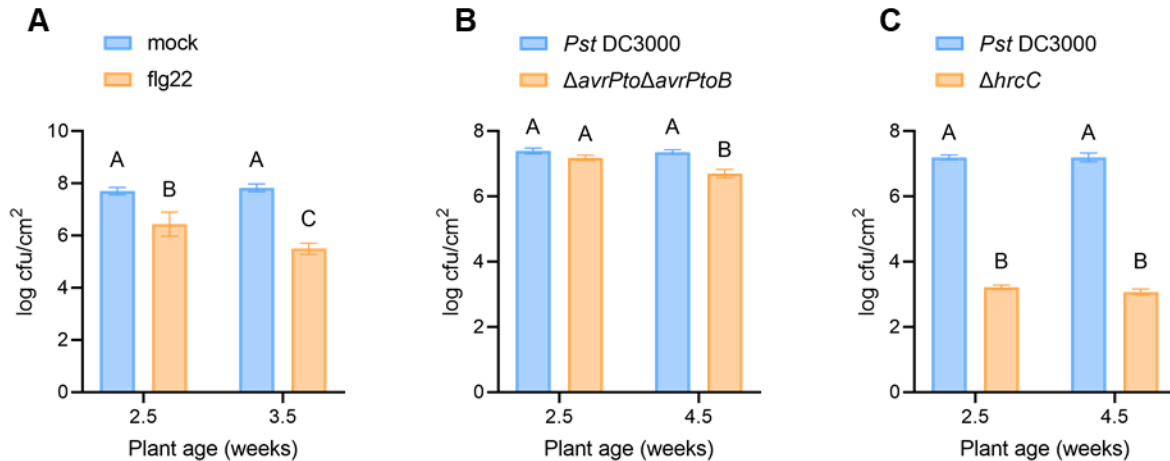


Figure 3.1: Immunity undergoes a maturation process in Arabidopsis plants conventionally grown in potting soil.

(A) flg22 protection assay showing enhanced resistance against *Pst* DC3000 triggered by pretreatment with 50 nM flg22 in 2.5-week-old and 3.5-week-old plants. Each column represents bacterial titer 24 hours after inoculation as log transformed colony forming units (cfu)/cm² and is the mean of 6 plants. Error bars indicate standard deviation. Different letters represent a significant difference ($p < 0.05$, two-way ANOVA with Tukey's HSD post-hoc test). Data contributed by Brian Kvitko. (B) Plants of the indicated ages were syringe infiltrated with a bacteria suspension of *Pst* DC3000 or *Pst* DC3000 (Δ avrPto/avrPtoB) at 1×10^6 cfu/mL. Each column represents bacterial titer 3 days after inoculation as log transformed cfu/cm² and is the mean of 3 plants. Error bars indicate standard deviation. Different letters represent a significant difference ($p < 0.05$, two-way ANOVA with Tukey's HSD post-hoc test). (C) Plants of the indicated ages were syringe infiltrated with a bacteria suspension of *Pst* DC3000 or *Pst* DC3000 (Δ hrcC) at 1×10^6 cfu/mL. Each column represents bacterial titer 3 days after inoculation as log transformed cfu/cm² and is the mean of 3 plants. Error bars indicate standard deviation. Different letters represent a significant difference ($p < 0.05$, two-way ANOVA with Tukey's HSD post-hoc test). Data for panels (B, C) contributed by Kinya Nomura.

[20]. With the *hrcC* strain we observed similar levels of virulence in young and old plants (Figure 3.1C) further indicating it is likely compromised immunity and not other pathogenesis-associated host processes that is responsible for the differential disease susceptibility between young and old plants.

3.3.2. Optimization of FlowPots and GnotoPots for studying immunocompetence

To assess a possible role of microbiota in age-dependent resistance, I needed to grow plants under gnotobiotic conditions with and without exposure to microbiota. Although FlowPots and Gnotopots have been shown to produce healthy plants (Chapter 2), whether these gnotobiotic conditions were optimal for analyzing immune responses had not been fully investigated. Indeed, in my initial experiments using FlowPots and GnotoPots, I found that PTI was greatly suppressed compared to plants grown conventionally in potting soil and an open-air growth chamber (Figures 3.2 A-B).

Both FlowPot and GnotoPot gnotobiotic systems utilize a similar soil-like substrate composed primarily of peat. However, GnotoPots contain a larger volume and increased concentration of liquid nutrients. The nutrient reservoir and larger pot size contributed to increased moisture in the GnotoPot system. This additional moisture resulted in an increase in the daytime relative humidity (RH) levels (~95% RH) compared to FlowPots (~85% RH). Both these values are increased compared to conventionally-grown plants which are grown with 50%-70% RH. I hypothesized that the increased RH was contributing to the suppression of PTI observed in GnotoPots. To test this, I measured *flg22*-induced production of ROS in colonized plants along a gradient of humidity levels. High humidity was achieved without modification to the

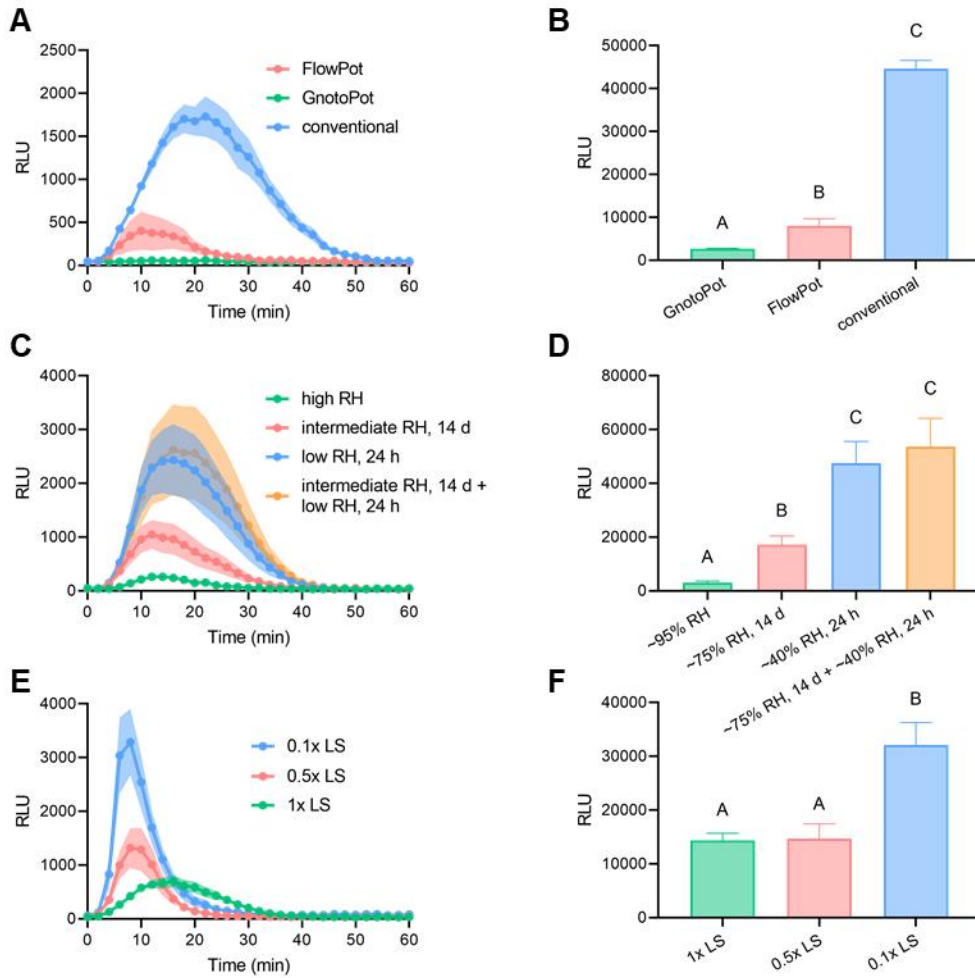


Figure 3.2: Excess nutrients and humidity suppresses flg22-induced immune responses in GnotoPots.

(A, B) ROS production induced by 100 nM flg22 in plants conventionally grown in potting soil, in FlowPots, and in GnotoPots. Conventionally grown plants supplied with 0.5x Hoagland solution as needed, ~65% RH. GnotoPot grown plants supplied with 1x LS, ~95% RH. FlowPots grown plant supplied with 0.5x LS, ~90% RH (A) ROS burst dynamics over 60 mins and (B) total ROS production. Results represent the mean of 8 plants \pm SEM. Different letters represent a significant difference ($p \leq 0.027$, Brown-Forsythe and Welch ANOVA with Dunnett's T3 post-hoc test). (C, D) ROS production induced by 100 nM flg22 in plants grown in GnotoPots with different levels of humidity. (C) ROS burst dynamics over 60 mins and (D) total ROS production. Results represent the mean of 8 plants \pm SEM. Different letters represent a significant difference ($p \leq 0.05$, Brown-Forsythe and Welch ANOVA with Dunnett's T3 post-hoc test). (E, F) ROS production induced by 100 nM flg22 in plants grown in GnotoPots supplied with 0.1x, 0.5x, or 1x LS nutrient solution concentrations. (E) ROS burst dynamics over 60 mins and (F) total ROS production. Results represent the mean of 8 plants \pm SEM. Different letters represent a significant difference ($p \leq 0.02$, Brown-Forsythe and Welch ANOVA with Dunnett's T3 post-hoc test).

GnotoPot system and served as our control group. Intermediate humidity levels were achieved by removing excess water from the bottom of the box 2 weeks prior to the experiment. This resulted in humidity levels that were similar to FlowPots, around 80-85% RH. Low humidity levels were achieved by partially removing the lids of the microboxes 24 h prior to the experiment. This resulted in humidity levels that were similar to ambient, which at the time was around 35-40% RH. A third treatment combined both intermediate (removing excess liquid two weeks prior to the experiment) and low (opening lid 24 h prior to the experiment) conditions. I observed a significant impact of humidity on the ability of GnotoPot-grown plants to respond to flg22 (Figures 3.2 C-D). A small but insignificant increase in the total amount of ROS produced in plants grown under intermediate RH for 2 weeks was observed, however the difference was more profound in plants that experienced a 24 low humidity treatment (Figures 3.2 C-D). This suggests that elevated levels of humidity were contributing to the observed suppression of PTI in GnotoPots, and this could be at least partially alleviated with a brief shift to low humidity.

Early versions of GnotoPots utilized an elevated concentration of nutrient solution to provide a nutrient-replete conditions sufficient for long-term growth. These early versions supplied plants with full strength (1x) Linsmaier and Skoog (LS) basal medium [21], a medium which is frequently used in *Arabidopsis* tissue culture. To determine whether elevated levels of nutrients were suppressing aspects PTI in GnotoPots, I worked with and mentored an undergraduate researcher, Jennifer Martz, to measure flg22-induced production of ROS in colonized plants along a nutrient gradient. Using the same volume of liquid, GnotoPots were prepared with full strength (1x) LS, half strength

(0.5x) LS and one tenth strength (0.1x) LS. The results indicated a significant impact of nutrients on flg22-mediated ROS production. Decreasing nutrient strength increased ROS burst magnitude and reduced time to reach the maximum ROS production (Figure 3.2 E). At intermediate nutrient levels (0.5x LS), ROS burst magnitude was moderately increased and time to reach the maximum was reduced compared to higher (1x LS) nutrient concentrations (Figure 3.2 E), however the total ROS produced was not significantly different (Figures 3.2 F). At low nutrient levels (0.1x LS), ROS burst magnitude was increased, time until maximum reduced, and total ROS was increased (Figures 3.2 E-F). This suggests that elevated levels of nutrients were contributing to the observed suppression of PTI in early versions of GnotoPots.

The individual effects nutrients and humidity had on flg22-induced production of ROS was significant. To get a more comprehensive understanding of the combined effect reduced nutrients and humidity have on PTI responses in GnotoPots, I measured PTI marker gene *FRK1* activation under initial conditions and optimized conditions. Initial, “unoptimized” GnotoPot plant growth conditions (discussed in Chapter 2) provided a high nutrient and high humidity environment (1x LS, $\geq 75\%$ RH) while in the optimized conditions reduced nutrients and provided lower RH (0.5x LS, $\leq 40\%$ RH). It was observed that both basal and flg22-induced *FRK1* expression was significantly increased in plants grown using the nutrient/humidity-optimized conditions (Figure 3.3 A). To assess whether the robust PTI responses observed in optimized GnotoPot conditions is associated with reduced disease susceptibility, I infiltrated plants with *Pst* DC3000 and observed that plants were less susceptible to infection when grown with the optimized conditions compared to the unoptimized conditions (Figure 3.3 C),

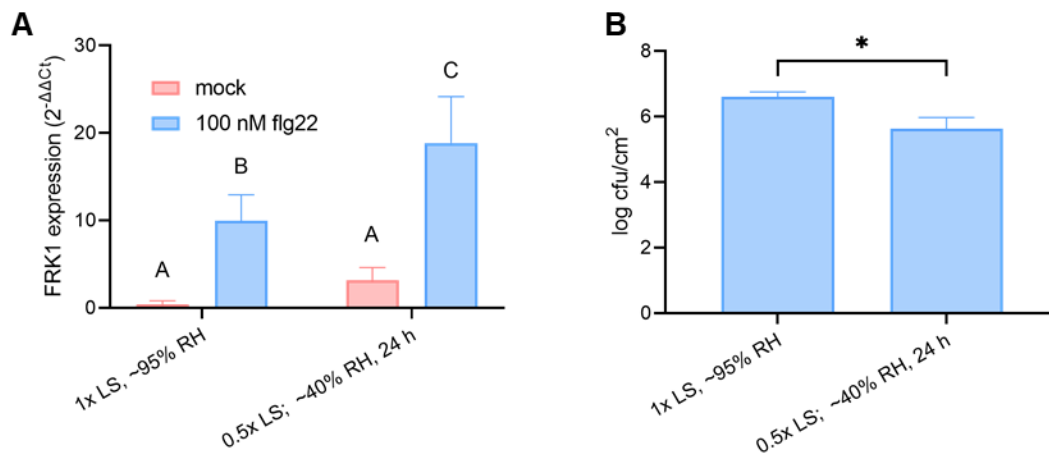


Figure 3.3: Optimized nutrient and humidity conditions promote more robust immune responses in colonized plants grown in GnotoPots.

(A) Basal and flg22-induced expression of *FRK1* in plants grown under a high (1x LS, ~95% RH) or low (0.5x LS; ~40% RH, 24 h) nutrient and humidity regimen. Total RNA was extracted 3 h after treatment with 100 nM flg22 or a mock solution. Expression levels expressed as relative to mock-treated holoxenic plants. PP2A was used for normalization. Results represent the mean values \pm SD of three biological samples consisting of three plants. Different letters represent a significant difference ($p < 0.05$, two-way ANOVA with Tukey's HSD post-hoc test). (B) Cell numbers of *Pst* DC3000 in plants grown under a high or low nutrient and humidity regimen. Each column represents bacterial titer 48 hours after inoculation as log transformed cfu/cm² and is the mean of 3 plants. Error bars indicate SD. Asterisk represents a significant difference ($p = 0.01$, Student's *t*-test).

suggesting that the suppression of PTI by elevated nutrients and high humidity could mask microbiota-mediated immunocompetence.

3.3.3. Immune maturation is dependent on colonization of plant tissues by microbiota

With the establishment of gnotobiotic conditions that allowed for the study of immunity over an extended period, we were able to address hypotheses regarding the involvement of microbiota in age-dependent immunity. First, we characterized the temporal maturation of flg22-mediated resistance in both colonized (holoxenic; HO) plants as well as plant grown without exposure to a microbiota (axenic; AX). The results indicated that HO plants colonized with a soil-derived microbial community exhibit progressively more robust flg22-mediated resistance that correlates with plant age (Figure 3.4 A) which is consistent with the experiment using naturally colonized plants grown conventionally in potting soil in a growth chamber (Figure 3.1 A). More notably, axenic (AX) plants mock-inoculated with an autoclaved soil slurry and grown devoid of a viable microbial community, were greatly reduced in age-dependent PTI phenotype (Figure 3.4 A). Expressing flg22-mediated resistance as the fold change in *Pst* DC3000 cell counts in flg22-treated plants compared to mock, confirmed that the relative flg22 protection becomes significantly more robust in HO plants but not in AX plants (Figure 3.4 B). Furthermore, *Arabidopsis* mutant *bak1-5/bkk1-1/cerk1* (*bbc* [22]; which is defective in PTI signaling downstream of many pattern recognition receptors, including the flg22 receptor FLS2, did not show flg22-mediated resistance in either HO or AX plants.

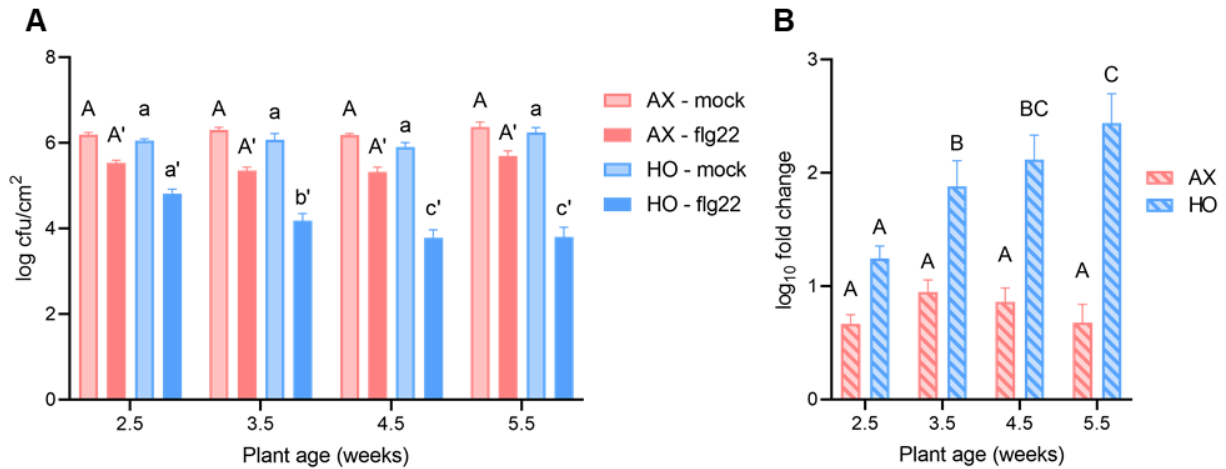


Figure 3.4: Role of microbiota in immune maturation.

(A) Age-dependent flg22 protection. Plants were treated 24 hours prior to inoculation with *Pst* DC3000 with either a water (mock) or 100 nM flg22 solution. Each column represents bacterial titer 24 hours after inoculation as log transformed cfu/cm² and is the mean of 3 plants. Error bars indicate SD. Different letters represent a significant difference ($p < 0.05$, two-way ANOVA with Tukey's HSD post-hoc test). Data contributed by Kinya Nomura. (B) Relative protection displayed as fold change in bacterial cell counts between flg22 and mock treated samples. Calculated from as the difference in log transformed bacterial cell counts between flg22 treated plants and mock treated plants. Error bars represent SD. Different letters represent a significant different ($p < 0.05$, two-way ANOVA with Tukey's HSD post-hoc test).

I next quantified induction of PTI marker gene *FLG22-INDUCED RECEPTOR-LIKE KINASE 1 (FRK1)* to further characterize age-dependent activation of PTI in HO plants and apparent lack thereof in AX plants. Basal expression of *FRK1* was similar within the same treatment group (i.e. HO or AX) for both 3.5- and 5.5-week-old plants; however the basal expression of *FRK1* was lower in AX plants compared to HO plants at both ages (Figure 3.5 A). After treatment with flg22 we observed induction of *FRK1* in response to flg22 in young HO plants, which became more robust in older plants. However, the magnitude of *FRK1* induction in AX plants was lower compared to HO plants and, notably, no significant age-dependent phenotype was observed (Figure 3.5 B), further indicating that AX plants is greatly reduced in age-dependent PTI.

3.3.4. Axenic *Arabidopsis* exhibit defects in pattern-triggered immunity

Temporal assays revealed that AX plants lack robust PTI, and that the difference in levels of immunocompetence between AX and HO plants becomes more pronounced with age. We therefore hypothesized that AX plants may possess an underdeveloped immune system as a result of the apparent lack of age-dependent PTI, especially at older ages. To rigorously test this, I conducted a series of immune-related assays in plants ranging from 4.5 to 5.5 weeks of age. In Chapter 2, I documented technical issues with using the FlowPot system for long-term growth of gnotobiotic plants, therefore most of the results presented in this Chapter were collected using plants grown in the GnotoPot system with the nutrient/humidity-optimized conditions described in Section 2.3.4. Consistently, I found AX plants exhibited significantly lower levels of PTI-associated immune responses compared to HO plants. In addition to reduced basal

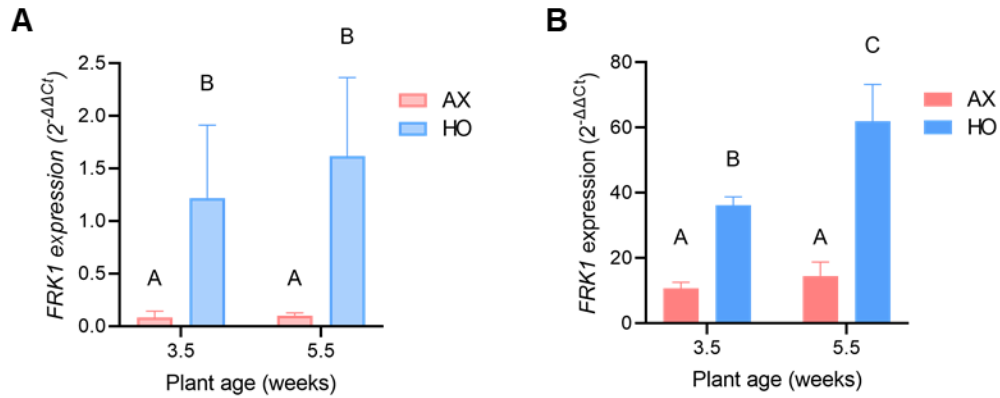


Figure 3.5: Role of microbiota in maturation of PTI.

(A) Basal and (B) flg22-induced age-dependent *FRK1* gene expression in 3.5-week-old and 5.5-week-old axenic and holoxenic plants. Total RNA was extracted 4 h after treatment with a mock solution lacking flg22 for basal expression or 100 nM flg22 for flg22-induced expression. Expression levels displayed as relative to mock treated 3.5-week-old HO plants for both panels. *PP2A* was used for normalization. Results represent the mean values \pm SD of four plants. Different letters represent a significant difference ($p < 0.05$, two-way ANOVA with Tukey's HSD post-hoc test).

and flg22-induced *FRK1* gene expression as observed previously in temporal analyses (Figure 3.4 C), 4.5-week-old AX plants exhibited significantly reduced flg22-induced ROS production compared to HO plants (Figure 3.6 A). In AX plants both the magnitude of maximum ROS production (peak amplitude) was reduced and the time to reach the maximum was delayed (Figure 3.6 B). PTI signaling in *Arabidopsis*, in part, involves signaling through a MITOGEN-ACTIVATED PROTEIN KINASE (MPK) cascade. Western blot analysis revealed that despite possessing similar levels of total MPK3 and MPK6 (Figure 3.7 A-B), less MPK was phosphorylated in AX plants after the activation of PTI by treatment with flg22 (Figure 3.7 C). RT-qPCR analysis indicated that both basal and flg22-induced expression of the *FLS2* receptor gene is significantly reduced in AX plant leaf tissue compared to HO plant leaf tissue (Figure 3.6 D). However, total *FLS2* protein abundance was only sometimes reduced in AX plant leaves (Figure 3.7 D). No notable difference in the co-receptor *BAK1* could be observed (Figure 3.7 E). Quantification of the defense hormone salicylic acid (SA), which is downstream of PTI signaling revealed that AX plants possess lower basal levels compared to HO plants.

I hypothesized that these immune defects observed in AX plants could ultimately contribute to reduced basal disease resistance in AX plants. To test this, I infiltrated plants with the foliar pathogen *Pst* DC3000. Two days after inoculation, *Pst* DC3000 cell counts were significantly elevated in AX plants compared to HO plants (Figure 3.6 G). Together, these results indicate that plants grown devoid of a microbiota in a soil-like peat substrate are defective in PTI-associated immune responses and hypersusceptible to disease.

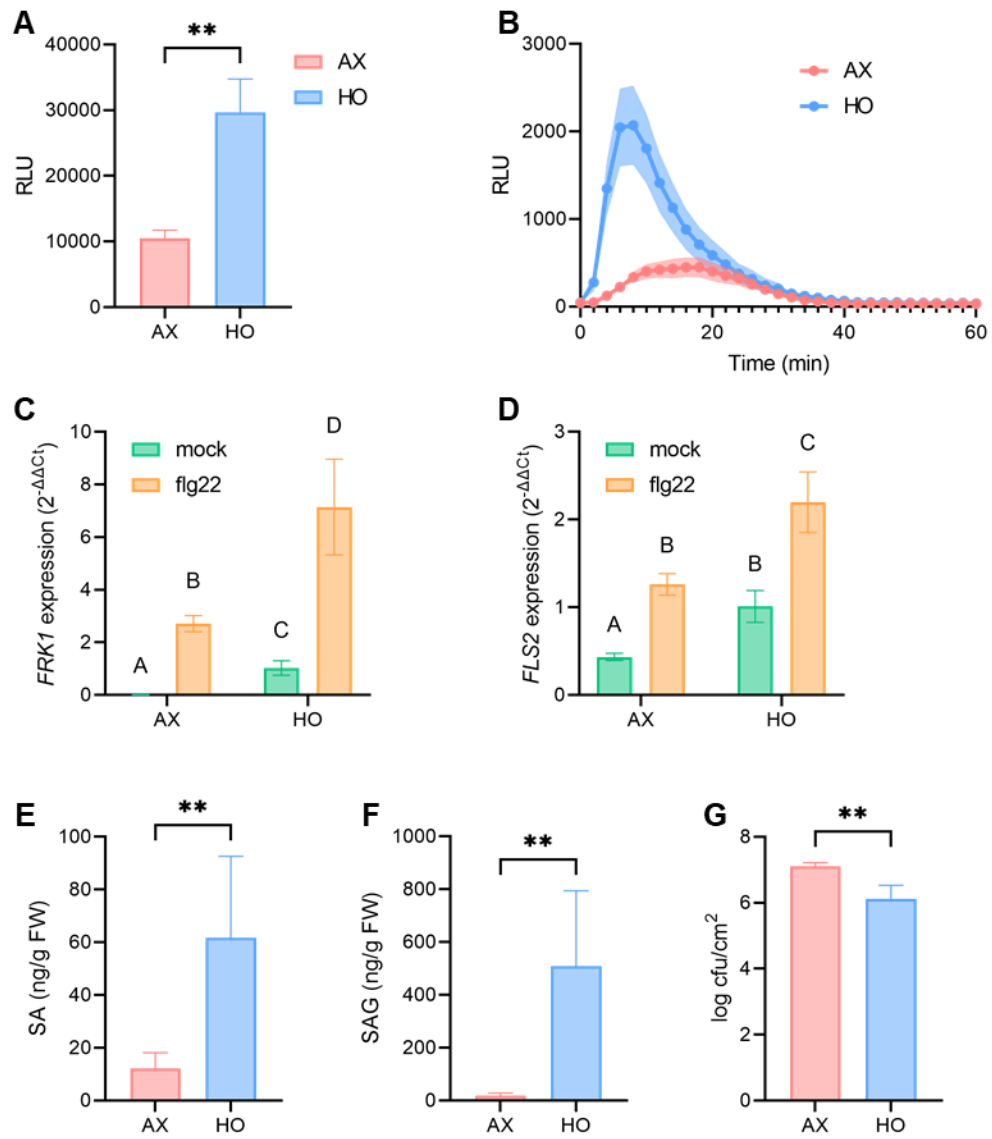


Figure 3.6: Axenic Arabidopsis plants exhibit defects in PTI compared to colonized plants.

Figure 3.6 (cont'd):

(A-B) ROS production induced by 100 nM flg22 in axenic and holoxenic plants colonized by the natural "MSU19" microbial community in GnotoPots. (A) Total ROS production and (B) ROS burst dynamics over 60 mins. Results represent the mean of 8 plants \pm SEM. The asterisk represents a significant difference ($p = 0.007$, Student's *t*-test). (C-D) Basal and flg22-induced expression of defense-related genes in axenic and MSU19-colonized holoxenic plant leaf tissue. (C) FRK1: Total RNA was extracted 3 h after treatment with 100 nM flg22 or a mock solution. (D) FLS2: Total RNA was extracted 1 h after treatment with 100 nM flg22 or mock solution. Results relative to colonized plants treated with elicitor solution lacking flg22 ($2^{-\Delta\Delta C_t}$ of mock HO plants = 1). PP2A was used for normalization. Bars represent the mean values \pm SD of three biological samples consisting of three plants. Different letters represent a significant difference ($p \leq 0.02$, unpaired *t*-tests with Welch's correction). (E-F) Total levels of (E) SA and (F) glycosylated SA in axenic and MSU19-colonized holoxenic plants. Each bar represents the mean values \pm SE of eight biological samples consisting of at least three plants. The asterisks represents a significant difference ($p \leq 0.003$, Student's *t*-test). (G) Cell numbers of *Pst* DC3000 in AX and HO plants. Each column represents bacterial titer 48 hours after inoculation as log transformed cfu/cm² and is the mean of 3 plants. Error bars indicate SD. Asterisk represents a significant difference ($p = 0.003$, Student's *t*-test).

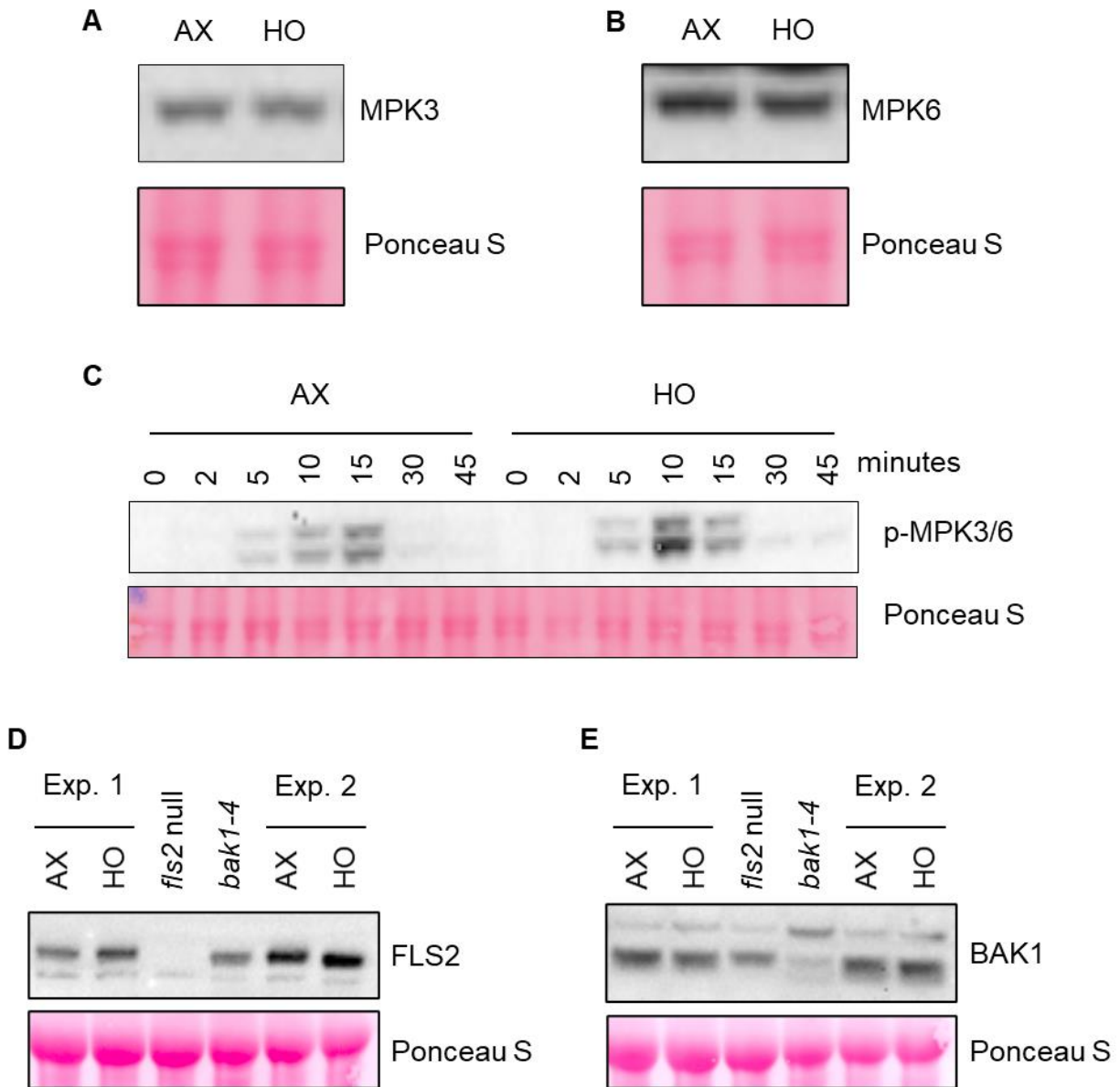


Figure 3.7: PTI-associated protein abundance in AX versus HO plants.

(A) Total MPK3 proteins or (B) total MPK6 proteins. Protein was detected with MPK3 or MPK6-specific antibodies. (C) Phosphorylated MPK3/6 proteins detected using an α -p44/42-ERK antibody. Four-week-old plants were treated with 100 nM flg22. Samples were taken at the indicated times after treatment.

(D) Total FLS2 protein or (E) total BAK1 detected in whole leaf tissue lysate of four pooled plants. Two experimental repeats show variability in FLS2 relative abundance. *fls2* null (SAIL_691C4) and *bak1-4* (SALK_116202) mutants contain T-DNA insertions which result in the lack of FLS2 or BAK1 production and are used as a negative control for detection. Ponceau S stain of all blots show equal loading.

3.3.5. A bacterial synthetic community (SynCom) confers immunocompetence

A 48-member SynCom composed of endophytic bacteria from leaves of healthy *Arabidopsis* Col-0 plants grown in potting soil in air-circulating growth chambers was recently developed in the He lab [23]. I conducted 16S profiling of the leaf endophytic bacterial communities in GnotoPot-grown plants inoculated with either a natural complex soil-derived microbiota (“MSU19”) or the 48-member SynCom (SynCom^{Col-0}). Similar phylogenetic compositions of bacteria were found regardless of the initial complexity of microbiome input, suggesting stringent selection of bacterial taxa for colonization inside leaves (discussed in Chapter 2). Given the similar composition and diversity of endophytic bacteria I hypothesized that SynCom^{Col-0} might phenocopy the natural soil-derived complex microbiota input and confer immunocompetence. To test this hypothesis, I compared the PTI phenotypes of plants grown with and without a soil-derived microbial community (HO vs AX) to those grown with and without a synthetic community (SynCom vs MgCl₂). Consistent with my previous findings, I observed significantly reduced flg22-induced production of ROS in AX plants compared to HO plants inoculated with a soil-derived community. Similarly, I observed significantly reduced flg22-induced ROS production in MgCl₂ mock-inoculated AX control plants compared SynCom^{Col-0}-inoculated plants. Notably, SynCom^{Col-0}-inoculated plants produced similar total ROS compared to HO plants while MgCl₂ mock-inoculated plants produced slightly reduced total ROS compared to AX plants (Figure 3.8 A, B), suggesting a bacterial SynCom can confer microbially-mediated immune phenotypes similar to that of a soil-derived community. I next quantified flg22-induced *FRK1* gene expression and observed significantly reduced basal and flg22-induced *FRK1*

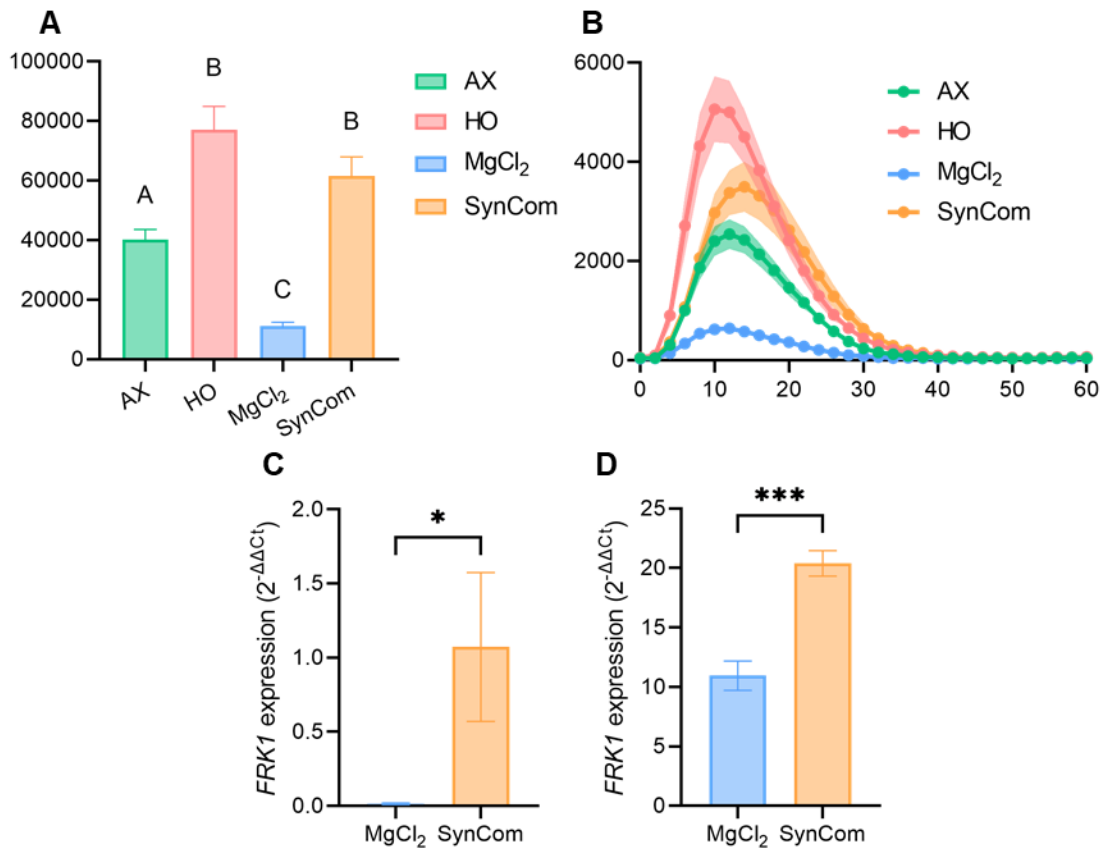


Figure 3.8: SynCom^{Col-0} restores immunocompetence similar to a natural soil-derived microbial community.

(A-B) ROS production induced by 100 nM flg22 in plants colonized by a MSU19 soil-derived community (HO) or a synthetic community consisting of 48 endophytic leaf bacteria from healthy Col-0 leaves (SynCom^{Col-0}). (A) Total ROS production and (B) ROS burst dynamics over 60 mins. Results represent the mean of 12 plants \pm SEM. Different letters represent a significant difference ($p < 0.03$, two-way ANOVA with Tukey's HSD post-hoc test). (C) Basal and (D) flg22-induced *FRK1* in axenic plants mock-inoculated with a sterile solution lacking microorganisms (MgCl₂) and SynCom^{Col-0}-inoculated plants. Total RNA was extracted 3 h after treatment with (C) a mock solution lacking flg22 or (D) 100 nM flg22. Results relative to basal expression in holoxenic plants. PP2A was used for normalization. Bars represent the mean values \pm SD of three biological samples consisting of three plants. Different letters represent a significant difference. Asterisks represents a significant difference (* $p = 0.02$, *** $p = 0.0006$, Student's *t*-test).

expression in MgCl_2 mock-inoculated plants compared to plants colonized by SynCom^{Col-0} (Figure 3.8 C-D), which was consistent with observations made earlier using a soil-derived microbial community (Figure 3.6 C) This result further suggests that a bacterial SynCom can confer immunocompetence similar to that of a soil-derived community.

3.3.6. Microbiota-conferred immunocompetence is dependent on growth substrate

Edaphic factors can alter the function of a plant microbiota [24]. An advantage of the GnotoPot system over other gnotobiotic plant growth systems is that it utilizes a peat-based growth substrate reminiscent of natural soil in terms of texture, organic matter and other biophysical properties. To determine whether a soil-like substrate is required for the microbially-mediated plant immune phenotypes, I repeated certain immune assays in a commonly used plate-based gnotobiotic system which utilized nutrient agar as a growth substrate. Seeds sown onto nutrient agar were inoculated with SynCom^{Col-0} or mock-inoculated with MgCl_2 . Visual inspection of plants 16 days post-germination indicated both groups appeared healthy and there were no visible signs of stress (Figure 3.9 A). RT-qPCR analysis revealed that basal expression of PTI-marker gene *FRK1* was significantly increased in SynCom-colonized plants (Figure 3.8 B), an observation consistent with plants grown in the peat substrate (Figure 3.6 C). Surprisingly, flg22-induced expression of *FRK1* was greatly reduced in SynCom-inoculated plants compared to mock-inoculated plants (Figure 3.8 C), which is opposite to what occurs in plants grown in the peat substrate (Figure 3.6 C).

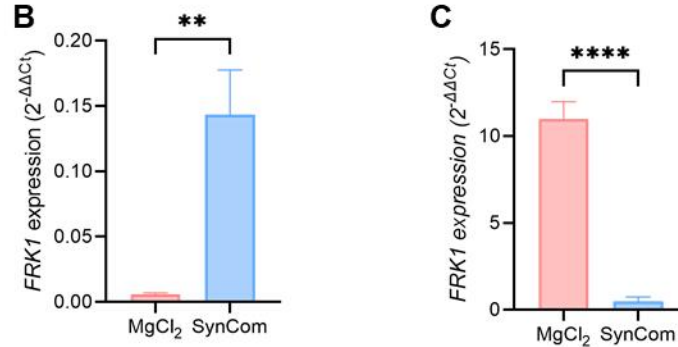
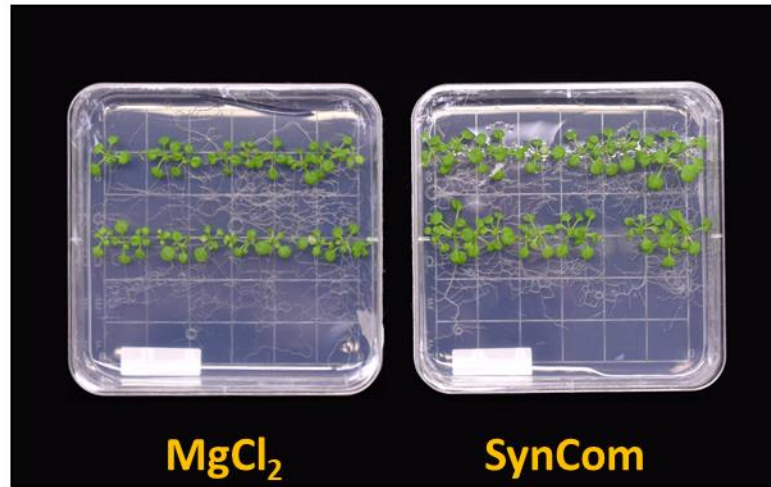
A

Figure 3.9: Microbiota-mediated immune phenotype is dependent on growth substrate.

(A) MgCl₂ mock-inoculated and SynCom^{Col-0}-inoculated *Arabidopsis* plants grown in sterile LS agar plates photographed 16 days post germination. (B) Basal and (C) flg22-induced *FRK1* expression in mock-inoculated and SynCom-inoculated plants grown on nutrient agar plates. Total RNA was extracted 3 h after treatment with 100 nM flg22. Bars represent the mean values \pm SD of three biological samples consisting of three plants. Different letters represent a significant difference. Asterisks represents a significant difference (** $p = 0.002$, **** $p = 6.04 \times 10^{-5}$, Student's *t*-test).

3.4. Discussion

In this Chapter, results are described that show *Arabidopsis* plants grown without exposure to a microbiota are greatly compromised in age-dependent immunity that normally occurs in plants colonized naturally by microbiota. The results indicate axenically-grown plants exhibit significant defects in PTI and are hypersusceptible to infection by a foliar pathogen. I also show that levels of immunocompetence associated with colonized plants can be restored by a bacterial synthetic community composed of culturable phyllosphere endophytic bacteria. Finally, my results suggest that the immune-modulation function of microbiota can be highly dependent on environmental conditions. These results have significant implications.

The ontogeny of flg22-triggered immunity was characterized in very young seedlings within six days after germination in axenic nutrient agar plates [25, 26], providing insight on the developmentally controlled maturation of immune responses immediately after germination in *Arabidopsis*. Results presented in this Chapter, however, provide evidence that flg22-triggered immunity exhibits an age-dependent maturation period that extends through at least the first several weeks of vegetative growth and that young *Arabidopsis* seedlings grown axenically in nutrient agar plates are immune-compromised. When flg22-mediated resistance was characterized throughout vegetative growth in both AX and HO plants, robust age-dependent PTI in colonized plants was observed, which was consistent with earlier observations in plants grown conventionally in potting soil. Strikingly, no age-dependent PTI resistance was observed in AX plants, suggesting a role for microbiota in the maturation of plant immunity. Subsequent temporal characterization of flg22-induced *FRK1* gene

expression corroborated notions that AX plants lack age-dependent immunity. These observations in *Arabidopsis* have conceptual parallels to findings in mammals where germ-free mouse models were used to discover an important contribution of endogenous microbiota in postnatal maturation of mammalian innate immunity [15, 16]. We found that older *Arabidopsis* plants are more resistant to pathogen infection compared to younger plants during vegetative growth, which is consistent with ARR measured across many different plant species. While ARR has typically been proposed to be caused by an undefined developmental process(es) that antagonizes immune responses [27], results presented in this Chapter support an alternative hypothesis that microbiota plays an important role in age-dependent immunity in plants.

Investigating the role of microbiota in immune maturation required the use of a gnotobiotic system capable of growing plants with or without viable microbes in otherwise identical conditions. This has been achieved in this study by using FlowPot and GnotoPot gnotobiotic systems with a peat-based substrate, which represents an important step forward mimicking the natural soil substrate. FlowPots had previously been used to characterize the role of microbiota in host phenotypes [23, 28], including immunity [29, 30], but were not conducive to the longer-term growth required for investigating age-dependent immune maturation, the focus of this study. GnotoPots, on the other hand, allowed plants to grow for a longer duration. For this reason, I chose to perform most gnotobiotic experiments in GnotoPots. As described in the Results section, however, I soon found that the original GnotoPot system was not suitable for immunity studies and it suppressed canonical PTI responses (Figure 2.3 A). I should point out that the immune suppression phenomenon in GnotoPots was not immediately

clear to me (or other users) in the beginning, so I spent a large amount of time to optimize the GnotoPot system for immunity study, which had not been anticipated or planned at the onset of my dissertation. In the end, I not only was able to discover the major sources of immune suppression in the GnotoPot system in comparison to the FlowPot system and conventionally grown plants, but also devised solutions to optimize GnotoPots. The optimized GnotoPot system will likely become an important tool for the large research community to characterize the contribution of microbiota in host immune phenotypes in the future.

My results from the GnotoPot system showing immune suppression by rich nutrients and high humidity are consistent with results from conventionally grown plants reported in the literature. For example, high humidity [31] and excess nutrients [32, 33] can inhibit immune signaling through various mechanisms, including inhibition of plasma membrane depolarization upon detection of flg22 [32]. Interestingly, I found that nutrient/humidity-mediated immune suppression was most obvious in the presence of microbiota, suggesting an intricate interplay between plant, microbiota, and nutrient/humidity conditions. With respect to humidity, restoration of PTI in GnotoPots was most profound after 24 h of acclimation to RH levels around 40% via removing the lid of the Microbox. This has the drawback of exposing plants to environmental microbes. However, for phenotypes measured in our study, this short-term microbe exposure did not appear to alter the phenotype of axenic plants compared to holoxenic plants. Future research is needed to determine the length of exposure time to air-borne microbiota that is required for alter microbiota-mediated immunity. In addition to removing the lid, RH levels could be slightly reduced by aseptically removing excess

moisture from the bottom of the Microbox. However, I found that this only partially relieved the humidity-induced suppression of host phenotypes. In the case of nutrients, the greatest flg22-induced production of ROS was observed at the lowest concentration of nutrient solution tested, 0.1x LS. However, due to issues involving hyperhydricity at this lower concentration as described in Chapter 2, intermediate concentrations of nutrient solution (0.25x-0.5x LS) were judged to be most suitable for PTI assays as presented in this Chapter.

The exact mechanism of microbiota-based age-dependent immune maturation requires future study. I hypothesized that a receptor-level defect upstream of ROS and MAPK signaling may be compromised PTI in axenic plants. Indeed, basal expression of *FLS2* is reduced in AX plants. However, preliminary western blot characterization of relative *FLS2* and *BAK1* protein levels in whole leaf tissue homogenates prepared from AX and HO plants grown in early versions of the GnotoPot system indicated *FLS2* levels were sometimes slightly reduced, but this was not always consistent. Determining the biological relevance of potential differences in *FLS2* protein abundance through the use of overexpression lines, for instance, is required. In my hands, however, an *FLS2* overexpression line driven by the 35S promoter accumulated less total *FLS2* compared to wildtype Col-0 plants so this will need to be revisited. No difference was observed in *BAK1* abundance and commercially available antibodies do not exist yet for *BIK1*. An *Arabidopsis* line expressing an epitope tagged *BIK1* driven by its native promoter has been described [34], which could function as an alternative to detecting native *BIK1*. Additionally, instead of total abundance, receptor subcellular localization and receptor/co-receptor proximity to one another could be a contributing factor to

compromised PTI signaling in AX plants. Future efforts to account for this spatial information by using methods such as cell fractionation or microscopy (as in the case of FLS2 described here [35]) may be warranted. Finally, future research should look into factors in addition to compromised PTI that may also contribute to the hypersusceptibility of AX plants. For instance, the lack of competition in the phyllosphere of AX plants could result in reduced microbial antagonism and increased nutrient availability associated with plant tissues.

Overall, results presented here demonstrating the compromised PTI and hypersusceptibility of axenic plants to infection add to similar results obtained by James Kremer using the FlowPot system [29]. In a separate study using FlowPots, Hou and colleagues also report axenic plants are more susceptible to both *Botrytis cinera* B05.10 and *Pst* DC3000 infection compared to plants colonized by a multi-kingdom synthetic community composed of bacteria, fungi, and oomycetes via an unknown mechanism. Together, these studies demonstrate that the compromised immune phenotypes observed in axenic plants are reproducible in multiple systems utilizing distinct peat-based substrates.

I found that a synthetic community composed of 48 culturable *Arabidopsis* phyllosphere bacteria (SynCom^{Col-0} described in [23]) was able to restore immunocompetence in GnotoPot-grown plants to levels similar to plants inoculated with a soil-derived community. Demonstrating the ability of a bacterial SynCom to restore immunocompetence opens the possibility of applying reductionist approaches to tease apart microbial factors involved in microbial-mediated immune maturation that would otherwise be too difficult with a highly complex community. Unexpectedly, in plates, I

observed stronger induction of flg22-responsive genes in AX plants compared to SynCom^{Col-0}-colonized plants, suggesting SynCom^{Col-0} is suppressing PTI responses in plate-grown plants. Interestingly, suppression of PTI by plant-derived bacterial communities in plate-based systems has similarly been reported in recent studies [36, 37]. These studies revealed that some individual isolates possess the ability to suppress plant immunity, which may either help colonization by other potentially beneficial bacteria or balance tradeoffs associated with defense. Whether synthetic community colonized plants are hypersusceptible to infection compared to axenic plants when grown in plates remains to be determined.

The emerging different results from nutrient agar- and peat-based gnotobiotic systems warrant further discussion. One possibility is that the different results are caused by using different microbiota, plants, or other experimental conditions in different studies. However, in my own study, input microbiota and plant genotype were identical in both plate and GnotoPots experiments, suggesting that the suppression of PTI observed in plates is the result of different gnotobiotic systems *per se*. The peat-based substrate of GnotoPots and agar-based substrate of plates are quite different. In particular, agar lacks a soil-like structure and organic matter relevant to soil [38]. A future study could examine whether compared to a soil-like substrate, altered composition or abundance of plant-associate microbiota in agar plates explain a surprisingly different microbiota immune output. Alternatively, microbiota-independent environmentally factors in agar plate and peat-based systems could be modulating the plant response to microbiota.

3.5 Methods

3.5.1. Arabidopsis growth conditions

Conventionally-grown plants were grown using potting soil composed of equal parts Suremix (Michigan Grower Products), medium vermiculite, and perlite. The resulting potting soil was autoclaved once to eliminate pests. Plants were grown in an air-circulating growth chamber with the following conditions: 60% RH, 22°C, 12 h day/12 h night photoperiod cycle and provided with a daytime photon flux of $\sim 90\text{-}100 \mu\text{mol m}^{-2} \text{s}^{-1}$ and supplemented with 0.5x Hoagland nutrient solution [39] as needed.

For peat-based gnotobiotic experiments, plants were grown in FlowPots or GnotoPots as indicated. Methods for preparation and inoculation are described in Chapter 2. Axenic plants were mock-inoculated with an autoclaved MSU19 soil slurry (50 g soil/ L water) and holoxenic plants were inoculated with the same unautoclaved soil slurry. For peat-based experiment using SynCom^{Col-0}, plants were inoculated with aliquots of SynCom^{Col-0} that preserved with 5% DMSO, cryogenically stored, and thawed at 37°C, as described in Chapter 2. Bacterial suspensions were adjusted to a $\text{OD}_{600} = 0.04$ ($\sim 2 \times 10^7$ cfu/mL) and contained a final concentration of 10 mM MgCl₂ and 0.5% DMSO. 1 mL was used for inoculation. Microbe-free plants for synthetic community experiments were mock-inoculated with a 1 mL mock-inoculum containing 10 mM MgCl₂ and 0.5% DMSO. Plants grown in peat-based gnotobiotic systems were harvested 4.5 weeks post germination for experiments, unless noted otherwise.

For LS agar plate-based experiments, plants were grown as described in [23]. Briefly, vapor-sterilized seed were sown on 0.5x LS containing 0.8% agar. Seeds were then inoculated with premixed SynCom^{Col-0} suspension (cryopreserved with 5% DMSO).

Prior to inoculation the suspension was adjusted to $OD_{600} = 0.02$ ($\sim 1 \times 10^7$ cfu/mL), 10 mM $MgCl_2$, 0.25% DMSO and individual seeds were inoculated with 2 μ L. Microbe-free plants for agar-based plate experiments were mock-inoculated with 2 μ L 10 mM $MgCl_2$ containing 0.25% DMSO. Plate-grown plants were harvested 4 weeks post germination.

3.5.2. Bacterial infection assays

For flg22 protection assays with conventionally-grown *Arabidopsis*, plants of the indicated ages were pretreated with a foliar spray of 500 nM flg22 containing 0.05% DMSO. 7 h after pretreatment with flg22 plants were infiltrated with 5×10^7 cfu/mL *Pst* DC3000 using a blunt-end syringe. Infected plants were partially covered with a dome to increase humidity. Bacterial populations were determined 24 h after infiltration.

For disease assays in conventionally-grown *Arabidopsis* using *Pst* DC3000 mutants, plants of the indicated ages were syringe-infiltrated with a 1×10^5 cfu/mL suspension of $\Delta avrPto \Delta avrPtoB$ [16] or *hrcC* [20]. Infected plants were allowed to dry then covered with a dome to increase humidity. Bacterial populations were determined 3 days after infiltration.

For flg22 protection assays in gnotobiotic *Arabidopsis*, plants were grown in FlowPots with 0.5x LS. Sow date was staggered, and plants of the indicated ages were treated at the same time to allow direct comparison. Plants were pretreated with 100 nM flg22 using a blunt-end syringe and allowed to dry until no longer glassy in appearance. flg22-treated plants were kept in Microboxes with the lid on overnight. 24 h after pretreatment, plants were syringe-infiltrated with *Pst* DC3000 at 1×10^6 cfu/mL. Infected

plants were allowed to dry then covered with a dome to increase humidity. Bacterial populations were determined 24 h after infiltration.

For the disease assay in gnotobiotic *Arabidopsis*, plants were grown in GnotoPots with 0.5x LS and infiltrated with *Pst* DC3000 at 1×10^6 cfu/mL with a blunt-end syringe. Infected plants were allowed to dry then covered with a dome to increase humidity. Bacterial populations were determined 24 h after infiltration.

3.5.3. ROS burst assays

Leaf disks (4 mm in diameter) were taken from the center of leaves from 4-5-week-old plants and floated with abaxial side down in a well of a white 96-well plate containing 200 μ L sterile water in each well. Plates were covered with foil and leaf disks were rested overnight to attenuate wounding response. 24 h later, water was removed from wells and replaced with 100 μ L of an elicitor solution containing 34 μ g/mL luminol (Sigma), 20 μ g/mL horseradish peroxidase (Sigma), and 100 nM flg22. Luminescence was measured (total photon counting) over 60 min immediately after the addition of elicitor solution using a SpectraMax L microplate reader (Molecular Devices). Plants used in ROS experiments were grown in GnotoPots with 0.25x-0.5x LS unless noted otherwise. Similar overall trends were observed in GnotoPot-grown plants when using LS concentrations less than 0.5x.

3.5.4. RT-qPCR analysis of flg22-induced gene expression

Plants of the indicated ages were treated with a foliar spray of elicitor solution consisting of 100 nM flg22, 0.1% DMSO, and 0.025% Silwet-L77 (Bioworld) or a mock

solution that lacked flg22. Foliar sprays were applied ensuring treatment solution came in contact with both the adaxial and abaxial side of leaves. For quantification of *FLS2* gene expression, tissues were harvested 1 h after treatment. For quantification *FRK1* gene expression, tissues were harvested 3 h after treatment. Upon harvest, the above-ground tissue was excised and transferred to 2 mL screw-top tubes before being frozen in liquid N₂ and stored at -80°C until further processing.

Total RNA was extracted from leaf tissue in Trizol (Thermo Fisher) using a Direct-zol RNA extraction kit (Zymo Research) according to the manufacturer's instructions using the optional on-column DNase treatment. Total RNA was eluted in water and normalized to 80 ng/μL on a NanoDrop 1000 spectrophotometer (Thermo Fisher). cDNA synthesis was accomplished in 10 μL volumes with SuperScript IV VILO master mix (Thermo Fisher) according to the manufacturer's instructions using 640 ng total RNA as input. Upon synthesis, cDNA was diluted 10-fold. qPCR was performed in duplicate on a minimum of three biological replicates in 10 μL reaction volumes containing 5 μL SYBR Green PCR master mix, 0.25 μL of each primer, and 2 μL of template cDNA on an ABI 7500 Fast qPCR instrument (Applied Biosystems) using the default settings. *PP2A* was used for normalization. The following primer sets were used to quantify gene expression:

FLS2-F: 5'-ACTCTCCTCCAGGGGCTAAGGAT-3'

FLS2-R: 5'-AGCTAACAGCTCTCCAGGGATGG-3'

FRK1-F: 5'-CTTCCATCGAGGTACAAAGATGAC-3'

FRK1-R: 5'-CAGTGCTCATGACAGTAGAAGC-3'

PP2A-F: 5'-GGTTACAAGACAAGGTTCACTC-3'

PP2A-R: 5'-CATTTCAGGACCAAACCTCTTCAG-3'

For age dependent gene expression experiments, plants were grown in FlowPots with 0.5x LS. Sow date was staggered and plants of the indicated ages were harvested at once. For other peat-based gene expression experiments, plants were grown in GnotoPots supplemented with 0.25x-0.5x LS.

3.5.5. Quantification of SA and SAG

Plant hormones SA and SAG were extracted as previously described [40]. In brief, 100 mg of leaf tissue harvested from 4.5-week-old plants grown in FlowPots was frozen and ground to fine powders with a TissueLyser (Qiagen) using two 45 s cycles at 28 Hz. Frozen powders were resuspended in 1 mL extraction buffer containing 80% methanol, 0.1% formic acid, 0.1 mg/mL butylated hydroxytoluene, and 100 nM deuterated abscisic acid (ABA-²H₆) in water. Samples were extracted overnight at 4°C with gentle agitation. The next day, samples were cleared by centrifugation at 12,000×g for 10 minutes, filtered through a 0.2 µm PTFE membrane (Millipore), and transferred to autosampler vials. 10 µL injections of prepared extracts were separated using an Ascentis Express fused-core C18 column (2.1×50 m, 2.7 µm) heated to 50°C on an Acquity ultra performance liquid chromatography system (Waters Corporation). A gradient of 0.15% formic acid in water (solvent A) and methanol (solvent B) was applied over 2.5 minutes at a flow rate of 0.4 mL/min. Separation consisted of a linear increase from A:B (49:1) to 100% B. Transitions from deprotonated molecules to characteristic product ions were monitored for ABA-²H₆ (m/z 269.1 > 159.1), SA (m/z 137.0 > 93.0), and SAG (m/z 299.1 > 137.0) on a Quattro Premier tandem mass spectrometer (Waters

Corporation) in negative ion mode. The capillary voltage, cone voltage, and extractor voltage were 3500 V, 25 V and 5 V, respectively. The flow rates were 50 L/h for the cone gas (N₂) and 600 L/h for the desolvation gas (N₂). ABA-²H₆ served as the internal standard for hormone quantification. Collision energies and source cone potentials were optimized using QuanOptimize software. Masslynx v4.1 was used for data acquisition and processing. Peaks were integrated and the analytes quantified based on standard curves normalized to the internal standard.

3.5.6. Protein extraction and immunoblot

Protein was extracted as previously described [41] with slight modification. First, frozen tissues were ground to fine powders with a with a TissueLyser (Qiagen) using two 45 s cycles at 28 Hz. Powders were taken up into a protein extraction buffer containing 50 mM Tris-HCl (ph 8.0), 150 mM NaCl, 10% (v/v) glycerol, 1% (v/v) Igepal CA-630 (NP-40) (Sigma), 0.5% (w/v) sodium deoxycholate, 1x Complete EDTA-free protease inhibitor tablet (Roche) and incubated on ice for 15 min with periodic inversion. Plant lysates were cleared by centrifugation at 10,000×g for 5 min and normalized via Bradford Assay (Biorad). Extracts were prepared for SDS-PAGE with a 5x loading buffer containing 10% (w/v) sodium dodecyl sulfate, 20% glycerol, 0.2 M Tris-HCl (pH 6.8), and 0.05% bromophenol blue and gradually denatured on a thermocycler using the following sequence: 37°C for 20 min, 50°C for 15 min, 70°C for 8 min, and 95 for 5 min. Protein was subsequently separated on NuPAGE 4-12% bis-tris gels (Thermo Fisher) for 2.5 h using 100 V. Proteins were then transferred to PVDF using an iBlot 2 dry blotting system (Thermo Fisher), blocked in 3% milk + 2% BSA and immunoblotted

overnight at 4°C with antibodies specific to *Arabidopsis* FLS2, (Agrisera), BAK1 (Agrisera), MPK3 (Sigma) or MPK6 (Sigma) at concentrations recommended by the manufacturer. Blots for detecting phosphorylated MAPK were blocked in 5% BSA and immunoblotted with a phosphor-p44/42 MAPK (Erk1/2) (Thr202/Tyr204) antibody (Cell Signaling). Horseradish peroxidase-conjugated anti-rabbit antibody produced in goat (Agrisera) was used as a secondary antibody and the resulting proteins of interest were visualized with SuperSignal West chemiluminescent substrate (Thermo Fisher). Ponceau S staining was performed to verify equal loading.

REFERENCES

REFERENCES

1. Boller, T. and G. Felix, *A renaissance of elicitors: perception of microbe-associated molecular patterns and danger signals by pattern-recognition receptors*. Annual review of plant biology, 2009. **60**: p. 379-406.
2. Daudi, A., et al., *The apoplastic oxidative burst peroxidase in Arabidopsis is a major component of pattern-triggered immunity*. The Plant Cell, 2012. **24**(1): p. 275-287.
3. Navarro, L., et al., *The transcriptional innate immune response to flg22. Interplay and overlap with Avr gene-dependent defense responses and bacterial pathogenesis*. Plant physiology, 2004. **135**(2): p. 1113-1128.
4. Bigeard, J., J. Colcombet, and H. Hirt, *Signaling mechanisms in pattern-triggered immunity (PTI)*. Molecular plant, 2015. **8**(4): p. 521-539.
5. Zipfel, C., et al., *Bacterial disease resistance in Arabidopsis through flagellin perception*. Nature, 2004. **428**(6984): p. 764-767.
6. Whalen, M.C., *Host defence in a developmental context*. Molecular plant pathology, 2005. **6**(3): p. 347-360.
7. Develey-Rivière, M.P. and E. Galiana, *Resistance to pathogens and host developmental stage: a multifaceted relationship within the plant kingdom*. New Phytologist, 2007. **175**(3): p. 405-416.
8. Panter, S. and D.A. Jones, *Age-related resistance to plant pathogens*. 2002.
9. Huot, B., et al., *Dual impact of elevated temperature on plant defence and bacterial virulence in Arabidopsis*. Nature communications, 2017. **8**(1): p. 1-12.
10. Wang, D., et al., *Salicylic acid inhibits pathogen growth in plants through repression of the auxin signaling pathway*. Current Biology, 2007. **17**(20): p. 1784-1790.
11. Yang, D.-L., et al., *Plant hormone jasmonate prioritizes defense over growth by interfering with gibberellin signaling cascade*. Proceedings of the National Academy of Sciences, 2012. **109**(19): p. E1192-E1200.
12. Lozano-Durán, R., et al., *The transcriptional regulator BZR1 mediates trade-off between plant innate immunity and growth*. elife, 2013. **2**: p. e00983.

13. Yang, D.-H., et al., *The multifaceted function of BAK1/SERK3: plant immunity to pathogens and responses to insect herbivores*. *Plant signaling & behavior*, 2011. **6**(9): p. 1322-1324.
14. Hooper, L.V., D.R. Littman, and A.J. Macpherson, *Interactions between the microbiota and the immune system*. *science*, 2012. **336**(6086): p. 1268-1273.
15. Fulde, M. and M.W. Hornef, *Maturation of the enteric mucosal innate immune system during the postnatal period*. *Immunological Reviews*, 2014. **260**(1): p. 21-34.
16. Lin, N.-C. and G.B. Martin, *An avrPto/avrPtoB mutant of Pseudomonas syringae pv. tomato DC3000 does not elicit Pto-mediated resistance and is less virulent on tomato*. *Molecular Plant-Microbe Interactions*, 2005. **18**(1): p. 43-51.
17. Hauck, P., R. Thilmony, and S.Y. He, *A Pseudomonas syringae type III effector suppresses cell wall-based extracellular defense in susceptible Arabidopsis plants*. *Proceedings of the National Academy of Sciences*, 2003. **100**(14): p. 8577-8582.
18. Gimenez-Ibanez, S., et al., *AvrPtoB targets the LysM receptor kinase CERK1 to promote bacterial virulence on plants*. *Current biology*, 2009. **19**(5): p. 423-429.
19. He, P., et al., *Specific bacterial suppressors of MAMP signaling upstream of MAPKKK in Arabidopsis innate immunity*. *Cell*, 2006. **125**(3): p. 563-575.
20. Yuan, J. and S.Y. He, *The Pseudomonas syringae Hrp regulation and secretion system controls the production and secretion of multiple extracellular proteins*. *Journal of bacteriology*, 1996. **178**(21): p. 6399-6402.
21. Linsmaier, E. and F. Skoog, *Organic growth factor requirements of tobacco tissue cultures*. *Physiol. plant*, 1965. **18**(1).
22. Xin, X.-F., et al., *Bacteria establish an aqueous living space in plants crucial for virulence*. *Nature*, 2016. **539**(7630): p. 524-529.
23. Chen, T., et al., *A plant genetic network for preventing dysbiosis in the phyllosphere*. *Nature*, 2020. **580**(7805): p. 653-657.
24. Song, C., K. Jin, and J.M. Raaijmakers, *Designing a home for beneficial plant microbiomes*. *Current Opinion in Plant Biology*, 2021. **62**: p. 102025.
25. Zou, Y., S. Wang, and D. Lu, *MiR172b-TOE1/2 module regulates plant innate immunity in an age-dependent manner*. *Biochemical and Biophysical Research Communications*, 2020. **531**(4): p. 503-507.

26. Zou, Y., et al., *Transcriptional regulation of the immune receptor FLS2 controls the ontogeny of plant innate immunity*. *The Plant Cell*, 2018. **30**(11): p. 2779-2794.
27. Carella, P., D.C. Wilson, and R.K. Cameron, *Some things get better with age: differences in salicylic acid accumulation and defense signaling in young and mature Arabidopsis*. *Frontiers in plant science*, 2015. **5**: p. 775.
28. Durán, P., et al., *Microbial interkingdom interactions in roots promote Arabidopsis survival*. *Cell*, 2018. **175**(4): p. 973-983. e14.
29. Kremer, J.M., *Characterization of axenic immune deficiency in Arabidopsis thaliana*. 2017: Michigan State University.
30. Hou, S., et al., *A microbiota–root–shoot circuit favours Arabidopsis growth over defence under suboptimal light*. *Nature Plants*, 2021. **7**(8): p. 1078-1092.
31. Panchal, S., et al., *Regulation of stomatal defense by air relative humidity*. *Plant physiology*, 2016. **172**(3): p. 2021-2032.
32. Jeworutzki, E., et al., *Early signaling through the Arabidopsis pattern recognition receptors FLS2 and EFR involves Ca²⁺-associated opening of plasma membrane anion channels*. *The Plant Journal*, 2010. **62**(3): p. 367-378.
33. Ding, S., et al., *Nitrogen forms and metabolism affect plant defence to foliar and root pathogens in tomato*. *Plant, Cell & Environment*, 2021. **44**(5): p. 1596-1610.
34. Lu, D., et al., *A receptor-like cytoplasmic kinase, BIK1, associates with a flagellin receptor complex to initiate plant innate immunity*. *Proceedings of the National Academy of Sciences*, 2010. **107**(1): p. 496-501.
35. Bücherl, C.A., et al., *Plant immune and growth receptors share common signalling components but localise to distinct plasma membrane nanodomains*. *Elife*, 2017. **6**: p. e25114.
36. Ma, K.-W., et al., *Coordination of microbe–host homeostasis by crosstalk with plant innate immunity*. *Nature Plants*, 2021. **7**(6): p. 814-825.
37. Teixeira, P.J., et al., *Specific modulation of the root immune system by a community of commensal bacteria*. *Proceedings of the National Academy of Sciences*, 2021. **118**(16).
38. Kremer, J.M., et al., *Peat-based gnotobiotic plant growth systems for Arabidopsis microbiome research*. *Nature protocols*, 2021. **16**(5): p. 2450-2470.

39. Hoagland, D.R. and D.I. Arnon, *The water-culture method for growing plants without soil*. Circular. California agricultural experiment station, 1950. **347**(2nd edit).
40. Zeng, W., et al., *A genetic screen reveals Arabidopsis stomatal and/or apoplastic defenses against Pseudomonas syringae pv. tomato DC3000*. PLoS pathogens, 2011. **7**(10): p. e1002291.
41. Chinchilla, D., et al., *A flagellin-induced complex of the receptor FLS2 and BAK1 initiates plant defence*. Nature, 2007. **448**(7152): p. 497-500.